THE UNIVERSITY OF
WARWICK

University of Warwick institutional repository: http://go.warwick.ac.uk/wrap

A Thesis Submitted for the Degree of PhD at the University of Warwick

http://go.warwick.ac.uk/wrap/34687

This thesis is made available online and is protected by original copyright.

Please scroll down to view the document itself.

Please refer to the repository record for this item for information to help you to cite it. Our policy information is available from the repository home page.

SOME PROPERTIES OF BOLTED JOINTS

Dissertation submitted to the

University of Warwick

for the degree of Doctor of Philosophy

by

T.V. Heath

June 1974

BEST COPY

AVAILABLE

Variable print quality

CONTENTS

ACKNOWLEDGEMENTS

The author wishes to thank:-

his supervisor, Dr. V. Marples, for his guidance especially in the latter period of the project,

the staff and technicians of the University of Warwick, in particular Messrs. J.D. Darmon, T. Farquar and C.C. Voiles for their continued and essential assistance,

and Mrs. B. Bramhall for her efficient service in the typing of the dissertation.

SOME PROPERTIES OF BOLTED JOINTS

by

T.V. HEATH

ABSTRACT

The roles of surface roughness and of surface flatness in determining the properties of structural joints are discussed. A method of measuring the effects of errors of form on joint stiffness is given.

Measurements of the dynamic stiffness of annular bolted joints were taken for varying preloads and on joints with different surface finishes. Results obtained were of a form not previously seen.

It was determined that the joint motion was the combination of a normal joint motion, which was uniform across the joint, and a dynamic deformation of the joint planforms resulting from the superimposition of a uniform dynamic load on to the non-uniform static joint preload provided by the bolts. This dynamic deformation varied as a function of position within the joint and in consequence the dynamic motion of the joint was not uniform with position. It was found that the phase relationship between the applied dynamic force and the resultant joint motion varied markedly with both bolt load and excitation frequency. A two degree of freedom mathematical model was developed to account for the unusual changes in the phase and magnitude of the dynamic joint stiffness, with these parameters. This model includes a negative stiffness. Experiments were performed to demonstrate the existence of this negative stiffness

and a method was then developed for determining the static motion of a rectangular joint subjected to non-uniform loading.

LIST OF SYMBOLS

A	Amplitude of joint motion
A_a, A_c, A_r	Areas within a joint
B	Distance of points on joint surface from a datum plane
E	Youngs Modulus
F	Bolt Load
I	Second Moment of Area of Section
N	Normal Reaction Force
P	Joint Load
Q	Pressure distribution under bolthead
R	Joint Flexibility (displacement per unit load)
S	Separation of joint planforms
T	Torque, Distance of points on joint surface from a datum plane
a,b,c,d,m	Constants
d	Distance of points within a joint from contact line
r	Radius
ε	Joint deflections
θ	Phase lag, helix angle on thread
ϕ	Rotation of joint plate, Angular position within joint
α	Semi-angle of thread form
μ	Coefficient of friction

Chapter 1

INTRODUCTION AND PREVIOUS WORK

1.1 INTRODUCTION

A joint may be defined as the region of contact between different components, or different sections of a single component, in any machine or structure. There are many types of joint, some of which are present in a structure simply to enable the fabrication of shapes and sizes not otherwise possible, whilst others have a more specific function such as to enable relative motion to occur between components, as in the case of a bearing, or to provide a fluid seal between sections of a machine. It is generally true to say that the classes of joint specifically designed for a purpose other than for simply connecting two components have been closely studied and are now the products of an advanced technology. It has only recently become widely appreciated however that the simple connecting joint also has properties which can have considerable influence on the static and dynamic properties of machine structures. A considerable volume of research by numerous authors has laid a firm foundation for the study of joints. Further work is now necessary to obtain a wider understanding of the mechanisms affecting joint properties and to enable the specification of joint design for the optimization of machine performance.

Joints are usually divided into two classes, fixed and moving. Fixed joints are connections between components in which there is no intentional motion tangential to the joint surface. Such joints are commonly formed by welding, riveting, bonding or by clamping under normal load, for

example by bolting or by the application of pneumatic or hydraulic pressure. Moving joints are necessary to enable relative motion to occur between adjacent components as in the case of rotary bearings or in machine slides. It is common for moving joints to be clamped under load for part of their lives as in the case of lathe tail stocks and as such the sliding joint can be converted to a fixed joint.

The type of fixing used in a joint depends largely on the strength requirement of the connection and whether the joint is to be permanent or has to be separated for maintainance or other reason. Welding and riveting can usually be relied upon to give nominally strong joints but these joints once formed do not readily lend themselves to separation. Bolts however can give fairly high interfacial preloads whilst still being very easy to strip and reassemble. This ease of use coupled with reliability and low cost has meant that for many years the use of bolts and other screw fasteners has been a primary method of securing joints. As a result of this widespread application the bolted connection deserves special attention in the study of joints; this work therefore is intended to determine the fundamental properties of bolted connections.

1.2 REVIEW OF PREVIOUS WORK

The main properties of a joint which affect the static and dynamic performance of a machine tool or other structural body are its stiffness and its damping capacity. It has long been appreciated that the majority of damping in machine tools comes from system rather than from material damping. Tobias (11) while investigating machine tool chatter

has measured the frequency responses of various machine tools and found damping ratios in the range of 0.006 to 0.135; a typical value being 0.03. This typical value is far larger than the internal damping of normal structural steels. Peters (9) performed experiments in which the damping ratios of cast iron and steel lathe spindles were measured in situ and remote from the machine. With the spindles remote from the machine structure values of 0.001 and 0.002 were obtained for the damping ratios of the steel and cast iron specimens respectively. Although the cast iron shows double the damping in the steel this is not significant when compared to the value of 0.03 obtained with the spindle in situ. From the shape of decay curves taken during experimentation it was concluded that the predominant source of damping in the mounted spindle was sliding friction in the spindle housing. It was further noted that the damping was a function of the preload applied to the mounting bearings and that there was an optimum preload for maximum damping. Peters set a value of damping ratio of 0.5 as a desirable lower limit for machine tool damping and suggested that additional damping could be introduced into machine tool structures to bring energy dissipation levels up to this value by using vico-elastic dynamic vibration absorbers and by the introduction of viscous damping into the spindles. Using these methods a damping ratio of 0.25 was obtained in a spindle and this damping was sufficient to eliminate chatter from cylindrical turning operations which had previously been highly disturbing. This example serves to illustrate the importance of damping in the control of structural vibration.

Damping in machine tool structures is also discussed by Andrew (8) who quotes values of material damping in the range of 0.003 to 0.005 for cast iron and 0.0015 to 0.0025 for steel. These are higher than the values given by Peters but are again insignificant when compared with the values of 0.016 to 0.05 given for complete machines. Andrew discusses two types of system damping both originating in the structural joints. Interfacial slip, where energy is dissipated in a motion tangential to the joint surface, and interfacial squeeze action where a fluid, normally machine oil, is pumped in and out of interfacial cavities within the joint. To demonstrate the damping effect of interfacial squeeze action an experiment was performed on a standard milling machine where the machine was stripped and, where possible without risk of machine damage, all the joints between components were degreased. The damping capacity of the machine was then measured. Oil and grease were then reintroduced into the machine and the damping again recorded. A 50% increase in energy dissipation was measured in the lubricated relative to the unlubricated state. Andrew agrees with Peters that the damping normally present in machine tool structures is undesirably low and concludes that if more damping is to be introduced into structural connections then squeeze damping offers greater potential for development than does slip damping.

Further measurements on squeeze damping have been made by Ungar and Carbonell (2). A series of tests was performed on irregularly shaped aluminium plates to which had been bolted stiffening beams. Irregular shapes of plates and assymetric locations of the beams were chosen

to ensure that when subjected to a forced harmonic excitation, a diffuse wave field would be generated in the panel. This was desirable to ensure that results were not unduly affected by dominant resonances in the test structure. The damping in the panel was measured from its reverberation time, and after correcting for material damping ratios of 0.004 were attributed to the presence of the beam. Rather surprisingly it was found that neither the clamping load with which the beams were held to the panel nor the surface finish of the mating parts had significant effect on the panel damping and it was therefore concluded that solid friction played little part in interfacial energy dissipation; the damping resulted primarily from the pumping of air between the plate and beam. This conclusion was confirmed when it was discovered that any restriction on the movement of air in the interfacial region, for example by welding the seam between beam and panel, led to a reduction in the measured damping and that furthermore the energy dissipation was found to decrease with the ambient air pressure.

A number of attempts have been made to calculate energy dissipation in squeeze films. The theory is normally based upon the Reynold's equation or on a similar approach. To obtain mathematical solutions to this problem authors have found it necessary to assume that the faces containing the squeeze film are parallel, or of constant separation. This is not an assumption which relates well to practical joints. Andrew, Cockburn and Waring (17) made measurements of the quadrature and in-phase stiffnesses of stacks of dry and oiled joints and found that whereas no damping could

be measured with the joints in the dry condition, there were considerable quadrature forces present when oil was introduced. It was found that the damping increased with oil viscocity and with a decrease in the effective separation of the joint planforms. The effective separation was considered to be a function of the surface finish of the joint planforms; the better the surface finish, the smaller the separation. The damping forces also increased with the frequency of excitation. A qualitative model was proposed to describe the effects of an interfacial oil film. This model consisted of a piston acting on a cylinder of oil which was connected to a reservoir through a restrictor. It was argued that the motion of the piston was equivalent to the joint motion and that the subsequent flow of oil through the restrictor represented the flow of oil between joint asperities. It was claimed that the properties of this model were similar to the results obtained experimentally; A close inspection of these results shows however that the similarity is tenuous.

Waring (16) performed further experiments on joint stacks using joint surfaces which had been lapped flat to within close limits. These surfaces were then held a known distance apart by 'pips' produced on the surface by indenting a hard ball under known load. Provided that cavitation did not occur in the interfacial oil film the results obtained from this arrangement compared well with those predicted from squeeze film theory.

It should be noted that when a stack of joints is tested rather than a single joint the displacement to be measured is increased in proportion to the number of joints

in the stack. This considerably eases the problems of measuring the very small displacements which occur in joints. Problems arise however in that it is very difficult to maintain parallelism of the joint surfaces in a stack and it is therefore difficult to prevent buckling in the column. In both the previously mentioned works the joints were annular in shape and a centrally placed inductive transducer was used to measure the joint displacements. Using a centrally mounted single pick-up makes it impossible to measure the effects of any buckling or tilting which might occur.

The frequency range investigated by Andrew, Cockburn and Waring (17) was 30 - 270 Hz. The properties of oil films subjected to higher frequencies, 300 - 1000 Hz, has been investigated by Hother-Lushington and Johnson (7). A mild steel beam was clamped at both ends and subjected to forced excitation at the centre. A resonance curve was obtained from which the damping in the beam was calculated. Two pads were then placed in position, centrally located above and below the beam with a separation of 1.5×10^{-3}in between the pad and beam on each surface. Oil, at constant pressure, was supplied to each pad and a new resonance curve obtained. Considerable damping was obtained from the oil. The amplitudes of motion measured in these experiments were far larger than those which might be expected in structural joints, and bulk cavitation of the oil occurred, also unlikely in joints. Nevertheless it was found that if the working fluid were considered as an oil/air mixture then reasonable correlation between squeeze film theory and practise was obtained.

Whilst it seems that damping might be most easily

introduced into structures by concentrating on the effects of squeeze films, sight must not be lost of the fact that a considerable proportion of the damping normally present is a result of frictional losses in tangential slip. Earles and Philpott (i) have investigated the frictional damping between dry steel contacts under oscillating tangential loads. The test specimen was clamped under normal load and was then subjected to an oscillating tangential force. The interfacial friction was measured as a function of the normal load and of the duration of the tests. It was found that during the initial period of experimentation there occurred considerable surface damage due to fretting; in consequence there was a rise in the coefficient of friction so that the energy dissipation rose. Subsequently however the loose particles resulting from the surface damage oxidised and the oxidised particles collected together and acted as a lubricant between the two surfaces. The operational coefficient of friction then decreased causing a drop in the level of damping. It was found that provided the amplitude of motion was insufficiently large for gross slip to occur then the damping in the joint stabilised, becoming invariant with time. Theoretical expressions were derived for the slip damping and these gave excellent correlation with the experimental results under conditions of partial slip. Agreement was not as good when gross slip occurred. A review of progress in the Analysis of interfacial slip damping is given by Goodman (18).

The damping in engineering structures is important to minimise the effects of structural resonance and to give a high resistance to the potential effects of shock excitation.

A factor of equal if not greater importance in machine tools is the static stiffness of the structure. A high stiffness is required to keep resonant frequencies high and to minimise vibration amplitudes in off resonant conditions of forced excitation. A high stiffness is also required to restrict machine deflections under constant tool loads thereby enabling high dimensional accuracy of components to be obtained. Connolly and Thornley (10) showed that joint deflections were a significant if not major contributor to overall structural deflections and criterion was given for determining the relative effects of joint and material deflections in joints of various configurations. Several factors have been shown to influence the normal static stiffness of metal-to-metal joints, the most important of these, omiting the effects of differing joint materials, being the preload applied to the joint, and the surface finish of the mating components. Much basic work has been performed by Thornley, Connolly, Barash and Koenigsberger, (14) and (15), on the influence of surface topography on the static performance of joints. During an early series of tests it was shown that provided a minimum preload, dependant on the type of surface, was exceeded, then the surface roughness of the planforms had no effect on the static stiffness of the joint. The value of the minimum preload decreased as the surface finish was improved; typical values being 0.1 tons/in^2 for a lapped surface and 3 tons/in^2 for a shaped surface. This conclusion may be a little misleading, since, as discussed by the authors, interface pressures in bolted joints are usually in the region of 2 tons/in^2 so that except for joints of particularly fine quality the

minimum preload is unlikely to be exceeded. It may therefore be taken that improving the surface quality of joint planforms increases the joint stiffness. It was subsequently shown by the same group of authors that in the preload range 0.02 to 2 tons/in^2 there was a linear relationship between joint stiffness and applied preload, and that the constant of proportionality was a function of the surface finish.

Deconinck (6) conducted research into dynamic stiffness of metal to metal joints subjecting test pieces to a low frequency vibration (3Hz). This frequency was chosen so that the effects of instrument phase shifts on measurements could be eliminated. This problem is much discussed by Day (19). No damping was measured in the joint although since many damping mechanisms are velocity dependant the low forcing frequency might have contributed to this result. The shape of the variation of joint stiffness with applied preload was approximated by Deconinck to a parabola and he also concluded that the surface roughness of the planforms did not significantly affect the stiffness. These findings are somewhat different from the later results obtained by Thornley et al.

Corbach (20) and Eisle and Corbach (21) demonstrated that in sliding joints the introduction of oil into the joint interface causes an increase in the dynamic stiffness. A similar effect for fixed joints was observed by Andrew, Cockburn and Waring (17). These conclusions are in turn contradicted by Day (19) who found that 'joints containing an oil film have a stiffness which is only increased within very narrow bands of a few specific frequencies, and that

at all other frequencies the stiffness is constant dependant only on preload. It is seen that there is still considerable controversy over the roles and the effects of surface finish and interfacial load on the normal stiffness of metal to metal joints.

The mode of deformation of contacting asperities in a joint has been much discussed. A review of research into the compression of such asperities is given by Jones, Howells and Probert (5). They show that by using complex derivations of the original Hertzian contact model, an elastic sphere being pressed against a rigid flat surface, a linear relationship between the real contact area in the joint and the applied load may be approached when elastic deformation is assumed. A similar relationship may also be obtained by considering the asperities to deform plastically and thus irrespective of the mode of deformation, a linear relationship between applied load and real contact area may be obtained.

Although considerable work has been performed by the above mentioned and many other researchers into the theoretical and experimental determination of joint properties, it is still not possible to predict with any certainty, the effect of joints on the dynamics of complex structures, and there is scope for much further work. The purpose of this dissertation is to examine the general properties of a simple bolted metal-to-metal connection and to make recommendation as to the manner in which joints may be prepared in order to improve the performance of machines and structures.

Chapter 2

THE EXPERIMENTAL DETERMINATION OF THE VARIATION OF CONTOUR AREA AS A FUNCTION OF JOINT DEFLECTION.

2.1 SURFACE FINISH AND JOINT PROPERTIES

The surface finish of a machined component is conventially described in terms of two parameters; surface roughness, and flatness error or error of form. The roughness of a surface indicates the texture of that surface. and is composed of errors of a short wavelength. It is primarily dictated by the machining process used in the production of the component and the cutting conditions prevalent during application of that process. Flatness errors are of a much longer wavelength and occur in general not as a function of the type of machining but as a result of inaccuracies in particular machines; for example, misalignment or wear in slideways; deformation of the tool under cutting forces and bending of machine structures due to incorrect mounting on foundations. It must be noted however that as shown by Thornley et al (15) certain machining processes can inherently lead to flatness errors. Flatness and roughness errors are simultaneously present on surfaces but are independant. It is in principle possible to produce a surface which is rough but is very flat or alternatively one which has a mirror finish but contains errors of form. Thus when considering the effects of surface finish on joint properties roughness and flatness must be treated as independant parameters.

A considerable volume of research has been performed into the manner in which surfaces behave when brought into contact although this work has largely been directed towards

gaining a greater understanding of surface friction. Kragelski and Demkin (13) define three types of contact area within a joint: -

1) APPARENT area of contact A_a which is the area defined by the physical dimensions of the contacting bodies.
2) CONTOUR area of contact A_c formed by the bulk compression of surface waves. This is the area of the regions of the surface containing touching asperities although contact is not complete within these areas.
3) REAL area of contact A_r which is the sum total of the actual areas of contact between mating asperities.

Three parameters are introduced to describe the effects of surface finish on real contact:

$$\eta_1 = \frac{A_r}{A_c}$$ is dependant on the surface roughness

$$\eta_2 = \frac{A_c}{A_a}$$ is dependant on the surface flatness

and $\eta_3 = \eta_1 \cdot \eta_2$ described the combined effects of roughness and flatness errors

From a series of experimental measurements on numerous surfaces it was found that the initial part of the bearing area curve could be represented by the expression:

$$\eta_1 = b\varepsilon^m$$

since in practical situations the real contact area rarely exceeds 1/5 of the apparent contact area then the expression covers the entire range of deflections normally occurring in joints. If it is now combined with the relationship of prime importance in the conventional theory of friction,

that the real contact area is proportional to the applied load; e.g. Greenwood and Williamson (22), Archard (12) then we have, assuming that for small deflections the contour area does not change significantly:

$$P = d\varepsilon^{m}$$

differentiating with respect to ε gives

$$\frac{dP}{d\varepsilon} = md\varepsilon^{m} = mP$$

but $\frac{dP}{d\varepsilon}$; i.e. the change in joint preload to give a unit change in deflection; is the normal stiffness of the joint and thus it is seen that the joint stiffness is directly proportional to the applied load on the joint.

The linear relationship between load and stiffness has been verified experimentally by Thornley et al (15). Good agreement was found during tests, on a number of joints with a variety of surface finishes. It was shown that as predicted from the work of Kragelsky and Demkin the 'm' value; i.e. the ratio of stiffness to load, increased as the surface roughness of the mating profiles diminished. After performing experiments on stacks of joints Andrew, Cockburn and Waring contradicted this finding concluding 'The stiffness is substantially independant of the roughness of the surfaces, depending primarily on the loads alone. There is general agreement that for given loads the joint stiffness is not dependant upon nominal planform area but that contacting asperities will deform until the real contact area is sufficient to support the applied load'. This statement is in fact difficult to justify in terms of the data published by Andrew et al which appears to substantiate the conclusions of Thornley rather than disprove them.

Day (19) also measured the normal stiffness of metal to metal joints, the curves of stiffness against preload showing three distinct regions. At low preloads the stiffness rises very slowly with applied load. This slow rate of increase is attributed to large bending deflections being produced during the formation of the joint. The second region showed the linear increase in stiffness with preload seen by Thornley and Andrew and in the third section the stiffness increased at a very slow rate indicating that the curve was tending to a limiting value. No satisfactory explanation was given for this.

The normal stiffness of a joint is dependant on the real area of contact within the joint and the real area of contact is limited to the contour area. It is normal that flatness errors are far larger than roughness errors and as such the rate of increase of contour area with joint deflection is far smaller than the rate of increase of real contact area within the contours. It is to be expected therefore that when the real area of contact approaches the contour area the joint stiffness will reach a limiting value which can only increase at a slow rate dependant on the rate of increase of contour area. It is likely that such saturation of contact within the contour area caused the results shown by Day.

Thornley et al (15) also showed that the 'm' value for a joint was critically dependant on the flatness of the planforms and we therefore see that the joint flatness affects both the ultimate strength of the joint and its rate of increase of stiffness with load. In view of the critical nature of joint flatness on joint performance an experimental procedure has been devised for measuring joint conformity;

conformity being defined as the rate of change of contour area with the separation of the joint surfaces.

2.2 MEASUREMENT OF FLATNESS DEVIATIONS

The method used to measure errors of form was similar to that used by Day and Marples (27). A schematic of the apparatus is shown in fig.1. The joint was set on a location plate via three vee-blocks set at 120° intervals in which sat three balls which were set into the passive face of the joint components. This method of support for the joint component was chosen since it provides a stable platform from which the joint can be removed and subsequently relocated accurately. The location plate was securely clamped to a levelling table, and the levelling table in turn to a rotary table. The rotary table was, after initial adjustment, clamped to the rigid surface plate which forms the base for the Rank-Taylor-Hobson Talylin, the instrument used to measure the flatness deviations. The Talylin has an optical flat which is as a straight line datum; any movement of the stylus is measured relative to this optical flat. The inclination of this datum line is finely adjustable by means of levelling screws. The set up procedure and method of operation of the system was as follows: -

1) The rotary table was moved into a position so that it rotated centrally under the mid-point of the Talylin traverse, and the traverse line of the Talylin traces between the 0 and 180° positions on the table. The rotary table was then clamped to the Talylin base plate.
2) The levelling table was placed centrally on the rotary table and securely clamped. A dial gauge was used to check on the concentricity of the two tables.

3) The levelling table was then levelled with respect to the measuring direction of the Talylin stylus. The levelling table is in two sections. The lower portion is clamped to the rotary table whilst the upper section is supported above this base by three legs spaced on equal radii at 120° intervals. The legs are kinematically constrained resting on a vee, a cone and a flat respectively, which locate on steel balls in the base plate. Two of the legs are fitted with micrometer screws to enable adjustment to be made to their lengths, and hence to the angle of inclination of the table. The Talylin stylus was moved to a position 2mm. from the end of its traverse and then gently lowered on to the surface of the table. The table was then rotated and adjustments made to the levelling screws as required to give equal deflections on the Talylin at the angular positions of each of the supporting legs.

4) The location plate was fixed in a central position on the levelling table.

5) The surface to be measured was set on the location plate and a datum plane was established, by levelling as described in section 3 at the three points on the joint surface corresponding to the angular positions of the levelling table legs.

6) The traverse line of the Talylin stylus is made parallel to the selected datum plane according to the following procedure. A trace of the surface profile is taken at an arbitrary angular setting, after which the joint is rotated by 180° and a second trace drawn. If the system had been set up correctly the second trace should follow closely the line of the first plot but in the opposite

direction. Each of the traces will consist of the joint profile inclined at an angle equal to the slope of the Talylin datum line with respect to the datum plane in the joint. Thus if the inclination of the Talylin datum line is adjusted by means of the jacking screws on the instrument suspension until the second trace is a mirror image of the first then the datum line and datum plane in the joint will be parallel. It should be noted that the two traces taken will not follow exactly the same line in the joint as a result of errors in the levelling process. When the datum plane is established in the joint the top plate of the levelling table is inclined to the plane of rotation of the rotary table. Thus the centre line of the assembly above this section is inclined by the same amount, with the result that the location plate and the test joint rotate eccentrically by an amount proportional to their height above the levelling table and approximately proportional to the angle of tilt. In general however this eccentricity is not sufficiently large to make a significant difference to the shape of the two profiles, and therefore does not affect the set up procedure.

Having set up the Talylin, traces of the surface profile of the joint were taken diametrically at angular intervals of $22\frac{1}{2}^{o}$. Brass plugs were fitted to the clamping bolt holes in the joint plates to enable the stylus to traverse these regions. Specimen traces for turned and ground surfaces are shown in fig.(2) the vertical magnification being 10^3.

2.3 .MEASUREMENT OF CONFORMITY

When two irregular surfaces are brought together, initial

contact is necessarily made at only one point. The surfaces will subsequently rotate about that point until a second contact is made. There will then be a further rotation about the line joining the first two contact points until the planforms meet at a third position. Even having established three contact points the joint is not necessarily stable. If the line of action of the closure force does not lie within the three points there will be a rotation about the line joining two contact points which is closest to the line of action of the force. This process will continue until either a stable position is reached or if there is no such position, the joint will adopt a position of limiting stability.

A numerical simulation of this closure process may be performed on digital measurements taken from Talylin traces as follows.

The flatness profile of the joint planforms are represented by measurements of the separation of each of the profiles from an arbitrary datum plane, the measurements being taken at regular angular and radial intervals around the joint. The greater the number of points chosen, the better the representation of the profiles. The datum plane is chosen for each surface so that it does not intersect either planform. If a zero for angular measurement is chosen for each planform then the distance above the datum plane of points in the joint top plate may be denoted by the function $T(r,\theta)$, and the distance below the datum plane of points on the joint base plate by $B(r,\theta)$. If it is then assumed that the two joint plates are aligned such that the datum planes for each profile coincide then the initial separation of the two plates is given by:

$$S(r,\theta) = B(r,\theta) + T(r,\theta) \quad \ldots\ldots\ldots(1)$$

If the planforms are now assumed to approach each other along a line perpendicular to the datum plane, contact will be made when the closure is equal to the minimum initial separation. S_{min}. At this stage the separation of each point is given by:

$$S_1(r,\theta) = S(r,\theta) - S_{min} \quad \ldots\ldots\ldots(2)$$

Dependant on the distribution of flatness errors more than one contact may be made simultaneously. Contact is established when S_1 becomes zero and thus by examining the value for S_1 at each of the points the number of contacts may be determined. It should be noted that at this stage S_1 cannot be negative. If there are three or more contacts then the system must be examined for stability. If there are two contact points then a third contact must be established before stability can be examined. These two situations will be described at a later stage. If there is just a single contact point, co-ordinates (r_1, θ_1), the joint will rotate about the perpendicular to the line joining the contact point to the point of application of the force. The perpendicular distance P of points (r,θ) from this line is :-

$$P(r,\theta) = r_1 - r\cos(\theta-\theta_1) \quad \ldots\ldots\ldots(3)$$

A rotation of ϕ towards the origin, the origin being taken as the point of application of the closure force, will cause a change in separation of $P\sin\phi$ so that the new separations S_2 will be given by :-

$$S_2(r,\theta) = S_1(r,\theta) - (r_1 - r\cos(\theta-\theta_1)\sin\phi \ldots(4)$$

Alternatively the rotation required to cause contact at any point is given by :-

$$\sin\phi_c = \frac{S_1(r,\theta)}{r_1 - r\cos(\theta-\theta_1)} \qquad \ldots\ldots\ldots(5)$$

If the value of $\sin\phi_c$ is computed for each position then discounting the point (r_1,θ_1) and all other points on the line of rotation the minimum positive value of $\sin\phi_c$ will give the angle necessary for the establishment of a second contact point. Having determined the value of $\sin\phi_c$ and hence the position of the second contact point the rotation is effected by substituting this value into equation 4. The total number of contact points is now checked again and if still less than three a second rotation must be performed to establish a third contact. This second rotation will be about the line joining the first contact points. In Cartesian co-ordinates the equation of the line is given by:-

$$y = mx + c \qquad \ldots\ldots\ldots(6)$$

where $m = \frac{y_2-y_1}{x_2-x_1}$ and $c = y_1 - mx_1$

The co-ordinates x and y are related to r and θ by the normal polar to cartesian transformations.

The perpendicular distance d(x,y) of the point (x,y) from the contact line is given by :-

$$d(x,y) = \frac{mx - y + c}{\sqrt{1 + m^2}} \qquad \ldots\ldots\ldots(7)$$

The sign convention adopted is that if c is made positive, then a positive value of d indicates that the point under consideration is on the original side of the line, whereas a negative d indicates that the contact line passes between this point and the origin. As previously stated a rotation ϕ towards the origin about the contact line will cause a change in separation of $d\sin\phi$. As a result of the sign convention for d this separation will be

positive if the rotation is towards the origin and negative if not. As previously the smallest positive rotation ϕ_{min} required to give contact is determined and thus a third contact point is found. The separation of points after the second rotation is given by :-

$$S_3(r,\theta) = S_2(r,\theta) - \frac{(mx(r,\theta) - y(r,\theta) + c)}{\sqrt{1 + m^2}} \quad \ldots.(8)$$

There must now be at least three contact points and it is necessary to examine the stability of the joint. The joint is stable if the centre of loading falls within the area enclosed by the contact points. It has already been assumed that the loading line passes through the origin and it is therefore necessary to compare the distribution of the contacts with respect to the origin. The lines joining the contact points must be established and that closest to the origin selected. The joint will be stable if the 3rd contact point is on the same side of this line as the origin; that is if the distance of the third contact point from the chosen line is positive. If the joint is found to be unstable then a new rotation is made about the contact line closest to the centre of loading so that a new contact is discovered to replace the point not on the line of rotation. This new contact regime is tested for stability in the same way as before, and if necessary further rotations must be made until a stable position is found.

Once stable contact has been established the application of preload to the joint will cause an increase in contact area by two methods. The original contact points will be compressed allowing further high regions to touch, and also since it is most unlikely that the original contacts lie

directly under the points of application of preload there will be bending forces operating on the joint plates. Further contacts might therefore be produced from bending deformations. The prediction of such bending deformations is beyond the scope of this work and it is assumed that a reasonable estimate of contour area as a function of joint displacement can be obtained by incrementally decreasing the separation of all points with the joint frame and noting the proportion of points at each stage for which the separation is zero or less.

The above procedure was applied to two annular joints; one formed from planforms with ground surfaces and the other from planforms with turned surfaces. Traces of the flatness profiles of the joint were taken as described and digital readings were taken from these traces at discrete intervals. Measurements were recorded at angular increments of $22\frac{1}{2}^{o}$ and radial increments of 4mm. A computer programme written to process these results is reproduced in Appendix 2. The inner and outer diameters of the annuli were 60 mm and 100mm; each digital reading therefore represented an area of approximately $65mm^2$. This area is not large when compared to the wavelengths of flatness errors anticipated; it is however necessary, if any meaning is to be given to the results obtained; to determine how representative of such an area any point is likely to be.

The method of predicting joint closure assumed that the surface profile followed a straight line between any two adjacent measuring points. The quality of representation of an incremental area by a point can therefore be examined by measuring the departure from such linearity. A closer

mapping was therefore made of four segments on the test joint surfaces each segment being 4mm wide and subtending an angle of 22°. Readings were taken at 2° and 0.5mm intervals. Using the method of least squares the best linear fit for the variation in the height of the surface was determined for each radial and angular sweep. The standard deviations of points on each sweep from the best fit straight line for that sweep were ten determined. The mean value of these deviations and their standard deviation were computed. The values obtained are shown in fig.3. If it is assumed that the standard deviations of points on the surface from a line on that surface from a normal distribution then it is known that 97.5% of deviations fall below a value two standard deviations above the mean of the deviations. Thus for the turned joint in 97.5% of cases the standard deviation of points from a radial line is less than 1.5μm and in the angular direction 1.51μm. The corresponding figures for the ground joint are in the radial direction 0.21μmand in the angular direction 0.13μm. When compared with the values of joint closure for 100% contour area (fig.4) it is seen that the magnitude of these standard deviations is approximately 10% of the total joint closure for both turned and ground joints.

Thus it may be concluded that although it is unlikely that the point chosen to represent an incremental area is in fact the point in that area which will first make contact, and as such the measured changes in contour area for small deflections will not be accurate; the effect on contour area measured for large deflections will not be significant.

The values of contour area measured are shown in fig.(4).

Apart from the obvious differences in the scale of the flatness errors for the two types of surface, the general trends of the two curves are very similar. The contour area increases initially at a slow rate; there is then a fairly rapid rise as the bulk of the surface material comes within contact zones followed by a period in which the conformity decreases as the contour area approaches the apparent area of the joint.

If it is assumed that the ultimate stiffness of the joint is proportional to the contour area the form of the variation in stiffness with applied load can be obtained.

Since $k = \frac{dP}{dx}$ it follows that

$$P = \int k \, dx$$

Thus by integrating the curves of fig.(4) with respect to the joint displacement the shape of the maximum stiffness which can be obtained from a smooth surfaced joint can be obtained as a function of applied load. Unless an absolute value is assigned to the joint stiffness the integration cannot be dimensioned and for this reason no scale has been assigned to the load axis; nevertheless comparisons can be drawn between the two curves. There is a striking similarity between the form of the 'synthetic' curves (fig.(5)) showing the relationship between joint load and stiffness for joints with flatness errors, and those produced by Day for joints with roughness errors. This tends to indicate that the effects of form errors on joint stiffness are the same as the effects of surface roughness but on a different scale; a result not altogether surprising when the relationship between roughness and flatness is

re-examined. The essential difference between flatness and roughness errors is the wavelength of the surface irregularity and on average the distribution of material, as a function of height, within a single cycle is likely to adopt a similar pattern whatever the wavelength. Thus, should a surface contain a single wavelength of flatness error, or should its dimensions be so large as to contain a number of wavelengths, then the distribution of material on the surface, as a function of height will adopt that standard pattern. It is therefore to be expected that the form of variation in the surface parameters η_1 and η_2 with joint deflection should adopt similar forms, albeit over different magnitudes of deflection.

2.4 SUMMARY

A method has been described for experimentally measuring the contour area of metal to metal joints and a regular form of variation in contour area with joint deflection proposed. It is suggested that a series of tests be performed to determine whether a parameter describing the effects of surface flatness on joint performance, similar to the 'm' value which describes the effects of surface roughness, exists, be it a function of the type of machining, or particular machine used to produce the surface. The effects of surface roughness and flatness could then be combined in a single parameter which could be used as an indication of the joint strength.

Chapter 3

EXPERIMENTAL MEASUREMENTS ON THE DYNAMIC MOTION OF ANNULAR BOLTED JOINTS

3.1 EXPERIMENTAL APPARATUS

An experimental rig was designed for the measurement of the small dynamic motions of a single metal to metal joint, and the associated phase shift of this motion with respect to the applied force. From these readings it was hoped to determine a measure of the stiffness and damping within the joint.

A general view of the mechanical apparatus is shown in fig.(6). The test joint was comprised of the contacting surfaces of the 'joint top plate', and the 'joint base plate'. These plates were manufactured in mild steel. The nominal contact region was annular, inner radius 30mm. and outer radius 50mm., giving an apparent contact area of $50.3 \times 10^2 mm^2$ to the joint. This annular planform shape was chosen on two counts. If the dynamic load is applied centrally to the joint top plate, and the width of the annulus is not large compared with its diameter then it may be assumed that the applied load will be distributed evenly over the joint surface. Furthermore the annular shape lends angular symmetry to the system thereby simplifying any mathematical analysis of the surface region. The joint top plate, fig.(7), was circular, being clamped to the base plate with four evenly spaced 6mm. bolts. Centrally situated on the upper surface of the top plate was a 6mm. stud which was used to connect a Kistler force link to the plate. Around the perimeter of the top plate were eight holes fitted to take Wayne-Kerr capacitive displacement transducers. The Wayne-Kerr displacement measuring system measures the capacitance of the gap between the face of the transducer

and the face to which it is brought into proximity; this capacitance is proportional to the separation pf the transducer and the test surface. Thus if the probe is rigidly clamped to the joint top plate with its face in proximity with the joint base plate the relative motion between these plates, i.e. the joint motion may be measured. The transducer is formed from a pair of concentric electrodes across which is a polarization voltage. These electrodes are surrounded by an insulated guard ring which allows the transducer to be clamped to the test structure without affecting the polarization voltage. Since it measures the total capacity of the gap between the transducer and the test surface, the system gives the mean separation of the joint in that region. When fitted with a probe type MA1 the maximum measuring range of the system is 0.025mm.

If the probe is not held perpendicular to the surface it is possible that some part of the transducer face may make contact before the mean separation comes within the operating range of the instrument. When the probe touches the measuring surface not only will there be unwanted mechanical interaction between the probe and the surface but there may also be an electrical short circuit across the transducer face. The system cannot operate under these conditions. The transducer is approximately 8mm. in diameter and thus assuming that it is a tight fit in the mounting hole, and that the transducer face and the measuring surface are flat, the hole must be perpendicular to the measuring surface to within 22' to ensure that the system is adequately set up. If the probe us tilted at an angle greater than this then it will be touching the joint base plate before the

mean separation of transducer face and the measuring surface comes within the range of the instrument. Considerable care was taken therefore during the manufacture of the top plate to ensure that close tolerances were maintained on the mounting hole diameter and on the perpendicularity of this hole to the joint surface. The displacement transducer was lightly clamped in position by means of a grub screw. A single transducer was used being moved to various positions during different parts of the tests. The centre of the clamping screw was 7mm above joint surface; the normal stiffness of the material of the joint top plate between the joint surface and the grub screw can therefore be calculated to be 149MN/mm. This is very much greater than joint stiffnesses measured by other researchers so that it is unlikely that any corrections need be made to results of joint motions to account for material deflections.

The joint base plate, fig.(8), consists of a flat circular plate with a raised annulus. The inner portion of this annulus mates with the joint top plate to form the test joint. The outer section of the annulus is the measuring surface for the displacement transducer. The two sections are separated by a rectangular groove. The purpose of this groove, in combination with the step in the profile of the top plate is to prevent any lubricant which may have been introduced into the test joint from seeping under the displacement probe. The presence of oil in the gap between the probe and the measuring face would change the capacitance of the gap thereby giving a false indication of the joint motion.

The joint base plate is rigidly clamped to a large

concrete block which acts as a base for the mechanical test structure. The clamping load between the joint assembly and the concrete block was provided by eight 10mm bolts giving an interfacial load approximately 30,000 kg. This compares with a maximum applied preload of 4,000 kg. or the test joint. Thus assuming that the joint contact has not reached a saturation level and that the surface quality of the base plate/block connection is not very much worse than that of the test joint then the motion of the test joint will not be greatly affected by the base plate/concrete block connection. In order to mainain a degree of isolation from the laboratory floor the block was mounted on a ribbed rubber mat. It is an unfortunate property of many of the materials used as vibration isolating mounts that their elastic moduli increase with the applied stress. Thus when a heavy mass is supported on such a material it is very difficult to obtain a sufficiently low mounting stiffness to give a low natural frequency and hence good isolation of low frequencies. The natural frequency of the concrete block on the ribbed rubber mat was measured at 67Hz. and from a decay curve the damping in this system was found to be 4.8×10^{4} Nsec/m. The mass of the block was 520 kg. By considering the test joint and concrete block as a two degree of freedom system it can be shown that for frequencies above 150 Hz. the mounting structure will have little effect on the performance of the test joint.

With reference to the formulae derived by McLeod and Bishop (23), the first natural frequencies of the joint top and base plates were estimated to be 890 Hz. and 3400 Hz.. In order to stay well below these bending resonances therefore,

the upper limiting frequency for the forced exitation of the joint was taken as 600 Hz.

A harmonic force was supplied to the joint from an electromagnetic vibrator which was slung from an overhead gantry. The vibrator was supported on steel wires which were passed over pulleys attached to the gantry, the equilibrium of the system being maintained by counterbalance weights. This method of suspension was chosen to enable easy movement of the vibrator during the setting up of the rig, and to ensure that there should be no preload on the vibrator table whilst it was in operation. The force generated in the vibrator was transmitted to the joint via a pushrod which was connected in turn to the Kistler load cell. To avoid resonance problems in the push rod its length was kept as short as possible, the shortness being determined by the length necessary to allow access for the displacement probes.

The electronic equipment used to generate the harmonic excitation on the joint and to measure the subsequent response is shown in diagramatic form in fig.(9). A sinusoidal wave was generated in the signal generator (1) and was then fed into a control amplifier (2). The output of the control amplifier was boosted in the power amplifier (3) so that the signal had sufficient force to drive the vibration generator (4). The input force level to the test joint was measured by a piezo-electric force transducer (5), and its associated charge amplifier (7). With switches A open, and B closed, the output of the charge amplifier was fed directly into the control amplifier thereby completing a force control loop. The control amplifier compared the input force level to the joint indicated by the force

transducer with a reference signal provided by the signal generator and automatically made adjustments to ensure that the force input remained constant as the frequency range was swept. A constant force input was useful on two counts. Firstly the effects of a non-linear response to a force input of varying magnitude were eliminated, and secondly the calculation of joint receptance was much simplified. If the force input is not held constant then to determine the joint receptance it is necessary to measure continuously the force input, the resultant displacement and the relative phase between these parameters. The receptance is then determined by the ratio of displacement per unit force. If however the force level is held constant then it is only necessary to measure the displacement level and the phase relationship between force and displacement. The receptance is then obtained by dividing the displacement by a constant and as such the work involved is much reduced.

The relative motion between the joint plates was measured using a capacitive displacement transducer (6) and its associated measuring equipment and demodulating filter (11) and (12). The displacements to be measured were sufficiently small that the output from the distance meter was inadequate in itself to drive the recording equipment. Further amplification was therefore supplied in the measuring amplifier (10) and the tracking filter (9). The tracking filter had a bandwidth of 5 Hz. and was automatically tuned via a signal from the signal generator so that the centre frequency of the pass band was equal to the excitation frequency. A dc. signal proportional to the magnitude of the joint displacement was available from the tracking

filter and this could be fed into the y-channel of an x-y plotter,(14). A dc. signal proportional to frequency, taken from the signal generator was used to drive the x scale of the plotter. The signal generator had an automatic sweep facility which enabled the excitation frequency to be varied at a pre-set rate between upper and lower limits. It was therefore possible to record automatically graphs of joint motion amplitude against frequency. An ac. signal proportional to joint displacement was also available from the tracking filter and this was fed into the phasemeter (13). The driving signal from the generator was also supplied to the phasemeter and a dc. output proportional to the phase difference between the signals was available to drive the plotter. The phase lag so measured consisted of the electrical delay between the initial production of the harmonic signal in the signal generator and the force generation in the vibration generator; the mechanical delay between the application of the force to the joint and the response in the form of a joint displacement; and the further electrical delay in the distance meter and subsequent amplifiers. Thus if the mechanical phase shift in the joint is to be measured the electrical phase shifts through the various instruments must be eliminated (or measured). With switches B open and A closed the signal from the force transducer was fed through the measuring amplifier and tracking filter so that the phase of the force signal relative to the output of the sweep oscillator could be measured. To ensure that the force level remained constant during the recording of both phase measurements the gain on the charge amplifier was reduced by an amount equivalent to the increased gain in the control loop caused by the introduction of the measuring

amplifier. It was found that provided the gain settings on the measuring amplifier were such that the input signal caused a visible meter deflection, and that the amplifier was not overloaded then the phase shift through the instrument was not dependant on the gain settings. Day showed that charge amplifiers may be used over a wide range of gain settings without incurring a significant phase shift. The two plots of the phase shifts of the force and displacement channels relative to the signal generator will therefore be subject to the same instrumental phase shifts save for the shift through the distance and vibration meter and the demodulating filter. If then these two readings are subtracted the majority of the instrumental phase shifts will be eliminated; the difference between the curves will be the summation of the mechanical phase lag in the joint plus the electrical delay in the distance meter and demodulating filter. Thus if the distance meter and demodulating filter are calibrated for phase the mechanical phase shift through the joint can be measured. Day (28) adapted a position sensitive photocell designed by Sydenham (24) to achieve such a phase calibration. The method was also used in this instance; the results are shown in fig.(10).

3.2 AMPLITUDE CALIBRATION OF DISTANCE METER

A block diagram of the equipment used in the amplitude calibration of the displacement measuring system is shown in fig.(11). A vibration generator (3) driven from a signal generator (1), through a power amplifier (2) was used to provide a unidirectional vibrating surface. The vibration generator was mounted on the glass bed of an S.I.P. Universal Measuring Instrument. The S.I.P. is

essentially a high quality travelling microscope with slides in three directions and scales reading to an accuracy of ± 0.5 m. A stroboscopic light (5) was placed beneath the glass table of the S.I.P. so that when looking down the microscope it illuminated the edge of the moving vibrator table. The stroboscope was powered by a Dawe Vari-phase Strobe Unit (4) which was in turn driven by the signal generator. Thus the flashing of the stroboscope was synchronised to the motion of the vibrator table so that the latter appeared stationary. The Vari-phase unit contained a manually operable delay circuit which enabled the timing of the stroboscope flash to be adjusted in relation to the phasing of the input signal from the signal generator. The image position of the vibrating generator table could therefore be moved between extreme positions so that the dynamic motion of the table could be statically measured on the S.I.P.

The displacement transducer was clamped to a vee-block and set in position to measure the movement of the vibrator table. The electrical output from the distance and vibration meter was compared with the motion measured mechanically on the S.I.P. By altering the excitation frequency and the amplitude of the motion voltage output per unit displacement and the frequency response of the system were determined. The results obtained are shown in figs.(10a) and (12b).

The output from the distance meter is in the form of a full wave rectified 50 kHz. signal which after passing through a low pass demodulating filter is converted to a dc. signal proportional to the mean separation of the probe and the test object onto which is superimposed the vibration waveform. The output from the demodulating filter is easily

measured with a digital voltmeter.

The transducer used during the dynamic calibration for both phase and amplitude was type MC1 with a maximum measuring range of 0.25 mm. as compared with the probe type MA1, maximum range 0.025 mm. which was used during the measurement of dynamic joint motions. The only effective difference between the two types of probe is however in the physical dimensions of their electrodes. The greater the separation of the probe and the test object the larger the area of the electrodes required to maintain the same capacitance in the gap. When operating under similar conditions referred to their maximum operating range different probes have nominally identical capacities so that although physically different the electrical nature of the distance and vibration meter is unaltered. A frequency response derived using one type of transducer is therefore equally applicable to all other sizes, so that having established this frequency response and the dynamic range of the instrument using one probe all that is required to obtain a calibration for other transducers is the static response.

To measure the static response of the distance meter the displacement transducer was clamped to the vertical slide of the S.I.P. The transducer was then lowered towards a steel parallel block mounted on the S.I.P. table until a reading was obtained on the distance meter display. The transducer was then moved further towards the block and the d.c. component of the demodulating filter output was plotted against the movement measured on the S.I.P. slide. The results of the static calibration are shown in fig.(12a).

It can be seen from the calibration curves that a linear frequency response was obtained between 100 and 700 Hz

and that the electrical output of the displacement measuring system rises linearly with the mechanical displacement amplitude. The dynamic calibration of the system with transducer type MC1 shows an output of 3.7 mv/μm and the static calibration 3.8 mv/μm. This difference is not significant however as can be seen from the spread of points on the curves of fig.(12) so that the dynamic and static responses may be considered equal. Fig.(10b) shows that there is a small phase lag through the distance meter and a larger delay in the demodulating filter. The total phase lag through the measuring system increases with frequency to a value of 4.8 deg. at 650 Hz.

During the actual measurements of joint motions the output of the Wayne-Kerr vibration measuring system was fed into a measuring amplifier and it was found that although the input impedance of this amplifier was nominally 1 MΩ it was not sufficiently large compared with the output impedance of the demodulating filter, nominally 24 kΩ, to avoid a slight loading of the output circuits. This loading was measured to be 3% and the measured calibration figures were adjusted accordingly.

3.3 THE MEASUREMENT OF BOLT CLAMPING FORCES

It has long been appreciated that the clamping load applied to a joint is of prime importance in determining joint performance; and thus in a study of the properties of bolted joints it is essential that the bolt loads should be measured accurately. Furthermore if the information derived from such an investigation is to be of use to industry then it is necessary that a simple means be available to tighten bolts to a required degree of accuracy. There are

two methods in common commercial use for tightening bolts to a predetermined load. The first is to measure the extension of the bolt using a screw micrometer and knowing the properties of the bolt material convert the strain reading into a measure of the applied load. This method suffers from numerous disadvantages. It is not particularly accurate, especially for small bolts; it necessitates free access to both ends of the bolt; and it is a time consuming and therefore expensive operation. The more usual method is to tighten the nut to a preset torque by using a torque wrench and to assume a fixed load/torque relationship for the particular type of bolt to enable the applied load to be calculated. Although such relationships are commonly quoted little attention is given to the accuracy of the method. A simple investigation was therefore performed to establish the suitability of applied torque as a measure of bolt load.

3.4 DERIVATION OF THE LOAD/TORQUE RELATIONSHIP FOR BOLTS

There are two contact regions which provide frictional resistance to the tightening of a nut on a bolt; the first being the interface between the threads of the nut and bolt, and the second is either the interface between the nut and washer, or that between the washer and the clamped object dependant on which of these surfaces slip occurs. It should be noted that the loading distribution at these interfaces is non-uniform both as a result of the deformation of components underload and of errors in their production.

Consider an incremental height of bolt thread opened out to form a wedge, fig.(13). The tightening of the nut on the thread then becomes analogous to forcing a block up

the wedge against friction and the proportion of the bolt load carried by that element of thread. Since the thread is vee shaped the normal reaction on the thread is inclined to an angle α to the plane of the developed wedge, 2α being the included angle of the thread. If N is the normal reaction the vertical component acting on the wedge will be $N\cos\alpha$. The frictional force acting on the wedge is however dependant on the total normal reaction and is therefore given by N. The forces acting on the element are shown in fig.(13).

Resolving these forces vertically and horizontally gives:-

$$dP_1 - \mu_1 N\cos\theta - N\cos\alpha \sin\theta = 0 \quad \ldots\ldots(9)$$

$$dF_1 + \mu_1 N\sin\theta - N\cos\alpha \cos\theta = 0$$

eliminating the normal reaction gives

$$\frac{dP}{dF_1} = \frac{\cos\alpha \tan\theta + \mu_1}{\cos\alpha - \mu_1 \tan\theta} \quad \ldots\ldots(10)$$

which when integrated over the complete height of the thread gives

$$P = \left\{\frac{\cos\alpha \tan\theta + \mu_1}{\cos\alpha - \mu_1 \tan\theta}\right\} F_1 \quad \ldots\ldots(11)$$

Assuming that this force acts totally at the mean thread radius the torque required to overcome thread resistance is:-

$$T_1 = Pr_i = F_1 r_i \left\{\frac{\cos\alpha \tan\theta + \mu_1}{\cos\alpha - \mu_1 \tan\theta}\right\} \ldots\ldots(12)$$

If the pressure distribution under the nut is described as a function of radius by Q(r) then the load carried by an annular element under the nut is given by:-

$$dF_2 = 2\pi r\, Q(r)dr \quad \ldots\ldots\ldots(13)$$

and the resistive torque supplied by the element is

$$dT_2 = 2\pi r^2 \mu_2 Q(r) dr \qquad \ldots\ldots\ldots(14)$$

and thus the total resistive torque at the nut, washer clamped object interface is:-

$$T_2 = 2\pi \int_{r_i}^{r_o} r^2 \mu_2 Q(r) dr \qquad \ldots\ldots\ldots(15)$$

if it is assumed that $Q(r) = F.D.(r)$ ie. that the spatial distribution of the load under the nut is not affected by the value of the load, then:-

$$T_2 = 2\pi F \int_{r_i}^{r_o} r^2 \mu_2 D(r) dr \qquad \ldots\ldots\ldots(16)$$

and hence the total resistive torque is equal to

$$T = T_1 + T_2$$

$$= F \left\{ \frac{\cos\alpha \tan\theta + \mu_1}{\cos\alpha - \mu_1 \tan\theta} + 2\pi \int_{r_i}^{r_o} r^2 \mu_2 D(r) dr \right\} \ldots(17)$$

or $T = F.S$

where $$S = \frac{\cos\alpha \tan\theta + \mu_1}{\cos\alpha - \mu_1 \tan\theta} + 2\pi \int_{r_i}^{r_o} r^2 \mu_2 D(r) dr$$

Thus we have the linear relationship between bolt load and applied torque commonly assumed in industry. Various tables and formulae are available from manufactures for the derivation of the constant of proportionality S.

In practise the coefficient of friction between two surfaces is not a constant but increases with interfacial pressure. There may also be a change in the frictional forces as a result of thread damage during the loading process. Thus μ_1 and μ_2 are functions of the bolt load

and are subject to a certain amount of random fluctuation. The simple load toque relationship therefore becomes non linear and is subject to scatter. An increase in the coefficient of friction causes a decrease in the gradient of the load torque curve so that the loading line follows the trend shown in fig.(14). There is usually a flattening of the nut during the loading cycle so that the spatial distribution of load also becomes a function of the applied load and a further non linearity is introduced into equation (7). In general as the bolt load increases the effective loading radius r_e* decreases and thus the resistive torque per unit bolt load also decreases. This leads to an increase in the gradient of the load torque curve as the bolt load increases. It is therefore seen that the combined effects of changes in friction coefficients and in loading distributions can cause the load torque line to move either above or below the straight line predicted by simple theory. The size of this divergence and the amount of random scatter will dictate the accuracy of using applied torque as a measure of bolt load.

3.5 EXPERIMENTAL INVESTIGATION OF THE TORQUE LOAD CHARACTERISTICS OF BOLTS

The apparatus used to measure the relationship between the load on a bolt and the applied orque is shown in fig.(15). The test bolt was clamped through a rectangular mild steel block. The surfaces on the block to which the bolt was clamped were ground in order to obtain an easily maintained controlled surface. The bolt head was restrained whilst load was applied to the nut so as to ensure that slip occurred in the region of the nut rather than at the bolthead. The bolt load was measured using a Kistler piezoelectric load

* r_e defined as $\frac{2\pi}{F}\int_{R_i}^{R_o} Q(r,F)\,dr$

washer which was fitted under the bolthead. A spherical ground washer was used in conjunction with the load cell to ensure that the bolt did not bend during loading. The torque wrenches used to apply load were of the ratchet type and on calibration were found to be repeatably accurate to within 3% of maximum applicable torque.

Tests were performed on 6mm and 12mm isometric nuts and bolts with rolled threads. The 12mm bolts were tested in the 'as from stores' condition, with oil lubrication, and in the dry state having been cleaned with acetone. The 6mm bolts were tested in the oil lubricated condition alone. A total of eight 6mm and ten 12mm bolts were tested each bolt being subjected to six loading cycles. On each cycle the bolts were loaded to just below their yield point. The maximum applied torques were 11 kgm for 12mm bolts and 1.2 kgm for the 6mm bolts. Least squares curve fitting techniques were used to determine the best fit straight line and the best fit second order curve through the experimental points. Since it is known that zero torque produces zero load the condition was made that the curves passed through the origin ie. curves of the form $P = aT$ and $P = bT^2 + cT$ were fitted. The standard deviations of the experimental points from these lines was also calculated. In order to determine the causes of scatter in the results the readings were processed in a variety of groups. First a single curve was fitted to the results from all the 6mm bolts. Secondly curves were fitted to the readings taken from the aggregate loadings on each individual 6mm bolt. By comparing the mean of the standard deviations obtained from the individual bolts with the overall mean the effect

of differences between bolts was assessed. Finally each loading cycle performed on a particular bolt was analysed separately and a mean standard deviation again calculated. From this value an estimate of the effect of differences between various loading cycles on the accuracy of torque loading can be made. The constants and standard deviations calculated for each group are shown in fig.(16). Fig.(17) shows the aggregate readings taken on 6mm. bolts and the best fit linear and second order curves.

Inspection of the results shows that whereas the values of standard deviation calculated for single loading curves show a very marked decrease when taking the quadratic rather than the linear curve fit, this decrease is not nearly so marked when considering the aggregate results. Thus although there may be a predominant non-linear trend in a particular loading cycle this trend is not repeatable for all bolts and that on average individual torque load curves are fairly evenly distributed about a mean straight line. It is also seen that there is little change in the standard deviation of results obtained by combining all the loading cycles from a particular bolt compared with the overall deviation. It may therefore be concluded that the scatter of results comes from difference between individual loading cycles of bolts rather than from differences between the bolts themselves.

Oiling the bolts prior to testing is seen to have little effect on the shape of the load torque curve when compared to the bolts in the 'as from stores' condition. This probably results from the fact that when taken from stores the nuts and bolts are covered in a thin film of protective oil. At the very high pressures prevalent in

bolt clamping the majority of any interfacial lubricant is squeezed from between the surfaces so that there is finally little difference between the effects of intended lubrication and residual protective oiling.

It was found that degreasing the nut, bolt and washer with acetone before loading led to a very rapid deterioration of the threads and the underside of the nut; these tests were therefore discontinued.

In an attempt to decrease the scatter of results obtained a series of tests were performed on bolts on which the mating surfaces of the nut and washer had been ground. It is seen that improving the surface quality of these regions does little to improve the repeatability of the loading curves showing that the major source of variance is in the threads. It is possible that grinding the nut and bolt threads might improve performance but it is considered unlikely that the improvement would justify the expense. The grinding of bolt threads was once a common industrial practise but has become uneconomic as techniques of thread rolling have improved. Ground bolts now tend to be used only in specialist applications. The internal grinding of nut threads is extremely difficult and very costly.

For both sizes of bolt tested the aggregate standard deviations were of the order of 10% of the working load of the bolt, (taking the working load to be 75% of the yield load). This is far outside the accuracy required for laboratory testing, it is however a reasonable limit for normal industrial purposes.

The method of measuring bolt loads finally chosen was to place a piezo electric load washer under each nut and

by feeding the signal from the load cell to a digital voltmeter via a charge amplifier obtain a reading of the bolt load. This method of load measurement has an advantage over simple torque loading quite apart from the increased sensitivity. As the load on each bolt is increased then a proportion of the load carried by other bolts is relieved. When monitoring each bolt individually this effect is easy to see, and compensation can be made. When using a torque wrench however this problem can only be overcome by repeated application of torque and particularly with the ratchet type wrench there is a danger of a shock overload as the ratchet is repeatedly broken.

3.6 DESCRIPTION OF DYNAMIC TESTS PERFORMED ON BOLTED JOINTS

After a number of preparatory tests four test joints were prepared, two with ground and two with turned surfaces. The surface roughnesses of the ground surfaces were between 0.065μm and 0.079μm CLA and those of the turned joint surfaces between 1.52μm and 1.7μm CLA. These values are typical for such surfaces. Before each test the joints were carefully cleaned with a degreasing agent and wiped with a leather cloth to remove any dirt particles from the contact regions. Tests were performed in this dry state and with oil lubrication. The oil, Duckams Zircon 6 a typical machine tool oil, chosen from Ref.3, was applied to the joint surface on the base plate before the joint components were clamped together. This ensured a uniform coverage of the lubricant.

Having clamped the test joint in position on the test rig a harmonic force of 20N rms was applied from the vibration generator and phase and displacement readings were taken at each of the eight measuring positions as the frequency of excitation was varied between 100 and 600 Hz.

Chapter 4

RESULTS FROM DYNAMIC JOINT TESTING

4.1 EXPERIMENTAL RESULTS

For the complete description of the dynamic motion of a structure it is necessary to know the amplitude of motion and the phase relationship between the forcing function and the displacement at every point on the structure. For the comparison of two systems, a single parameter, or a small group of parameters is required which is representative of the motion, and which can be determined for both systems.

It is the function of the vibration engineer to reduce overall vibration levels in mechanical systems not only to improve operational accuracy and to reduce structural fatigue but also to minimise noise generation and operator discomfort. The root mean square vibration amplitude averaged across the surface of a joint gives a simplified but convenient measure of overall joint motion and has therefore been chosen as a starting point for describing joint performance. In computing rms flexibility no account is taken of the phase relationships between different sections of the joint and as such there is no differentiation between the normal motion and any bending which may be present, nor is any indication given as to the level of energy dissipation, or damping in the joint.

Plots of rms flexibility against bolt preload are shown in figs.(18) and (19) for joints with turned and ground surfaces in the dry state and with oil lubrication. The frequency of the forced excitation is in each case 200 Hz. As would be expected for dry joints there is a rapid drop in joint vibration amplitudes as the bolt preload is

increased from zero. The joint normal stiffness is dependant upon the actual contact between the two mating surfaces. When the joint planforms are first brought together contact occurs only at a smaller number of relatively large asperities; when preload is applied these asperities are compressed to enable contact to be made between smaller peaks. Thus as the preload increases the real contact area increases and the joint stiffness becomes greater. Furthermore since the load required to compress the existing contacting asperities is dependant on the number of mating points it is to be expected that the rate of increase of stiffness with load falls with rising load. The joint flexibility will therefore exhibit a very rapid drop as the preload increases from zero, as is seen in the results, but the rate of decline in flexibility lessens as the load is further increased.

It is an unexpected feature of the results obtained that there is a tendency for the flexibility to increase at high preloads. This cannot be explained in terms of the previous work performed on structural joints described in the first chapter and will be discussed at a later stage.

The most striking observation made on the curves of rms flexibility is that except at very low preloads, the turned joints exhibit substantially less motion than do those with ground surfaces. This is contrary to all expectation as previous research has shown that the normal stiffness of joints increases with the quality of the surface finish of the mating components. At this stage it is important to note that results were taken from two joints with ground surfaces and from two joints with turned surfaces

and that as is seen in figs.(18) and (19) the results from joints of similar types are in close agreement. This confirms that the difference between the results from the turned and ground joints is a function of the surface finish rather than of any random influence.

At low preloads the introduction of oil into the test joint gives rise to a marked fall in the measured flexibility relative to the dry state. This improvement in joint performance decreases as the bolt load rises and at high preloads there is a small but repeatable deterioration in the oiled joint compared with the dry. When oil is introduced into a joint it rests in the cavities formed between the mating peaks on the joint planforms. When the joint is subsequently excited the oil provides a resistance to motion. Dependant on the degree of captivity of the oil, ie. the restriction imposed on the movement of oil in the joint interface regions by the contacting asperities, this resistance may be in the form of viscous damping, as in a squeeze film, or it may be elastic in nature, resulting from the finite bulk compressibility of the oil.

It is proposed that the oil forms a link between the joint planforms which is stiff compared with the air which was present in the dry case. As the joint preload is increased the oil is squeezed from between the planforms and the small pockets which gave support to the joint at low preloads are replaced by direct metal to metal contact. Hence as the stiffness of the joint is increased through enlargement of the real contact areas the oil cavities are eliminated so that the contribution of any interfacial lubricant to joint stiffness diminished.

It is seen that for the turned joints at high preloads,

the introduction of oil into the joint causes an increase in flexibility. This also occurs in the case of ground joints but to a far lesser extent. Again the reasons for this unusual behaviour are not immediately obvious and are discussed at a later stage.

In summary, the graphs of rms. flexibility against applied preload reveal three unexpected features which must be accounted for in any theory relating to the dynamics of bolted joints.

1) Improving the surface quality of the mating planforms leads to an increase in the measured flexibility of the joint.
2) At high preloads, increasing the applied preload causes a small but significant rise in the measured flexibility.
3) At high preloads the introduction of an interfacial oil film increases the measured flexibility.

As previously stated, the rms joint flexibility gives no indication of the distribution of motion in the joint, nor does it involve the phase relationship between the force and displacement at the various measuring positions around the joint. Figs. (20) to (23) show the variation in flexibility at different positions on the joint for different bolt preloads. Both the magnitude of the flexibility and the phase lag between the force and displacement are shown for a turned and for a ground joint.

It can be seen that not only does the flexibility very in magnitude around the joint, but that in many cases some segments of the joint are moving in antiphase with respect to the remainder. In the preload range of 800 kg to 4000 kg a distinct trend is apparent in the phase of the

motion of the turned joint in the dry state, fig.(20). At a preload of 800 kg the joint displacement is totally out of phase with the exciting force; as the preload is increased the motion of some sections of the joint undergo a 180° phase shift and start to oscillate in phase with the exciting force whilst the amplitude of motion decreases. The proportion of the joint oscillating in phase increases as the load becomes larger until at the maximum preload of 4000 kg there is only one of the eight measuring positions at which the joint motion is still out of phase with the applied force. It is interesting to note that the region of preload on the plots of rms flexibility in which the measured flexibility reaches a minimum corresponds well to the preload at which the joint motion undergoes a 180° phase shift with respect to the harmonic exciting force.

In the majority of the measurements taken the phase lag between the displacement at the measuring position and the force input was very close to either 0 or 180°, so that adjacent points were moving either in-phase or directly in phase opposition. In the case of the turned oiled joints however there was no such clear cut relationship between the motion of the different regions within the joint. The phase lag between the joint displacement and the force input varied over a wide range of values. This phase variation between adjacent measuring positions indicated that the peak deflection of the points within the joint planforms did not occur at the same time. When one point was at a maximum deflection adjacent points were either approaching or had just passed this state. This means that a point of maximum joint motion moved around the joint annulus;

i.e. that a travelling wave existed within the joint. For such a travelling wave to have been present it is necessary that bending of the planforms occurred and it is therefore seen that planform bending can form a major part of joint motion. Since a static phase measurement was measured at each position this travelling wave must have been repetitive over one cycle of the joint. If the wavelength of the travelling wave was not such that the wave repeated after each rotation of the joint then a constant variation in the phase lag at each position would have been seen.

The form of motion in which different sections of the same joint are moving in antiphase requires either that the joint is rocking with an amplitude greater than the normal motion or that bending of the planforms occur on a considerable scale. Rocking in the joint can be represented by the expression

$$D_1 \cos\phi + D_2 \sin\phi \qquad \ldots\ldots\ldots(18)$$

where ϕ is the angular position in the joint.

By subtracting the normal motion of the joint from each of the eight measurements taken around the joint, and fitting a curve of the form (18) to the resulting data the degree of rocking in the joint can be assessed.

The normal motion was defined as the average displacement across the joint, due consideration being given to the temporal phase of this displacement with respect to the applied force. This is a true average as opposed to the average of the rectified results given previously. Thus the amplitude of normal motion is given by:

$$A = A_i^2 + A_q^2$$

where $$A_i = \frac{1}{8} \sum_{n=1}^{8} A_n \cos\theta_n$$

and $$A_q = \frac{1}{8} \sum_{n=1}^{8} A_n \sin\theta_n$$

A_n refers to the amplitude of motion at position n, and θ_n the temporal phase lag of the motion at this position. A_i and A_q are therefore the means of the in-phase and quadrature components of the joint displacement. The effective phase lag of the normal motion was taken as:

$$\theta = \tan^{-1} \frac{A_q}{A_i}$$

Now consider the work done in the joint. Assume that the dynamic load is evenly distributed around the joint annulus.and that each measuring point is representative of one eigth of the total joint. The harmonic force acting on each segment of the joint is then:

$\frac{F}{8}$ sin wt the forcing function being Fsin wt

The component of velocity in phase with this force is

$$WA_n \sin\theta_n \sin wt$$

And thus the work done per cycle of excitation is given by ΔE where:

$$\Delta E = \int_0^{2\pi/w} \frac{F}{8} WA_n \sin\theta_n \sin^2 wt \, dt$$

$$= \frac{\pi}{8} F A_n \sin\theta_n$$

The total work done in the joint is therefore:

$$E = \frac{\pi}{8} F \sum A_n \sin\theta_n$$

but $$\sum A_n \sin\theta_n = 8 A_{qn} = 8 A \sin\theta$$

thus

$$E = \pi AF\sin\theta$$

It is therefore seen that provided that the reading taken at each measuring position is representative of the motion within a one eighth segment of the joint then the energy dissipated in the joint can be calculated simply from the amplitude and phase of the normal motion as defined.

The definition of normal vibration across the joint and the equating of the energy dissipated by this motion to the total energy lost in the joint implies that there is no damping in any rocking or bending modes of vibration which might be present. This is erroneous but is necessary if a rocking mode is to be isolated from the remainder of the vibration. If a situation exists, such as that in the turned oiled joint, where a travelling wave forms a significant part of the joint motion, then the deflected profile of the joint changes shape as a function of time and as such it becomes unrealistic to think in terms of analysing for bending and rocking motions. The deflected shape of the turned oiled joint under a preload of 1600 kg is shown in fig.(24) for different parts of the forcing cycle. It is seen that the profile changes quite markedly throughout the half cycle shown. Under these circumstances the planforms must be bending, but the degree of bending itself varies as a function of time. Fig.(25) compares the mean level of motion in the joint with the standard deviation of points from this mean as a function of time. To obtain a single value representative of the bending in the joint the mean level of these standard deviations was taken and this is compared with the level of normal vibration in fig.(26).

The phase of the motion of points on the ground joint and the turned dry joint was approximated to either 0 or 180° and the normal vibration level for the particular joint was subtracted from the results. The method of least squares was then used to fit a curve of the form (18) to the resulting data, and the amplitude of the rocking motion thereby determined. The coefficients D_1 and D_2 are given by:

$$D_1 = \frac{\Sigma y_n \sin\phi_n \Sigma \sin\phi_n \cos\phi_n - \Sigma y_n \cos\phi_n \Sigma \sin^2\phi_n}{(\Sigma \sin\phi_n \cos\phi_n)^2 - \Sigma \sin^2\phi_n \Sigma \cos^2\phi_n}$$

$$D_2 = \frac{\Sigma y_n \cos\phi_n \Sigma \sin\phi_n \cos\phi_n - \Sigma y_n \sin\phi_n \Sigma \cos^2\phi_n}{(\Sigma \sin\phi_n \cos\phi_n)^2 - \Sigma \sin^2\phi_n \Sigma \cos^2\phi_n} \qquad (19)$$

All summations are assumed to be made for n = 1,8.

It can be seen that if there are sufficient points so that the summations can be considered integrals then the expressions (19) become exact expressions for a Fourier analysis on this mode of motion. Although eight points cannot be considered large it is sufficient to give a good approximation to the level of rocking within the joint. The ratio of the amplitude of the rocking motion to that of the normal motion is plotted as a function of preload in fig.(27).

It is only for the dry joints at low preloads that the rocking amplitude becomes greater than the normal motion and it is only in these cases that rocking alone could have caused the relative phase differences observed between the various sections of the joints. In the majority of cases therefore, there musthave been considerable bending of the joint planforms. The degree of this bending is again

represented by the standard deviation of the motion of individual points from the average normal motion of the joint. The standard deviations are shown, relative to the normal motion, in fig.(26) and in absolute terms in figs.(28) and (29).

In general the preload range may be split into two distinct regions. At low preloads, the normal and bending amplitudes are changing very rapidly, whereas for higher loads a change in preload has little effect on joint performance. At high loads the bending recorded in the ground joint is small compared with the normal motion, for the turned joint however this is not so. A comparison of the bending amplitudes for the turned and ground joints shows that the curves bear a fairly close resemblance, so that although a change in surface finish caused a marked change in the normal vibration there was no corresponding change in the bending motions. This is possible since whereas normal motion is determined by the absolute value of normal stiffness the bending forces in the joint occur as a result of non-uniform stiffness distributions between the planforms.

The distribution of asperities on the surface of the mating components of a joint is in general random, although certain machines appear to produce repeatable flatness errors, the stiffness distribution is therefore also generally random. The peaks are sufficiently small however, and sufficiently numerous, that on a macroscopic scale one region of a flat surface will have similar properties to another region on the same surface, particularly after the initial crushing of primary contact peaks. It is therefore to be expected that there will be a region at low preloads where

with contact occurring at only a few high spots the joint stiffness may be very unevenly distributed and in consequence the joint will be very susceptible to bending. As the preload increases and contact is made over a wider area, the stiffness distribution becomes more even and the bending will therefore rapidly subside. As the load rises the major regions of contact might also change so that the form of the bending motions will also change.

The stiffness distribution in the joint will be greatly affected by any flatness errors in the planforms. If the joint is subject to flatness errors there will be non uniform contact in the joint. This non uniformity will not be eliminated simply by increasing joint preload so that bending caused by lack of flatness will remain throughout the preload range. There is therefore little decrease in bending amplitudes after the first rapid fall. It is interesting to note that flatness errors are commonly greater than joint deflections so that there will be regions in joints where contact is never made.

At low preloads the introduction of oil into a joint causes a marked decrease in bending amplitudes. The decrease in bending is far greater than the fall in the level of normal vibration. This supports the theory that interfacial oil provides support in the regions of the joint where there is limited metal to metal contact. The oil evens out the load carrying capacity of the joint thereby suppressing bending. At high preloads there is little difference between the bending of the oiled and non oiled joints so that as was seen in the curves of R.M.S. flexibility the oil only has influence at low preloads.

In summary the following statements may be made about the bending motions in the test joints:-

1) At low preloads the joints suffered large bending and rocking motions which rapidly subsided as the preload was increased.

2) The variation of the bending and rocking motions with joint preload and the magnitude of these vibrations was similar for both turned and ground joints. Because of the relative magnitudes of the normal motions for the two surfaces however, bending formed a major part of the motion of the turned joint but only a minor part of the motion of the ground joint.

3) The introduction of interfacial oil into the joint reduces bending and rocking motions, particularly at low preloads.

Graphs of the variation with preload of the computed amplitudes of normal flexibility and the associated effective phase angle are shown in figs. (30) and (31). As before plots are given for a ground and a turned joint, with interfacial oil and in the dry state. The variation of the normal flexibility with preload shows much the same characteristics as the curves of rms flexibility; the plots of effective phase angle do however show some striking features. It can be seen that across the preload range the average motion of the dry turned joint undergoes two phase shifts of 180° . At low preloads the joint motion is in phase with the exciting force at intermediate preloads the motion is out of phase with the excitation and at high preloads the force and displacement are once more in phase. The preload at which the second phase change occurs is close to the load for minimum normal motion and there is

a sharp fall in the amplitude of normal motion in the region of the first phase change. There is therefore an association between a 180° phase shift in the joint motion and a drop in the normal flexibility. For the oiled joint the rate of change of phase angle is much slower than in the dry case. The first phase change is almost absent and the second change is spread over the majority of the preload range. Nevertheless it can be seen thatwhen the normal motion is a minimum the displacement is 90° out of phase with the exciting force.

For the ground joints the average motion is always in phase with the excitation. It will be remembered however that at low preloads there were individual segments of the joint exhibiting a 180° phase shift but that this shift was eliminated as the preload increased.

It has been stated that the deflected form of the turned oiled joint varied as a function of time, as a result of a travelling wave being present within the joint. At higher frequencies such waves were found to be present in other joints. It was found that the frequency response of the joint motion at any particular measuring point fell into one of three main types; these are illustrated in fig.(32) and are described as follows.

a) The dynamic flexibility remained approximately constant throughout the frequency range and the motion was out of phase with the force input. As the frequency was increased there was a gradual fall in phase angle.

b) The phase lag fell from 180° as the frequency increased passing through 90° at some point within the frequency band. In the majority of cases, as illustrated, the

amplitude of motion increased throughout the frequency range. In other situations however the amplitude of motion decreased or remained constant whilst retaining a similar phase characteristic to that described.

c) The amplitude of motion is substantially constant and the phase lag remains close to zero throughout the frequency range.

Although the frequency responses type a, b and c occurred most frequently in the joints from which the examples of fig.(32) were taken, they were by no means unique to these joints. Thus responses of type (b) were found in turned dry joints and those of type (a) in ground dry joints etc.

It is interesting to note that at some frequency in type (b) the motion of the joint lags the force input by 90 , a condition normally associated with resonance, and yet there is no corresponding large change in flexibility normally associated with the resonant condition. This indicates either that the system is very highly damped or that the joint cannot be represented by a simple single degree of freedom model.

Whenever the joint motion changed phase as a result of increasing the forcing frequency, the phase change always occurred from the 180 position towards a zero phase lag. That is the joint motion always moved from being predominantly out of phase to being predominantly in-phase when the phase change was caused by a change of frequency. Changes in motion passing from the in-phase to the out of phase condition only occurred through increasing the joint preload.

It was found that the frequency response of the joint varied not only between joints under different conditions but also at different measuring points under nominally identical conditions on a single joint, see fig.(33), and as such the form of the frequency response must be greatly affected by any non-uniformity within the joint. Since the major non-uniformity within a joint is the distribution of contact then flatness deviation must be a prime factor in determining the frequency response at a particular point within a joint.

A study of the results from the test joints has revealed several features which cannot be explained in terms of the simple joint model described earlier. They are:-

1) The measured flexibility was greater for the ground joints than for the turned joints.
2) Above a certain preload increasing the preload caused the flexibility of the turned joint to rise.
3) At high preloads the introduction of oil into the joint caused an increase in the measured flexibility.
4) Changing the joint preload may result in a 180° temporal phase shift in the joint motion with respect to the applied force. At the preload to cause this phase shift the flexibility drops to a minimum.
5) Joint motions show an unusual frequency response which varies markedly as a function of position within the joint.

A new joint model is now described which accounts for all these unusual features.

4.2 DISCUSSION OF JOINT MODEL

When two plates are clamped together with a bolt the

force on the top plate is zero at all points except in the area directly under the bolthead. The interfacial pressure between the plates is at a maximum directly under the bolthead and decreases with the distance from the bolt. The distribution of load is therefore different on opposite faces of the joint planforms so that there are bending forces operative in the system. As shown by Connoly and Thornley (10) these bending forces may be sufficient to cause a separation of the planforms at some finite distance from the bolthole. As the bolt load is increased the pressure distribution in the joint changes. The maximum interfacial pressure, that is the pressure directly under the bolt, increases at a faster rate than the bolt load and the point at which the planforms separate moves towards the bolt. The load is therefore carried over a progressively smaller area. The joint deflection per unit load, denoted R_x, is a function of the bolt preload and the position of the measuring point in the joint. If the position is very close to the bolthole then R_x will be positive; if the position is at the point of instantaneous rotation of the joint then R_x will be zero; and if it is beyond this point then R_x may be negative. Thus it is seen that the joint deflection per unit load can take any real value.dependant on the point of measurement.

If a uniformly distributed load is now applied to the joint superimposed on the bolt preload, then the joint will undergo a gross deflection by an amount determined by the normal stiffness. The bolt stiffness and the joint normal stiffness are a parallel combination, so that the extra load on the joint is borne by the bolt and joint in proportion to their stiffnesses. The bolt stiffness is usually very

small compared with the joint stiffness and thus all the load may be considered to be borne by the interface. Although uniformly distributed on the upper surface the extra load will be borne at the interface by the existing load carrying regions, ie. the area immediately surrounding the bolt. Further bending forces will therefore be created and the joint will therefore adopt a new deformation profile equivalent to that for a bolt load equal to the sum of the actual bolt load and the uniformly distributed load. The measured joint deflection at any point will be the sum of the normal motion and that due to the change in the deformation profile in the joint.

A mathematical representation of this situation is given in fig.(34a). The uniformly distributed load F is applied to a series combination of two springs k_n and k_x. k_n represents the normal stiffness of the joint and $k_x = {}^1/R_x$ represents the 'deformation stiffness', ie. the change in bolt load required to produce a unit deflection in the joint. It must be emphasised that k_x is a position dependant function whereas k_n is assumed to be constant for any joint configuration and preload.

Each mode of motion will have associated damping. This is represented by placing viscous dampers, rates c_x and c_n, in parallel with the two springs, fig (34b). The dynamic flexibility of the system is then given by:

$$R = \frac{1}{k_x + ic_xw} + \frac{1}{k_n + ic_nw}$$

$$= \frac{A + iB}{C}$$

where

$$A = (k_x + k_n)(k_xk_n - c_xc_nw^2) + w^2(c_x + c_n)(c_xk_n + c_nk_x)$$
$$B = w\ (c_x + c_n)(k_xk_n - c_xc_nw^2) - (c_xk_n + c_nk_x)(k_n + k_x) \quad ..(20)$$
$$C = (k_xk_n - c_xc_nw^2)^2 + w^2(c_xk_n + c_nk_x)^2$$

In a practical joint it is to be expected that the majority of damping arises from viscous pumping of interfacial oil, or in the case of a dry joint a lesser degree of damping will be obtained from the pumping of air and from interfacial friction. In both situations the same source of damping will dissipate energy from both the normal and deformation modes of motion and in this case it might be expected that the values of c_n and c_x would be similar. Making the assumption that $c_n = c_x$ and substituting $c_n = c_x = c$ in equations (20) gives:

$$R^1 = \frac{(k_n + k_x)(k_nk_x + c^2w^2) - iwc(k_n^2 + k_x^2 + 2c^2w^2)}{(k_nk_x - c^2w^2)^2 + c^2w^2(k_n + k_x)^2}$$

or $$R^1 = R^*e^{i\phi}$$

where

$$R^* = \sqrt{\left[\frac{(k_n+k_x)(k_nk_x+c^2w^2)^2 + w^2c^2(k_n^2+k_x^2+2c^2w^2)^2}{(k_nk_x - c^2w^2)^2 + c^2w^2(k_n + k_x)^2}\right]} \quad .....(21)$$

and $$\tan\phi = \frac{wc(k_n^2 + k_x^2 + 2c^2w^2)}{(k_n + k_x)(k_nk_x + c^2w^2)}$$

Equations (21) may be written in non-dimensional form by substituting

$$a = k_x/k_n \quad \text{and} \quad b = wc/k_n$$

Thus

$$R^*k_n = \frac{\sqrt{\left[(1 + a)(a + b^2)^2 + b^2(1 + a^2 + 2b^2)^2\right]}}{(a - b^2)^2 + b^2(1 + a^2)^2}$$

$$\text{and } \tan\phi = \frac{b(1 + a^2 + 2b^2)}{(1 + a)(a + b^2)}$$

Graphs of R^*k_n and against a are shown, for various values of b, in fig.(35).

It is seen that as the ratio k_x/k_n is changed then not only does the amplitude of motion vary to a marked degree but also the phase relationship between the force and displacement changes. As a is decreased from a positive value, through zero, the motion of the joint switches from being predominantly in phase with the applied force to being predominantly out of phase. As the stiffness ratio is further decreased there is a second phase change and the joint motion becomes once more predominantly in phase. It should be noted that in the region of a = -1, ie. in the region of the second phase change R^*k_n falls to a minimum. This should be compared with the results shown in fig.(30).which indicate that the motion of the practical joint fell to a minimum when the phase lag between the applied force and the joint motion passed through 90 .

It is known from the work of previous researchers that k_n is a function of joint preload. It is to be expected that k_x also varies with the load applied to the joint and as such the stiffness ratio a may in turn be considered to be a function of load. Thus by varying joint preload the flexibility of the joint model may be altered.

The validity of the joint model depends on the existence of negative values of k_x and on a variation of k_x with preload commensurate with the experimental results shown in figs.(30) and (31). A series of tests were therefore performed to determine values of k_x for the trial joints.

Chapter 5

STATIC LOADING OF JOINTS AND THE CALCULATION OF VALUES OF NORMAL STIFFNESS

5.1 EXPERIMENTAL APPARATUS

The static loading of the test joints was performed on a Dennison T60ct Transverse and Compression Testing machine.

In the dynamic tests the joints were clamped with equal loads on four symmetrically placed bolts. To simulate this loading in static tests a rig was designed to convert the single central force produced by the Dennison machine into four equal loads distributed at the bolt holes. A photograph and a diagrammatic representation of the loading rig are shown in figs. (36) and (37). The roller G on the loading rig contacts with the loading anvil on the compression tester. The roller is situated midway between the secondary loading bars AC and FD. When load is applied the rig is free to rotate about the line IH so that by taking moments about this line it is seen that the vertical forces at B and E must be equal. The secondary loading bars AC and FD are free to rotate on the primary loading bar at points B and E. These two points are centrally located in AC and FD respectively and thus for equilibrium to be maintained the load at B must be evenly distributed between the reactions at A and C, and that at E between the reactions at F and D. Hence each of the four joint loading points bears one quarter of the total applied load.

The two halves of the test joint were located by four dummy bolts which passed through the joint base plate and protruded into the bolt holes in the joint top plate;

[redacted]. Load was applied to the joint through four more dummy bolts situated in the top plate bolt holes. The lengths of the dummy bolts was such that there was no contact between the locating and load bearing sets. The load bearing dummy bolts had a centrally situated conical seat to provide stable accommodation for the balls in the loading rig. The bolt holes in the joint were a clearance fit for the dummy bolts to enable movement of the bolts to accommodate the slight variations in distances between loading points caused by rotation of the loading rig. The joint assembly rested on a soft aluminium sheet which was in turn situated on the loading table of the compression tester. The aluminium sheet served two functions. Firstly it protected the loading table of the test machine against damage from the concentrated loads on the dummy boltheads. Secondly, it reduced inequalities in the loads carried by the dummy bolts in the lower planform thereby giving a more regular loading distribution. The lower joint planform is an order of magnitude stiffer in bending than the joint top plate, the modulus of rigidity being proportional to the cube of the thickness of the plate, so that the effects of unequal loading on the lower dummy bolts will be small compared with the effect of similar inequalities in the loading of the upper dummy bolts. Nevertheless it is important to guard against the possibility of widely differing bolt loads.

As in the dynamic testing, joint deflections were measured using the Wayne Kerr distance and vibration meter. Since static deflections were being investigated it was the direct component of the demodulated output of the distance meter which was required for analysis. The output from the

demodulating filter was therefore fed into a dc digital voltmeter on which a reading proportional to the separation between the joint base plate and the face of the measuring probe was displayed. Since the initial formation of the joint is random and the joint is subject to large deflections at very low pre-loads, the datum for displacement readings is, in effect, arbitary. The displacement reading for a joint preload of 40 kg. was taken as a reference. The joint deflections under static loading were large compared with the dynamic movements previously measured and it was therefore possible to use a less sensitive capacitive probe during the static testing. The transducer used was type MC1 with a maximum measuring range of 0.25 mm. The increased range of the transducer made the setting up of the probe very much easier than in the dynamic situation.

It was established during primary testing that provided that the joint was not broken and that the maximum preload in the joint's history was not exceeded then for the second and subsequent loading cycles the load deflection curve for a joint followed the same course to within close limits. This is to be expected from the work performed by previous researchers into the properties of structural joints, for example, Day (19) and Thornley (14). During the first loading of a joint there is both plastic and elastic deformation. On unloading the recovery is entirely elastic and on subsequent reloading there will be no further plastic deformation unless the previous maximum preload is surpassed. This feature of joint performance is important since it enables measurements of deflection to be made at several positions on the joint during different loading cycles, thereby

making it possible to plot the deformation profile of the joint using a single displacement monitor.

5.2. EXPERIMENTAL PROCEDURE

The joint planforms were degreased with acetone and wiped with a leather cloth before being assembled. The function of the leather cloth was to remove any particles of fluff or dust left by the previous cleaning cloth. The test joint was then assembled on the bed of the compression test machine as is shown in fig.(36). Load was then applied from the compression tester to a total maximum of 4,000 kg., this value being the same as the maximum total preload supplied by the clamping bolts during dynamic testing, and was held at this level for a short while to allow the joint to stabilise. Throughout subsequent testing the joint preload was not allowed to exceed this level, nor was it allowed to fall below 40 kg. ensuring that there was always preload acting on the planforms and that the joint surface was not disturbed. The displacement measuring transducer was next inserted in the first measuring position and adjusted to give a meter reading of approximately 0.15 mm. This mid range initial setting was necessary since it was not known whether the joint planforms would approach each other under load, or whether they would separate. The load was incrementally increased to 4,000 kg. the display on the voltmeter being noted at each stage. Readings were also taken as the joint was unloaded to ensure that the results remained consistent. On reaching the lower limiting load of 40 kg. the measuring probe was moved to the next desired position and the procedure repeated. Readings were taken from both turned and ground joints.

5.3. PRESENTATION AND DISCUSSION OF RESULTS

The load deflection curves obtained from the turned and ground joints tested are shown in figs.(38) and (39). The position at which the readings for these curves were taken were the same as those used in the dynamic testing; ie. at angular increments of 22.5° to the bolt positions. It is seen that in general the initial application of load to the joint causes a closure of the planforms, but that the rate of closure rapidly falls and as the preload increases the joint planforms begin to separate. It is clear that there are wide differences between the displacements in the joint at different measuring positions. Since the measuring points are symmetrically placed with respect to the bolt holes these differences must be a function of the flatness errors in the planforms. To minimise the effect of these flatness errors on an overall picture of the joint deflection at an angular position 22.5° removed from a bolt hole, the average of the four readings for each joint was taken and the values obtained plotted on fig.(40).

The curves for the turned and ground joints show a similar form. There is a period where increasing joint preload causes a joint closure, the rate of closure then decreases eventually becoming negative and after this point any further increase in preload causes a separation of the planforms. The turned joint is however far more sensitive to changes in load than is the ground joint, furthermore the load at which the joint starts to separate is higher for the ground joint than for the turned.

The phenomenon of an increase in clamping load causing a separation within the joint is of considerable importance.

In particular it is of great interest in situations where a bolted connection is used to provide not only a tight joint but is also required to act as a seal; for example in the cylinder head block connection in internal combustion engines. It appears possible that tightening the joint beyond a certain level may actually decrease the effectiveness of the joint as a seal rather than increase it as might be thought.

The gradient of the average load deflection curves gives the deformation flexibility R_x , and the inverse of this flexibility is the deformation stiffness k_x . Graphs of k_x against applied preload are shown in fig.(41). At low preloads k_x is positive and increasing; it becomes infinite at the load F_∞ , the load at which the measuring position becomes the point of instantaneous rotation of the joint, and on further increase of load k_x decreases rapidly in magnitude from minus infinity, reaches a maximum value and then increases once more in magnitude whilst still retaining a negative sign.

It has been proposed in the previous chapter that the joint motion at any point is a combination of a normal motion and a component arising from the change in the deformation profile of the joint brought about by a change in the effective bolt load. The deformation in the joint is represented by the stiffness k_x plotted in fig.(41) and the effect of combining this stiffness with a joint normal stiffness of the type measured by Day will now be considered. Day found that the normal stiffness of a joint rose sharply with initial preload, the rate of increase in stiffness with load falling with increasing preload. Curves of this form are compared in fig.(42) with curves for k_x of the

form measured in the static loading tests; k_x and $- K_n$ are plotted.

Dependant on the relative magnitudes of k_n and k_x there may be zero one, or two intersections between the two curves. Consider first $-k_{n1}$ which cuts the plot of k_x twice at F_1 and F_2. If the damping in the system is assumed to be small, so that terms in cw can be neglected, then the joint flexibility is given by:

$$R_0 = \frac{k_n + k_x}{k_n k_x} \qquad \text{.....(22)}$$

or $$R_0 k_n = 1 + {}^1/a$$

Thus for

$0 < F < F_\infty$	$a > 0$	and	$R_0 k_n > 0$
$F_\infty < F < F_1$	$a < -1$	and	$R_0 k_n > 0$
$F_1 < F < F_2$	$-1 < a < 0$	and	$R_0 k_n < 0$
$F_2 < F$	$a < -1$	and	$R_0 k_n > 0$

Since k_n is always positive it is seen that in the range $F_1 < F < F_2$ the joint motion is out of phase with the forcing function whereas for the remainder of the preload range the force and displacement will be in phase.

As the preload is increased from zero there will be a region in which the motion is in phase with the applied force, there will be a second region in which the force and displacement are in antiphase, and there will finally be a region in which the force and displacement are once more in phase. This is the sequence observed in the motion of the turned dry joint.

If as for curve-k_{n2} the magnitude of the normal stiffness is sufficiently large that there is no second intersection of the curves of k_x and $-k_n$ then for all preloads

above F_3 the motion would be out of phase with the forcing function. If as for $-k_{n3}$ the magnitude of the normal stiffness is always less than the deformation stiffness then there will be no phase changes the force and displacement always being in phase. This corresponds to the form of motion seen for the ground joints. The correspondence between the motion observed in practise and the form of motion predicted from fig.(42) indicates that the form of the deformation stiffness k_x measured in the static loading tests is of the form required to substantiate the series spring joint model.

The introduction of damping into the joint does not radically alter the form of the variation of joint motion with preload but tends rather to smooth out these changes, see fig.35. From equations 21 it is seen that $\phi = 90^\circ$ for

$$(k_n + k_x)(k_n k_x + c^2w^2) = 0$$

and thus the joint motion changes phase when

$$k_n = -k_x \qquad \text{ie. } a = -1$$

or

$$k_x = -c^2w^2/k_n \qquad \text{ie. } a = -b^2$$

Examining the values obtained for k_x indicates that the situation where $k_x = -c^2w^2/k_n$ will not be met in practise and as such the change in phase of the joint motion resulting from varying the preload can be assumed to result from the condition of 'a' passing through -1 as the load is increased.

If the effects of damping are once more considered to be small then an estimate of the normal stiffness of the joints may be made.

From equation 22

$$k_n = \frac{k_x}{1 - k_x R_0}$$

Thus by combing the measured values of k_x with the results from the dynamic testing values of k_n can be determined. The results obtained by such combination are shown in fig.(43).

The plots of normal stiffness against preload for the turned and ground joints are similar in shape to those obtained by Day. The stiffness of the turned joint increases with increasing preload but the rate of increase falls as the load rises. The stiffness of the ground joint increases steeply from zero but rapidly becomes assymptotic to a value of approximately 8 GN/m. Although it rises initially at a slower rate the stiffness of the turned joint attains a substantially higher value at high preloads than that of the ground joint and the stiffness is still rising at the end of the preload range. The difference between the two joints is solely in the properties of the planform surfaces. The normal stiffness is determined by the real contact area between the planforms. The real contact area is determined by the apparent contact area and the quality of contact in this area. The quality of contact between the surfaces is increased by preloading the joint so as to compress the contacting asperities thereby enabling new contacts to be made between smaller asperities. The quality and type of machining used to produce the surface determines the distribution of asperities in terms of their size. The better the surface finish the smaller the asperities and the more uniform the asperity height, so that a ground surface requires a relatively small normal deflection compared with a turned surface to give comparable improvements in the quality of contact. Similarly however because of the smaller depth of the surface region, when the planform

is subjected to bending it requires only a small upwards deflection of the upper joint plate to cause separation in a ground joint compared with the deflection required to cause a separation in a turned joint. Thus we see that although the normal stiffness of the ground joint rises rapidly at first due to improvement in the quality of contact, this improvement is not maintained since, due to bending of the planforms, the area of the contact region is decreasing at a corresponding rate. The depth of the surface region of the turned joint is such that the normal stiffness is less sensitive to bending, the net effect of increasing the joint preload and the effects of joint bending being to increase the joint normal stiffness throughout the preload range.

The introduction of oil into the joint makes little difference to the measured values of normal stiffness, save for the ground joint at low preloads. In this region the measured stiffness with oil is much higher than for the dry state, thereafter the readings are very similar. This pattern is possible if the rate of decrease in the area of the contact regions is greater than the rate of increase in the quality of the contact. It should be noted however that the values of k_x used in the calculation of normal stiffness were static readings. Under static conditions interfacial oil has an infinite time in which to seep to a position of zero gauge pressure so that although it may offer temporary support to the planforms on initial application of load, this support cannot be maintained. It is not therefore possible to measure the true deformation stiffness of a joint containing interfacial oil by the method previously described. If however the period of oscillation is small

compared with the response time of the oil the in phase component of the dynamic stiffness will be increased. Furthermore as was seen in fig.(28) and (29) the effect of interfacial oil is to reduce bending motions. It is therefore to be expected that the value of k_x for an oiled joint will be somewhat different than for a dry joint.

5.4 FREQUENCY RESPONSE OF THE JOINT MODEL

Examples of the frequency responses observed at different positions and under varying conditions in the test joints were shown in figs.(32) and (33).

The frequency response of the joint model may be gauged by plotting across the curves of fig.(35) for constant values of 'a'. It can be seen that whereas responses of type(a) and(c) are generated by the model, type(b) does not occur; ie. at no value of k_2/k_1 does the dynamic flexibility of the motion increase whilst the phase lag between force and displacement decreases through 90° . It should be remembered however that the arbitrary assumption was made that $c_n = c_x$. If the damping in the joint model is altered so that $c_n = 0$ then from equations (20):

$$R^*k_n = \frac{\sqrt{[(a\ (1+a) + b^2)^2 + b^2\ ]}}{a^2 + b^2} \qquad \ldots\ldots(23)$$

$$\text{and } \tan\phi = \frac{b}{a(1+a) + b^2}$$

In this situation $\phi = 90^\circ$ for

$$a(1+a) + b^2 = 0$$

So that the joint motion changes phase when

$$a = \tfrac{1}{2}\left[-1 \pm \sqrt{[1 - 4b^2]}\right] \qquad \ldots\ldots(24)$$

Thus if $b > \frac{1}{2}$ the discriminant becomes negative and no phase change occurs. Such large damping is however unlikely and for small damping equation (24) may be approximated to:

$$a = \tfrac{1}{2}(-1 \pm (1 - 2b^2))$$

$$= (-1 + b^2) \text{ or } -b^2$$

As before the experimental values of k_x indicate that the situation of $a = -b^2$ will not occur, so that phase change resulting from a change in preload will take place in the region of $a = -1$ whether the assumption of $c_n = c_x$ or $c_n = 0$ is made.

Curves of $R^* k_n$ and for $c_1 = 0$ are shown in fig.(44). It is now seen that in the region of $a = -0.65$ a frequency response of type b occurs.

It is not intended that either of the assumptions made as to the joint damping, ie. $c_n = c_x$, or $c_n = 0$, should apply universally across the test joints or indeed that these conditions should necessarily exist at all. The assumptions have merely been made to demonstrate the type of frequency response which can be generated by a model of the form chosen. Curves are plotted in fig.(45), for comparison with those in fig.(32), to show that the joint model can generate frequency responses similar to those seen in the test joints.

Except in the regions where k_x approaches $-k_n$ the phase lag measured in the joint does not deviate markedly from 0 or 180° so that the damping forces are seen to be small compared with the in phase forces in the joint. In the region where k_x approaches $-k_n$ the phase angle measured is dependant as much on the stiffness ratio as on the joint damping and as such it is difficult to estimate the magnitude

of the damping forces. Furthermore there is no justification to suppose that the damping measured at the particular position chosen relative to the boltholes would be representative of that in the remainder of the joint and as such no estimate of joint damping has been made.

The joint motion has so far been discussed only in terms of the motion of a single point on the planform. Although the normal stiffness is ideally considered uniform across the joint the deformation stiffness is a function of position so that the joint motion is also a function of position. If the spatial distribution of k_x were known it would be possible to predict the flexibility of any point on the joint and hence determine the rms joint flexibility. To give some measure of the variance of k_x with position additional readings were taken on the compression test machine at points on and midway between two bolt holes on a ground and a turned joint. In fig.(46) the deflections measured are plotted against position relative to a bolthole. It is to be expected that the curves would be symmetrical about the position midway between the boltholes, this is not however seen in practise. Since the joints are not perfectly flat there is rocking and bending in the joint quite apart from that caused by the bolt loading. Thus the measured deflection is a combination of the controllable effects of the bolt loading distribution and the random effects of the surface form errors. The effects of tilting in the joint are clearly seen in the results for both turned and ground joints where at one bolt the joint closes under load whereas at the other the joint separates. In general the deflections measured in the ground joint are far smaller than those measured in the turned. As previously stated

the joint bends because the forces acting on the upper surface are not distributed in the same manner as those on the lower planform. When the joint deflects it tends to move in such a manner as to equalise these loads. Thus there is a compression of the surface material under the boltholes and a separation midway between the bolts. The interfacial pressure is at a maximum under the applied load. The deflection required to relieve interfacial pressure is much smaller in a ground joint than in a turned joint and hence the deformation caused by the concentrated loading is much smaller.

From the deflection measurements taken in the single quadrant values of k_x for different positions and preloads were determined. The joint flexibility was then calculated at various positions and the results combined to give a plot of rms flexibility against preload. This rms flexibility is compared with the normal flexibility in fig.(47). It is seen that there may be considerable differences between the normal and rms flexibilities of the single joint quadrant and that this difference is greater in the case of the turned joint than in the case of the ground.

From the results of the static and dynamic loading tests on the joints the following conclusions can be drawn:-

1) The motion of a bolted joint subjected to a uniformly distributed dynamic load is a function not only of that dynamic load but also on the magnitude and distribution of the bolt preload.
2) The motion at any point in a bolted joint is a combination of the direct effects of the dynamic load and those of the change in the effective joint preload caused by the application of the dynamic load.

3) The overall stiffness of a joint with a non uniform static loading distribution is not simply related to the surface finish of the joint planforms. The surface finish affects not only the normal stiffness of the joint but also the deformation profile of the joint under static loading.

Chapter 6

THEORETICAL AND EXPERIMENTAL DETERMINATION OF THE VARIATIONS, WITH POSITION, OF JOINT STIFFNESS

It has been shown that the static, and hence the dynamic deflections in a bolted joint are not uniform throughout the joint but are functions of position. This non uniformity is caused by the uneven distribution of pressure at the joint interface which results from bolt loading. Furthermore it has been shown that the deflection profiles produced by this uneven loading are such that remote from the bolts there may be a separation of the joint components rather than the desired closure. This has two serious effects on the performance of the joint. Firstly any sealing properties of the joint will be severely effected if there is a gap between the joint plates and secondly the resonant frequencies in bending of the clamped portions of the joint assembly will be lower in a joint containing a region of separation as compared to a uniformly clamped section thus greatly affecting the transmission of vibration through and radiation of noise from the structure. It therefore becomes important that it should be possible to predict theoretically the manner in which a joint deforms under non uniform loading.

The problem of predicting the static delection in a joint formed between two nominally flat rectangular plates is analagous to that of a beam on an elastic foundation. Consider fig.(48), fig.(48a) shows two rectangular bars clamped together with a bolt at either end. The modulus of rigidity of the bars (EI) is proportional to the cube of the beam depth and the ratio of the depths of the bars is therefore such that the stiffness of the lower beam in

bending, is an order of magnitude greater than that of the upper beam. The joint deflection, that is the relative motion between upper and lower bars, may therefore be approximated to the motion of the upper beam. Schematically, fig.(48b) the upper beam may be considered as being subjected to two point loads, equal to the bolt loads, whilst being supported on an elastic foundation, the stiffness of which is equal to the joint stiffness. It is assumed that if the bar is long compared with the bolt size and with its width then the bolt load may be considered as evenly distributed across the width and that the effect of the load being distributed over a small area rather than being concentrated at a point may also be neglected.

The differential equation describing the deflected shape of a beam of uniform section is

$$EI \frac{d^4y}{dx^4} = w(x) \qquad \text{.....(25)}$$

The origins of this equation are well known and may be examined in any standard work on elastic stress analysis, eg.(26). In the case of a beam on an elastic foundation the loading on the beam is provided by the stiffness of the elastic support so that

$$EI \frac{d^4y}{dx^4} = -k^*(x).y \qquad \text{.....(26)}$$

where k^* is the stiffness of the foundation per unit length of beam.

Thornley (15) has shown that for a joint subject to a uniform normal loading the following relationship between stiffness, load and deflection holds between certain ranges of interfacial pressure.

$$k = mP = a\,e^{my} \qquad \text{.....(27)}$$

If it is assumed that over an incremental length of the beam the interfacial pressure and joint deflection remain constant then this expression may be used to express the foundation stiffness per unit length as a function of joint deflection or interfacial pressure; ie

$$EI\,\frac{d^4y}{dx^4} = -mp^*y = -a^*e^{my}.y \qquad \text{....(28)}$$

This equation has no exact solution and as yet attempts at numerical solution have failed. An approximation to the joint deflection can however be made by assuming that the joint stiffness is uniform across the planforms, ie.

$$k^* = \frac{mP}{L} \qquad \text{.....(29)}$$

In this case the equation describing the deflected shape of the joint becomes

$$EI\,\frac{d^4y}{dx^4} = -\frac{mP}{L}\cdot y \qquad \text{.....(30)}$$

an equation which has exact solutions for any particular values of P. The change in the deflection of any particular point in the joint with load may be determined by plotting deflection curves for a series of applied loads and reading across these curves to obtain the desired result.

Solution of equation (30) yields

$$y = e^{\beta x}[c_1 \cos\beta x + c_2 \sin\beta x] + e^{-\beta x}[c_3\cos\beta x + c_4\sin\beta x] \qquad \text{.....(31)}$$

where $\beta^4 = \frac{mP}{4EIL}$ .....(32)

and c_1, c_2, c_3 and c_4 are constants to be determined from the boundary conditions imposed on the beam. In the situation shown in fig.(48) it is assumed that the segment of beam

under consideration is a small section of a flange clamped by many bolts so that the gradient of the beam at the bolt is zero. A second boundary condition is given by the fact that at the bolts the shear force in the beam must be equal to half the bolt load. Thus equation (31) must satisfy the conditions:-

$$\frac{dy}{dx} = 0 \quad \text{and} \quad EI\frac{d^3y}{dx^3} = \frac{P}{2} \quad \text{at} \quad x = \pm L \qquad \ldots.(33)$$

Since the beam is symmetrical about the position $x = 0$ then $y(x) = y(-x)$ and thus $c_1 = c_3$ and $c_2 = -c_4$. Thus

$$y = 2c_1\cos\beta x \cosh\beta x + 2c_2\sin\beta x \sinh\beta x \qquad ..(34)$$

By applying boundary conditions (33) it can be shown that

$$\frac{c_1}{c_2} = \frac{\cot\beta L + \coth\beta L}{\coth\beta L - \cot\beta L} = G_3(\beta L) \qquad ....(35)$$

$$\text{and } c_2 = \frac{P}{8\beta^3 EI.H(\beta L)} \qquad .....(36)$$

where

$$H(\beta L) = -G_3(\beta L)\{\sin\beta L\cosh\beta L + \cos\beta L\sinh\beta L\} + \cos\beta L\sinh\beta L - \sin\beta L\cosh\beta L$$

Given the physical dimensions of the joint, and the Youngs Modulus and 'm' value of the joint material it is possible to use equations (34), (35) and (36) to give an approximation to the deflection profile of the joint.

In order to test the accuracy of this method an experimental rig was designed to simulate the situation described in fig.(48). A photograph of this apparatus is shown in fig.(49).

When a joint is formed under preload from bolts then the order and the manner of tightening the bolts will greatly affect the nature of the joint formed. The above theory has been derived for determining the deflection in a span where the joint is formed under two equal bolt loads. In practise it is not possible to simultaneously tighten bolts to the same load and so the chosen model cannot be matched exactly. If however load is supplied from a compression testmachine, and load equalising devices are used as was done in the static loading tests on annular joints, (see Chapter 5) then a good simulation can be achieved. In the apparatus shown in fig.(49) the load is supplied from the ram of the compression test machine to the top loading beam through a centrally located hardened steel roller. The beam is thus free to rotate about this roller thereby ensuring that equal loads are transmitted to the vertical loading pillars. The vertical loading pillars are similarly connected to the top loading beam and the load carried by each foot of the pillars must therefore be equal. Looking at a section through the longitudinal axis of the joint the loading on the joint is exactly the same as that which would be provided by bolts, fig.(48c). The distribution of load in the lateral direction is not representative of bolt loading. Deflections in this direction are however not yet of primary interest. The distribution of fig.(48c) is then approximated to the chosen model of fig.(48b). Although a better approximation to the point loading assumed in the mathematical model could have been obtained from the experimental rig this would have required that the clamping effects of the bolts were ignored and the boundary condition of zero gradient at $x = \pm L$ were waived.

The planforms of the joints tested were rectangular, 6 x 20 cm and were manufactured in EN8 steel. Top joint plates of thickness 1 and 2 cm with both milled and ground surfaces were tested. The thickness of the lower joint plate was in all cases 6cm. and the ratios of the flexural rigidities of the lower and upper joint plates therefore had a minimum value of 27. It is safe to assume therefore that the lower joint plate was rigid compared to the upper section of the joint.

The deflections in the joint were measured using a Wayne-Kerr distance meter type 731 with a capacitive transducer type MC1; maximum range 0.25mm. Deflections were measured at five positions equally spaced along the longitudinal axis of the joint between the vertical loading pillars. As in previous static loading tests the joint was initially loaded to the maximum test load and held at this level for a brief period. This was to ensure that during the subsequent testing only elastic deformations would be measured. The joint was then unloaded to 40kg. and the displacement probe inserted in the first measuring position. The displacement reading at a preload of 40kg. was taken as a datum. The joint was now reloaded in stages to the maximum total test load of 4,000 kg.; deflection readings being taken at each stage. The deflections were also noted as the joint load was subsequently decreased to 40kg. At no time was the joint preload allowed to fall below this minimum value so that at no time during testing did the joint planforms become separated or repositioned. On reaching the lower limiting load the measuring transducer was moved to the next position and the procedure repeated. The results obtained are shown in figs.(50) - (53). Also plotted are the theoretically

derived deflection curves with 'm' value chosen to give the best fit when compared with experimental results.

Although there are marked similarities between the theoretical curves and the experimental values the correlation between the two sets of figures cannot be claimed to be good. In general the deflections measured experimentally are much larger than those predicted and there is also a marked difference in the 'lie' of the two sets of curves in relation to the datum line. The overall shape of the predicted and measured results do however have much in common. Both sets of readings show a maximum joint closure under the loading points and both also show a maximum separation, or minimum closure of the planforms at the centre of the span. Again it is seen that there are positions in the joint where for a particular load the joint deflection does not change with applied load, ie. at that position and load the joint stiffness is infinite.

The large discrepancy in the 'lie' of the results relative to the chosen datum may be traced to two causes. At low preloads the joint stiffness is very low so that a small change in load gives a relatively large change in deflection. Assuming that the order of stiffness involved may be estimated from the expression $k = mP$ then taking an 'm' value of $10^6 m^{-1}$ the joint stiffness at the datum load of 40 kg. will be of the order of 40×10^6 kg/m. The likely error in the load measurement on the compression test machine was 20 kg. this being the smallest division on the load scale; the machine having been calibrated shortly before use, and therefore the largest likely error in deflection reading would be of the order of 0.5μm. This is very small

compared with the apparent shift in datum between the experimental and theoretical results. It therefore seems unlikely that this shift occurs solely as a result of inaccuracies in measuring datum load.

The linear relationship between load and stiffness is quoted by Thornley (15) to be valid between the ranges of mean interfacial pressures of 0.02 tons/in^2 to 2 tons/in^2. At a total joint preload of 40 kg. the mean interfacial pressure is only 0.002 tons/in^2 and even allowing for the fact that the majority of the load is carried in the regions directly under the loading points it is unlikely that the minimum interfacial preload for the linear load stiffness relationship is exceeded. At such low preloads the actual joint stiffness is lower than is predicted from the linear model (see Day(19)) and the joint deflections are therefore greater than would be expected from this model. Furthermore at very low preloads the contact points are not evenly distributed thoughout the load bearing surfaces and the joint planforms are therefore liable to tilting and bending motions until a stable support is achieved. The assymetry of the experimental results with respect to the transverse axis of the beam is evidence of such tilting.

The magnitude of the tilting and bending present in the joint is dependant to a large extent on the flatness of the mating profiles. To gauge the order of magnitude of these flatness errors a mapping was made of the joint surfaces of the ground bar 2cm thick and the ground base bar. The readings taken along the centre line of the joint are shown in fig.(54). It is seen that at zero preload there is a gap of up to 3 m between the two planforms. The joints must therefore deflect by this amount before contact can

be made over the entire surface. The size of the zero shift apparent in this joint is similar to the gap observed at zero preloads and thus although it is possible that much of the flatness errors might be taken out at loads below 40 kg. it is likely that errors of form are major contributors to the datum shift and assymetry observed in the experimental results.

It should be noted that since the linear load stiffness relationship is not applicable at low preloads then the errors resulting from inaccuracies in load measurement will be greater than those previously estimated. It is not thought however that the difference would be solely responsible for the measured datum shift.

It has been argued that the majority of the differences between the predicted deflection profiles and the experimental data result from a poor match between the experimental model and the test joint at low preloads. If this is so then a better correlation between experiment and theory might be expected if the datum load were shifted to a higher value. A new datum of 3,000 kg. was therefore chosen, corresponding to a mean interfacial preload of 0.105 tons/in^2 and the theoretical and experimental deflections at 4,000 kg. were related to this datum. The results obtained are shown in fig.(55). It is seen that there is now excellent correlation between the two sets of curves particularly in the case of the ground joints.

We may therefore conclude that although the theoretical approached outlined compares badly with experimental results at low joint preloads there is a very good correlation at higher loads when the theoretical model fits the experimental

situation more closely. Since it is possible to predict changes in deflection at high preloads it is now possible to derive the stiffness of the joint as a function of position. It should then be possible by application of energy methods to determine the fundamental natural frequency in bending of the bars constituting the joint and a relationship between natural frequency and bolt load could then be derived. This relationship would be of considerable importance in the control of the transmission of audio frequency noise through structures.

It is suggested that the applicability of the method be further tested and if shown to be of repeatable value in the prediction of the static and resonant properties of one dimensional joints then an investigation should be made into extending this method to joints such as clamped plates where the forming preload is non-uniformly distributed in two dimensions.

Chapter 7

CONCLUSIONS

1. When considering the effects of surface topography on joint performance researchers have tended to concentrate on the effects of surface roughness; the effects of surface flatness are however of equal importance in determining joint properties.

2. A method has been described by which the contour area within a joint may be determined from measurements taken on the surfaces of the joint planforms, the stability of the joint may also be examined. This method should be extended to account for changes in the orientation of the joint planforms resulting from different stiffnesses occuring at the different points of contact.

3. The maximum stiffness which a joint can attain is limited by the flatness errors in the joint planforms.

4. In a bolted joint bending of the joint planforms can be a major contributor to joint motion.

5. The standard deviation of bolt loads produced by a given torque on the nut is approximately 10% of the working load of the bolt; this is insufficiently accurate to enable the applied torque to be used as a measure of bolt load during laboratory testing.

6. The rate of change of bolt load with applied torque can increase as a result of deformation of the nut face causing a decrease in the effective loading radius under the nut. The rate of change of bolt load with applied torque may also decrease if thread friction increases or if the effective loading radius increases.

7. The normal motion of a bolted joint is not constant throughout the joint but varies as a function of the point of measurement. This variation in joint motion is caused by the non-uniform distribution of load within the joint, which results from bolt loading, and by the effects of flatness errors in the joint planforms.

8. If a bolted joint is subjected to a uniformly distributed normal dynamic load then in general increasing the bolt preload leads to an increase in joint stiffness. In certain preload ranges, however, increasing bolt preload causes an increase in the flexibility of some sections of the joint and can lead to an increase in the rms motion of the joint.

9. In a bolted joint subjected to a uniformly distributed normal dynamic load, the deflected shape of the joint may vary as a function of time. A travelling wave can exist around the periphery of an annular joint.

10. Increasing joint preload, while holding all other parameters constant, can lead to a 180° phase shift in the dynamic motion of a bolted joint relative to the force input to the joint.

11. The dynamic motion of a bolted joint is dependant on both the magnitude and distribution of the bolt preload.

12. The motion of a bolted joint cannot be represented by a single degree of freedom model.

13. The dynamic motion of a bolted joint may be considered as the summation of a normal motion which is uniform across the joint, and a change in the deformation profile of the joint resulting from achange in effective bolt load

when a uniformly distributed dynamic load is superimposed on the static bolt load.

14. A mathematical model representing a bolted joint may be formed by placing two springs in series. The first spring represents the normal stiffness of the joint and is defined as 'the uniformly distributed incremental load which in the absence of other loads will give a unit normal deflection in the joint'. The second spring represents the 'deformation stiffness' of the joint, which is defined as 'the incremental bolt load, which in the absence of other loads will give a unit deflection at the position of interest within the joint'. The normal stiffness is a constant for the joint and is positive. The deformation stiffness varies as a function of position and may take any real value positive or negative. Each stiffness has associated damping which is represented in the joint model by a viscous dashpot in parallel with each spring.

15. The surface finish of joint planforms affects both the normal and deformation stiffnesses; under certain conditions decreasing the surface roughness of the planforms forming a bolted joint can lead to an increase in rms joint flexibility.

16. The introduction of oil into the joint interface reduces dynamic bending of the joint.

17. Above a certain preload limit the deformation stiffness of a rectangular bolted joint may be predicted by the method described in Chapter 6.

18. A mechanism has been described for simulating four equal bolt loads from the force delivered by the ram of a

compression test machine.

19. Joint separations of the order of 5μm were measured in joints subjected to static bolt loads.

20. The separation of joint planforms caused by increasing a non-uniformly distributed preload is of great importance in determining joint properties. This separation should be further studied to determine its affect on the manner in which load is borne at the joint interface and on the transmission of vibrational energy across joints.

Appendices

Appendix 1. Computer programme for the determination of joint contour area.

```
 &ALGOL; L;
LIBRARY
ALGOL

    1   "BEGIN"
    2   "INTEGER"N,M;
    3   "INTEGER"Q;
    4   "READ"M,N;
    5   START;"BEGIN"
    6   "INTEGER"INT;
    7   "INTEGER"I,J,K,L;
    8   "REAL""ARRAY"TH,BH,S,D,SINFI,X,YC1:N,1:M],RC1:N],THETAC1:M];
    9   "ARRAY"CHC1:N,1:M];
   10   "BEGIN"
   11   "REAL" GP,X1,X2,Y1,Y2,C,DS,DTHETA,DRAD, SMIN,FN,KL,R1,THETA1,R0,R2,THETA******
   12       2,PI,MINSFI;
   13   "REAL"ZH;
   14   "INTEGER"LM;
   15   "INTEGER""ARRAY" A,BC1:3];
   16   "PROCEDURE"STAP(AN,DDRAD,RRO,OM,ON,OX,OY,IS,BN,THE,COUNT);
   17    "VALUE"DDRAD,RRO,OM,ON,OX,OY,THE;
   18    "REAL"DDRAD,RRO;
   19   "ARRAY"THE,OX,OY,IS;
   20   "INTEGER""ARRAY"AN,BN;
   21    "INTEGER"OM,ON;
   22   "INTEGER"COUNT;
   23   "BEGIN""REAL"RADMAX,RADMIN,THEMAX,THEMIN,IC,IZH,IFH,ID,ISMIN,CON;
   24   "REAL"DIS12,DIS23,DIS31,DISMIN;
   25         "ARRAY"RAD,IT,IR,IX,IYC1:3],OD,ISFIC1:ON,1:ON];
   26   "ARRAY"CN,DNC1:3];
   27   "INTEGER"IN,OJ,OI;
   28   RADMAX:=0; RADMIN:=1000;
   29   "FOR"IN:=1"STEP"1"UNTIL"3"DO""BEGIN"
   30     RADCINJ:=(ANCINJ-1)*DDRAD+RRO;
   31   IXCINJ:=RADCINJ*COS(THELBNCINJJ);
   32   IYCINJ:=RADCINJ*SIN(THELBNCINJJ);
   33   "END";
   34   "IF"IXC1J=IXC2J"THEN"DIS12:=IXC1J"ELSE""BEGIN"
   35   DIS12:=(IYC1J-IXC1J*(IYC2J-IYC1J)/(IXC2J-IXC1J))/(SQRT(1+((IYC2J-IYC1J)/******
   36   (IXC2J-IXC1J))*2));
```

```
"END";
"IF"IX[3]=IX[2]"THEN"DIS23:=IX[3]"ELSE""BEGIN"
DIS23:=(IY[2]-IX[2]*(IY[3]-IY[2])/(IX[3]-IX[2]))/(SQRT(1+((IY[3]-IY[2])/******
(IX[3]-IX[2]))↑2));
"END";
"IF"IX[1]=IX[3]"THEN"DIS31:=IX[1]"ELSE""BEGIN"
DIS31:=(IY[3]-IX[3]*(IY[1]-IY[3])/(IX[1]-IX[3]))/(SQRT(1+((IY[1]-IY[3])/******
(IX[1]-IX[3]))↑2));

"END";
"IF"ABS(DIS23)<ABS(DIS12)"THEN"DISMIN:=ABS(DIS23)"ELSE"DISMIN:=ABS(DIS12******
);
"IF"ABS(DIS31)<DISMIN"THEN""BEGIN"
        IR[1]:=RAD[1];  IT[1]:=THETBN[1];
        IR[2]:=RAD[3];  IT[2]:=THETBN[3];
        IR[3]:=RAD[2];  IT[3]:=THETBN[2];
   CN[2]:=AN[2]; DN[2]:=BN[2];
    AN[2]:=AN[3]; BN[2]:=BN[3];
     AN[3]:=CN[2]; BN[3]:=DN[2];
"END"
  "ELSE""BEGIN" "IF"ABS(DIS23)<ABS(DIS12)"THEN""BEGIN"
        IR[1]:=RAD[2];  IT[1]:=THETBN[2];
        IR[2]:=RAD[3];  IT[2]:=THETBN[3];
        IR[3]:=RAD[1];  IT[3]:=THETBN[1];
     CN[1]:=AN[1]; DN[1]:=BN[1];
     AN[1]:=AN[3]; BN[1]:=BN[3];
     AN[3]:=CN[1]; BN[3]:=DN[1];
"END"
  "ELSE""BEGIN"
    "FOR"IN:=1"STEP"1"UNTIL"3"DO""BEGIN"
        IR[IN]:=RAD[IN];  IT[IN]:=THETBN[IN];
    "END";
    "END";
  "END";
"FOR"IN:=1"STEP"1"UNTIL"3"DO""BEGIN"
  IX[IN]:=IR[IN]*COS(IT[IN]);
  IY[IN]:=IR[IN]*SIN(IT[IN]);
"END";
```

```
"COMMENT" NEXT SECTION SETS UP CONTACT LINE NEAREST ORIGIN AND EXAMINES
  STABILITY;
CON:=1;
"IF"IX[1]=IX[2]"THEN""BEGIN""IF"IX[1]<0"THEN"ID:=IX[3]-IX[1]
  "ELSE"ID:=IX[1]-IX[3]; "END"
"ELSE""BEGIN"
   IC:=IY[1]-IX[1]*(IY[2]-IY[1])/(IX[2]-IX[1]);
   IZM:=(IY[2]-IY[1])/(IX[2]-IX[1]);
   IFM:=SQRT(1+IZM↑2);
"IF"IC=0"THEN""GOTO"END;
  "IF"IC<0"THEN""BEGIN"IC:=-IC;
                       IZM:=-IZM;
                       CON:=-CON;   "END";
  ID:=(IZM*IX[3]-IY[3]*CON+IC)/IFM;
"END";
ISMIN:=1;
"IF"ID"GE"0"THEN""GOTO"END;
"IF"IX[1]"NE"IX[2]"THEN""BEGIN"
"FOR"OI:=1"STEP"1"UNTIL"ON"DO""BEGIN"
"FOR"OJ:=1"STEP"1"UNTIL"ON"DO""BEGIN"
  OD[OJ,OI]:=(IZM*OX[OJ,OI]-CON*OY[OJ,OI]+IC)/IFM;
"IF"ABS(OD[OJ,OI])<1.-50"THEN""GOTO"THEEND;
  ISFI[OJ,OI]:=IS[OJ,OI]/OD[OJ,OI];
  "IF"ISFI[OJ,OI]>0"AND"ISFI[OJ,OI]<ISMIN"THEN""BEGIN"
   ISMIN:=ISFI[OJ,OI]; AN[3]:=OJ; BN[3]:=OI; "END";
THEEND:"END";
"END";
"END"
"ELSE""BEGIN"
  "FOR"OI:=1"STEP"1"UNTIL"OM"DO""BEGIN"
"FOR"OJ:=1"STEP"1"UNTIL"ON"DO""BEGIN"



"IF"IX[1]<0"THEN"OD[OJ,OI]:=OX[OJ,OI]-IX[1]
   "ELSE"OD[OJ,OI]:=IX[1]-OX[OJ,OI];
 "IF"OD[OJ,OI]"LE"0"THEN""GOTO"ANEND"ELSE"
   "BEGIN" ISFI[OJ,OI]:=IS[OJ,OI]/OD[OJ,OI];
      "IF"ISFI[OJ,OI]<ISMIN"THEN""BEGIN"   ISMIN:=ISFI[OJ,OI];
                                          AN[3]:=OJ;  BN[3]:=OI;  "END";******
```

```
111    "END";
112    ANEND;"END";
113    "END";
114    "END";
115    "FOR"OI:=1"STEP"1"UNTIL"ON"DO""BEGIN"
116    "FOR"OJ:=1"STEP"1"UNTIL"ON"DO""BEGIN"
117      ISLOJ,OI]:=ISLOJ,OI]-ODLOJ,OI]*ISMIN;
118    "END";
119    "END";
120    "GOTO"REEND;
121    END;COUNT:=1;
122    "PRINT"(/L3\,SOLUTION STABLE,/L3\\);
123    REEND;"END";
124    "COMMENT" M= NO OF ANGULAR INTERVALS,N= NO OF RADIAL INTERVALS,
125                I DENOTES ANGULAR POSITION, J DENOTES RADIAL POSITION;
126    PI:=3,14159;
127    OI=0;
128    DS:=2₁₀-4;
129    DTHETA:=22;5*PI/180;
130    DRAD:=4;
131    RO:=30;
132    SMIN:=1₁₀9;
133    "FOR"I:=1"STEP"1"UNTIL"3"DO""BEGIN" AC I]:=BC I]:=0;"END";
134    "FOR"I:=1"STEP"1"UNTIL"M"DO""BEGIN"
135    "FOR" J:=1"STEP"1"UNTIL"N  "DO""BEGIN"
136        "READ"THCJ,I];
137              THCJ,I]:=(5-THCJ,I])/1000;
138        "END";
139    "END";
140    "FOR"I:=1"STEP"1"UNTIL"N"DO""BEGIN"
141      "FOR"J:=1"STEP"1"UNTIL"N"DO""BEGIN"
142        "READ"BHCJ,I];
143              BHCJ,I]:=(5-BHCJ,I])/1000;
144        "END";
145        "END";
146    INT:=0;
147    START;INT:=INT+1;
148    "FOR"I:=1"STEP"1"UNTIL"M"DO""BEGIN"
149    "FOR"J:=1"STEP"1"UNTIL"N"DO""BEGIN"
150        SCJ,I]:=BHCJ,I]+THCJ,I];
151      "IF"SCJ,I]<SMIN"THEN"SMIN:=SCJ,I];
152              "END"; "END";
```

```
153   K:=0;
154   "FOR"I:=1"STEP"1"UNTIL."N"DO""BEGIN"
155   "FOR"J:=1"STEP"1"UNTIL."N"DO""BEGIN"
156      S[J,I]:=S[J,I]-SMIN;
157      "IF"S[J,I]=0"THEN""BEGIN"
158         K:=K+1;
159         "IF"K"LE"3"THEN""BEGIN"
160            A[K]:=J;
161            B[K]:=I;
162            "END";"END";"END";"END";
163   "FOR"I:=1"STEP"1"UNTIL."N"DO""BEGIN"
164   "PRINT"(/L1\\);
```

```
165     "FOR"J:=1"STEP"1"UNTIL"N"DO"
166       "PRINT"SAMELINE,FREEPOINT(3),1000*S[J,I],(/S4\\);
167   "END";
168   "PRINT"DIGITS(3),K;
169   R1:=(A[1]-1)*DRAD+RO;
170   R2:=(A[2]-1)*DRAD+RO;
171   THETA1:=(B[1]-1)*DTHETA;
172   THETA2:=(B[2]-1)*DTHETA;
173   "FOR"J:=1"STEP"1"UNTIL."N"DO"R[J]:=(J-1)*DRAD+RO;
174   "FOR"I:=1"STEP"1"UNTIL."N"DO""BEGIN"
175        THETA[I]:=(I-1)*DTHETA;
176      "FOR"J:=1"STEP"1"UNTIL"N"DO""BEGIN"
177         X[J,I]:=R[J]*COS(THETA[I]);
178         Y[J,I]:=R[J]*SIN(THETA[I]);
179            "END"; "END";
180   "IF"K>2"THEN""GOTO"CC;
181   "IF"K=2"THEN""GOTO"BB;
182   MINSF:=1;
183   X1:=R1*COS(THETA1);  Y1:=R1*SIN(THETA1);
184   "FOR"J:=1"STEP"1"UNTIL."N"DO""BEGIN"
185   "FOR"I:=1"STEP"1"UNTIL."N"DO""BEGIN"
186     "IF"ABS(X1)<1.-50"THEN""GOTO"JACK"ELSE"
187      D[J,I]:=(X[J,I]*Y1/X1-Y[J,I])/SQRT(1+(Y1/X1)↑2);
188       "GOTO"ILL;
189    JACK:D[J,I]:=X[J,I];
```

```
190   JILL;
191     "IF"ABS(D[J,I])<1.-50"THEN""GOTO"FRED"ELSE""BEGIN"
192   SINFI[J,I]:=S[J,I]/D[J,I];
193     "IF"ABS(SINFI[J,I])<MINSFI"THEN""BEGIN"  MINSFI:=ABS(SINFI[J,I]);
194                                              A[2]:=J;  B[2]:=I;
195       "END";
196      "END";
197     FRED:"END";
198   "END";
199   K:=0;
200   "FOR"J:=1"STEP"1"UNTIL"N"DO""BEGIN"
201   "FOR"I:=1"STEP"1"UNTIL"N"DO""BEGIN"
202      S[J,I]:=S[J,I]-D[J,I]*SINFI[A[2],B[2]];
203      "IF"S[J,I]<1.-20"THEN"K:=K+1;
204      "END";
205   "END";
206   "PRINT"DIGITS(3),K;
207   "FOR"I:=1"STEP"1"UNTIL"N"DO" "BEGIN"
208   "PRINT"(''L1'');
209    "FOR"J:=1"STEP"1"UNTIL"N"DO"
210     "PRINT"SAMELINE,FREEPOINT(3),1000*S[J,I],(''S4'');
211   "END";
212   R2:=(A[2]-1)*DRAD+RO;
213   THETA2:=(B[2]-1)*DTHETA;
214   "IF"K>2"THEN""GOTO"CC;
215   BB:X2:=R2*COS(THETA2);
216      Y2:=R2*SIN(THETA2);
217   "IF"X2=X1"THEN""GOTO"JEN;
218   C:=Y1-X1*(Y2-Y1)/(X2-X1);
219   ZM:=(Y2-Y1)/(X2-X1);
220   FM:=SQRT(1+ZM↑2);
221   "IF"C<0"THEN""GOTO"EB;
222   "FOR"I:=1"STEP"1"UNTIL"N"DO""BEGIN"
223   "FOR"J:=1"STEP"1"UNTIL"N"DO""BEGIN"
224      D[J,I]:=(ZM*X[J,I]-Y[J,I]+C)/FM;
225           "END";
226       "END";
```

```
227   "GOTO"EF;
228   EB:"FOR"I:=1"STEP"1"UNTIL"N"DO""BEGIN"
229   "FOR"J:=1"STEP"1"UNTIL"N"DO"
230    D[J,I]:=- (ZH*X[J,I]-Y[J,I]*C)/FH;
231            "END";
232   "GOTO"EF;
233   JEN:"FOR"I:=1"STEP"1"UNTIL"N"DO""BEGIN"
234       "FOR"J:=1"STEP"1"UNTIL"N"DO"D[J,I]:=X2-X[J,I];
235      "END";
236   EF:MINSF:=1;
237   "FOR"I:=1"STEP"1"UNTIL"N"DO""BEGIN"
238      "FOR"J:=1"STEP"1"UNTIL"N"DO"
239     "BEGIN"
240     "IF"D[J,I]<1.-50"THEN""GOTO"FF;
241         SINF[J,I]:=S[J,I]/D[J,I] "IF"SINF[J,I]<0"THEN""GOTO"FF;
242         "IF"J="E"A[1]"THEN""GOTO"GG;
243         "IF"I=B[1]"THEN""GOTO"FF;
244      GG:"IF"J="E"A[2]"THEN""GOTO"GH;
245         "IF"I=B[2]"THEN""GOTO"FF;
246   GH:"IF"SINF[J,I]<MINSF"THEN""BEGIN"MINSF:=SINF[J,I];
247            A[3]:=J; B[3]:=I; "END";
248      FF:"END";
249   "END";
250   "PRINT"SCALED(3),MINSF;
251   "FOR"I:=1"STEP"1"UNTIL"N"DO""BEGIN"
252   "FOR"J:=1"STEP"1"UNTIL"N"DO"
253      S[J,I]:=S[J,I]-D[J,I]*MINSF; "END";
254   LAB10:LM:=0;
255   STAB(A,DRAD,RO,N,N,X,Y,S,B,THETA,LM);
256   "IF"LM=0"THEN""GOTO"LAB10;
257   "FOR"I:=1"STEP"1"UNTIL"N"DO""BEGIN"
258   "PRINT"''L1'';
259    "FOR"J:=1"STEP"1"UNTIL"Q"DO"
260      "PRINT"SAMELINE,FREEPOINT(3),1000*S[J,I],''S4'';
261   "END";
262   CC:K:=0;
263   ZZ:L:=0;
264   Q:=Q+1;
265   "IF"Q>30"THEN""GOTO"QOUT;
266   "FOR"I:=1"STEP"1"UNTIL"N"DO""BEGIN"
267   "FOR"J:=1"STEP"1"UNTIL"N"DO""BEGIN"
268      "IF"S[J,I]"LE"0"THEN"L:=L+1;
```

```
269       SC[J,I]:=SC[J,I]-DS;
270       "END"; "END";
271     K:=K+1;
272     KL:=100*L/(H*N);
273     "PRINT"DIGITS(3),K,SANELINE,"'S10'",FREEPOINT(4),KL;
274     "IF"L"NE"H*N"THEN""GOTO"ZZ;
275     "END";
276     "IF"INT"GE"8"THEN""GOTO"QQUT"ELSE""BEGIN"
277     "FOR"I:=1"STEP"1"UNTIL"H"DO""BEGIN"
278     "FOR"J:=1"STEP"1"UNTIL"N"DO""BEGIN"
279     CH[J,I]:=BH[J,I];
280     "END";
281     "END";
282     "FOR"J:=1"STEP"1"UNTIL"N"DO""BEGIN"
283     BH[J,1]:=CH[J,16];
284     "FOR"I:=2"STEP"1"UNTIL"16"DO"
285     BH[J,I]:=CH[J,I-1];
286     "END";
287     "END";
288     "GOTO"START;
289     "END";
290     QQUT:"END";
```

```
  502    NC
 2392  CODE
 2894 TOTAL
```

```
 &DIAG;                                                    C
DIAG
```

```
 &RUN;                                                     C
AION
DRO
```

```
2,50      2,05      6,75      6,75      1,05      ,150
1,85      1,65      ,800      ,900      ,550      ,550
2,30      1,75      ,700      1,10      ,700      ,400
1,95      1,65      ,750      ,600      ,600      ,050
2,35      1,10      6,75      6,75      ,700      ,250
2,10      1,55      ,750      ,980      1,00      ,450
2,25      1,75      1,00      1,05      ,900      ,700
1,70      1,53      ,450      ,950      1,00      ,250
2,65      1,60      6,75      6,79      ,950      ,500
2,15      1,65      ,700      ,900      1,00      ,000
2,60      1,55      1,00      1,00      ,600      ,650
2,20      1,50      ,850      1,30      ,650      ,350
1,75      1,55      4,85      4,85      ,750      ,350
2,15      1,75      ,550      ,830      ,750      ,050
1,75      1,90      1,10      1,10      ,650      ,500
2,35      1,80      ,750      1,00      ,580      ,150
  1
  1
2,49      2,04      6,74      6,73      1,03      ,131
1,85      1,65      ,800      ,900      ,550      ,550
2,31      1,76      ,715      1,12      ,718      ,419
1,97      1,67      ,777      ,630      ,633      ,085
2,38      1,13      6,79      6,79      ,742      ,296
2,13      1,58      ,783      1,02      1,05      ,500
2,28      1,78      1,04      1,09      ,942      ,746
1,72      1,55      ,477      ,980      1,03      ,285
2,66      1,61      6,76      6,77      ,968      ,519
2,15      1,65      ,700      ,900      1,00      ,000
2,59      1,54      ,985      ,984      ,582      ,631
2,18      1,48      ,823      1,27      ,617      ,315
1,72      1,52      4,81      4,81      ,708      ,304
2,12      1,72      ,512      ,788      ,704      ,000
1,72      1,87      1,06      1,06      ,608      ,454
2,33      1,78      ,723      ,970      ,547      ,115
1,00,,-06

,SOLUTION STABLE,
```

2,44	1,99	6,69	6,68	,979	,076
1,79	1,59	,738	,835	,482	,479
2,25	1,70	,644	1,04	,640	,338
1,91	1,60	,704	,552	,551	,000
2,31	1,06	6,71	6,71	,665	,215
2,07	1,52	,726	,957	,978	,429
2,23	1,73	,965	1,04	,890	,692
1,69	1,52	,442	,944	,997	,250
2,64	1,59	6,74	6,75	,950	,503
2,14	1,64	,692	,894	,997	,000
2,58	1,53	,985	,987	,590	,642
2,17	1,47	,626	1,28	,628	,329
1,71	1,51	4,61	4,81	,715	,315
2,11	1,70	,504	,782	,701	,000
1,70	1,85	1,04	1,04	,590	,438
2,29	1,74	,688	,935	,512	,079

1	1,042
2	5,208
3	10,42
4	22,92
5	37,50
6	53,13
7	58,33
8	59,38
9	66,67
10	77,08
11	80,21
12	84,38
13	88,54
14	90,63
15	91,67
16	91,67
17	91,67
18	91,67
19	91,67
20	91,67
21	91,67

```
 22          91,67
 23          91,67
 24          91,67
 25          91,67
 26          93,75
 27          93,75
 28          93,75
 29          93,75
 30          93,75

STORE LEFT 31210  LSED 10037

 &END;
CPU TIME =  0000  31,199  REAL TIME   00 01 00
```

Appendix 2

LIST OF FIGURES

49. Static Loading rig for rectangular steel joints.

50-53. Experimental and theoretical values of the variation in the closure of milled and ground rectangular joints with position in the joint and with applied load.

54. Surface profile along the mid-axis of a ground rectangular joint.

55. Experimental and theoretical values of the closure of ground and milled rectangular joints between preloads of 3000kg. and 4000kg.

Appendix 3

REFERENCES

1. Earles, S.W.E. & Philpot, M.G. 'Energy dissipation at plane surfaces in contact'. Journal of Mechanical Engineering Science. Vol.9. No.2. 1967

2. Ungar, E.E. & Carbonell, J.R. 'On panel vibration damping due to structural joints'. A.I.A.A. Journal. Vol.4 No.8. 1966

3. M.T.I.R.A. 'Rationalisation of lubricating oils for machine tools'. Machine tool industry research association. July 1968.

4. Grieve, D.J., Kalizer,H. & Rowe, G.W. 'The effect of cutting conditions on bearing area parameters'. Proceedings for the 9th International Machine Tool Design and Research Conference. 1968. University of Birmingham.

5. Jones, M.H., Howells, R.I.L., Probert, S.D. 'Solids in Static Contact'. Wear 1968. No.12.

6. Dekoninck, C. 'Experimental investigation of the normal dynamic stiffness of metal joints'. International journal of Machine Tool Design and Research Vol.9 1969.

7. Hother-Lushington, S. & Johnson, D.C. 'Damping properties of thin oil films subjected to high frequency alternating loads'. Journal of Mechanical Engineering Science. Vol.5 No.2. 1963.

8. Andrew, C. 'Damping in fixed joints'. M.T.I.R.A. conference on 'Damping Machine Tool Structures'. April 1969.

9. Peters, J. 'Damping in machine tool construction'. Proceedings 6th International Machine Tool design and research conference, Manchester 1965

10. Connoly, R. & Thornley, R.H. 'The significance of joints on the overall deflection of machine tool structures'. Proceeding 8th International Machine tool design and research conference. Manchester 1967.

11. Tobias, S.A. 'Machine tool vibration'. Handbook of shock and vibration (Harris and Crede). Chapter 40. McGraw Hill.

12. Archard, J.F. 'Elastic Deformation and the laws of friction'. Proceedings of the Royal Society (London). A.243 (1957).

13. Kragelsky, I.V. & Demkin, N.B. 'Contact areas of rough surfaces'. Wear 3. 1960.

14. Thornley, R.H., Connoly, R., Barash, M.M. & Koenigsberger,F. 'The effect of surface topography upon the static stiffness of machine tool joints'. International journal of machine tool design and research. 1965 Vol.5.

15. Thornley, R.H., Connoly, R. & Koenigsberger, F. 'The effect of flatness of the joint faces upon the static stiffness of machine tool joints'. Proceedings of the Institution of Mechanical Engineers 1967-68, 182.

16. Waring, A.E. 'The damping of fluid-filled metal to metal joints undergoing normal vibration'. Ph.D. Thesis University of Bristol 1969.

17. Andrew, C., Cockburn, J.A. & Waring, A.E. 'Metal surfaces in contact under normal forces, some dynamic stiffness and damping characteristics'. Proceedings of the Institution of Mechanical Engineers 1967. Part 3k.

18. Goodman, L.E. 'A review of progress in analysis of interfacial slip damping'. A.S.M.E. Colloqium on Structural Damping 1959.

19. Day, P.E. 'Experimental investigation of the stiffness of a clamped joint under normal loading'. Ph.D. Thesis University of Warwick.1970.

20. Corbach,K. 'The dynamic stiffness of fixed and moving joints in machine tools'. Mashinemarkt, Jg. 72 (1964) No.79. (Translation by U.M.I.S.T. 1969).

21. Eisle, F. & Corback, K. 'Dynamic stiffness of slides and joints on machine tools'. Maschinenmarkt, Wurzburg, 70.Jg.No.89. 1964. (Translation by M.T.I.R.A. T.136).

22. Greenwood, J.A. & Williamson, J.B.P. 'Contact of nominally flat surfaces'. Proceedings of the Royal Society of London, Series A. 295. 1966

23. McLeod, A.J. & Bishop, R.E.D. 'The forced vibration of circular flat plates'. Mechanical Engineering Science, Monograph No.1. 1965

24. Sydenham, P.H. 'Position sensitive photo-cells and their application to static and dimensional metrology'. Optica Acta 1969. 16(3).

25. Kragelskii, I.V. 'Friction and wear'. Butterworths. 1965.

26. Timoshenko & Young. 'Elements of strength of materials'. Van Nostrand. 1935

27. Day, P.E. & Marples, V.M. 'A technique for measuring the flatness errors on machined surfaces'. Journal of Physics E. Scientific Instruments. 1972. Vol 5

28. Day, P.E. & Marples, V.M. 'Phase calibration of displacement sensitive vibration transducer systems'. Journal of physics E. Scientific Instruments. 1971 Vol 4

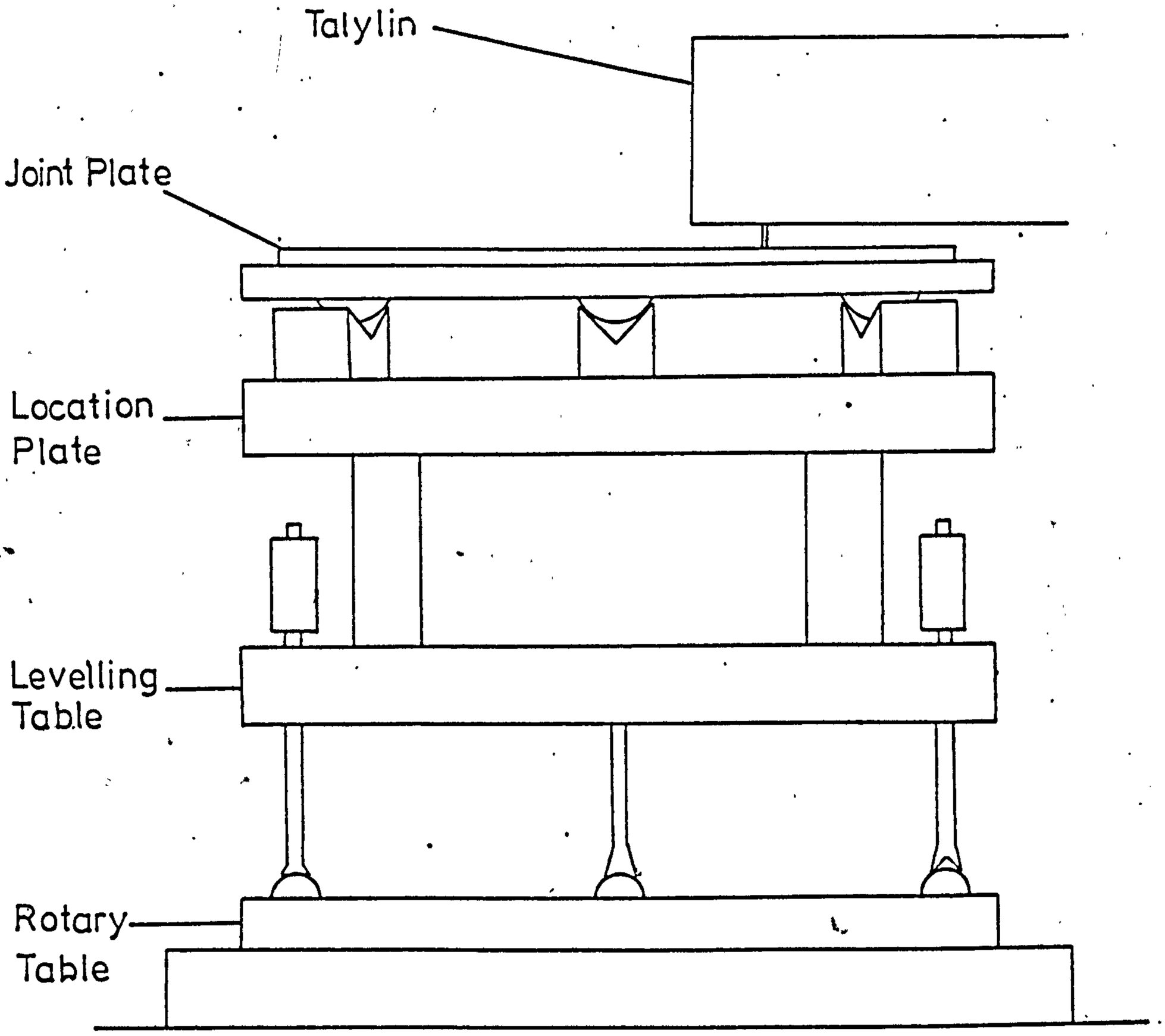

Fig 1 Schematic of mounting of joint plates for measurement of surface flatness

Vertical Magnification x 1000

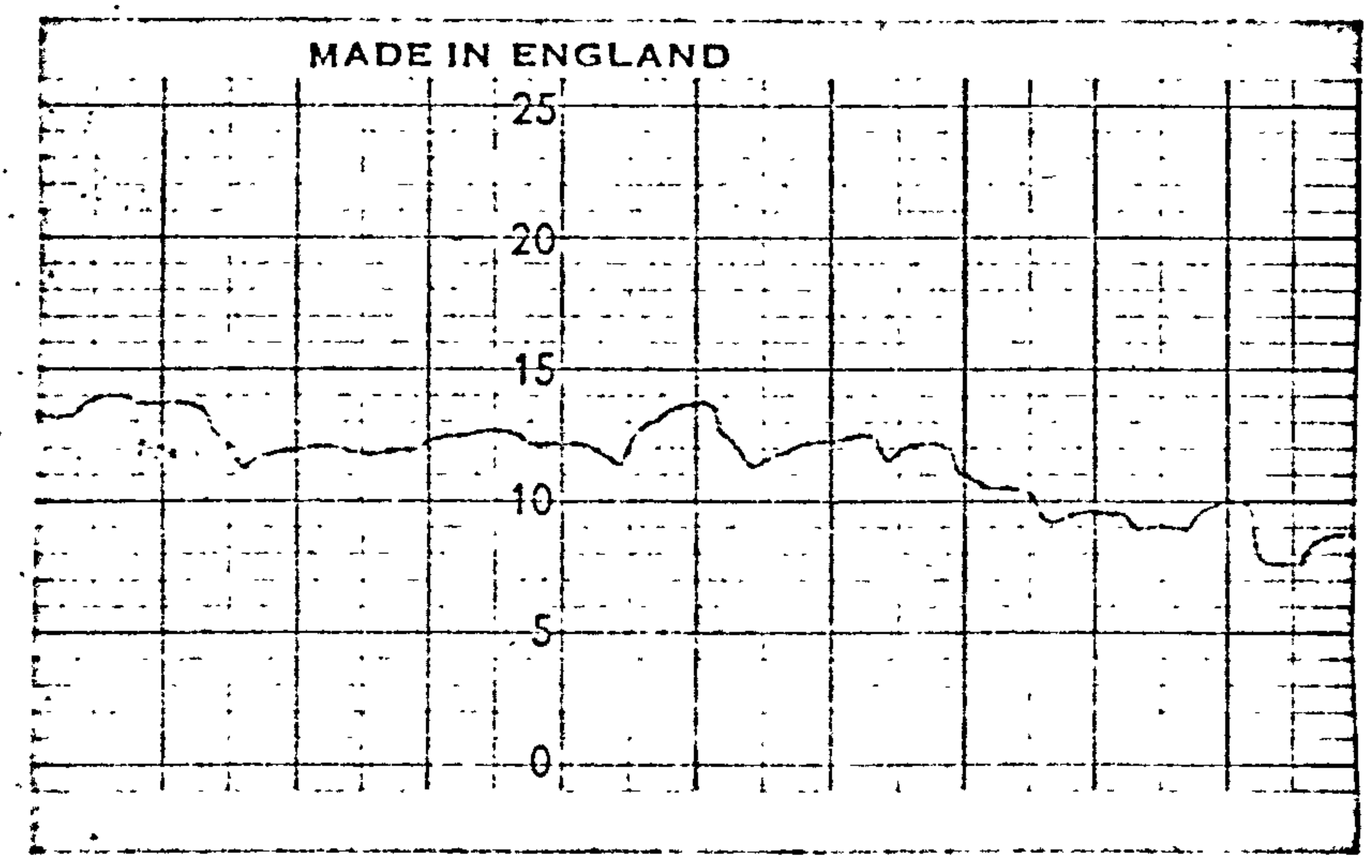

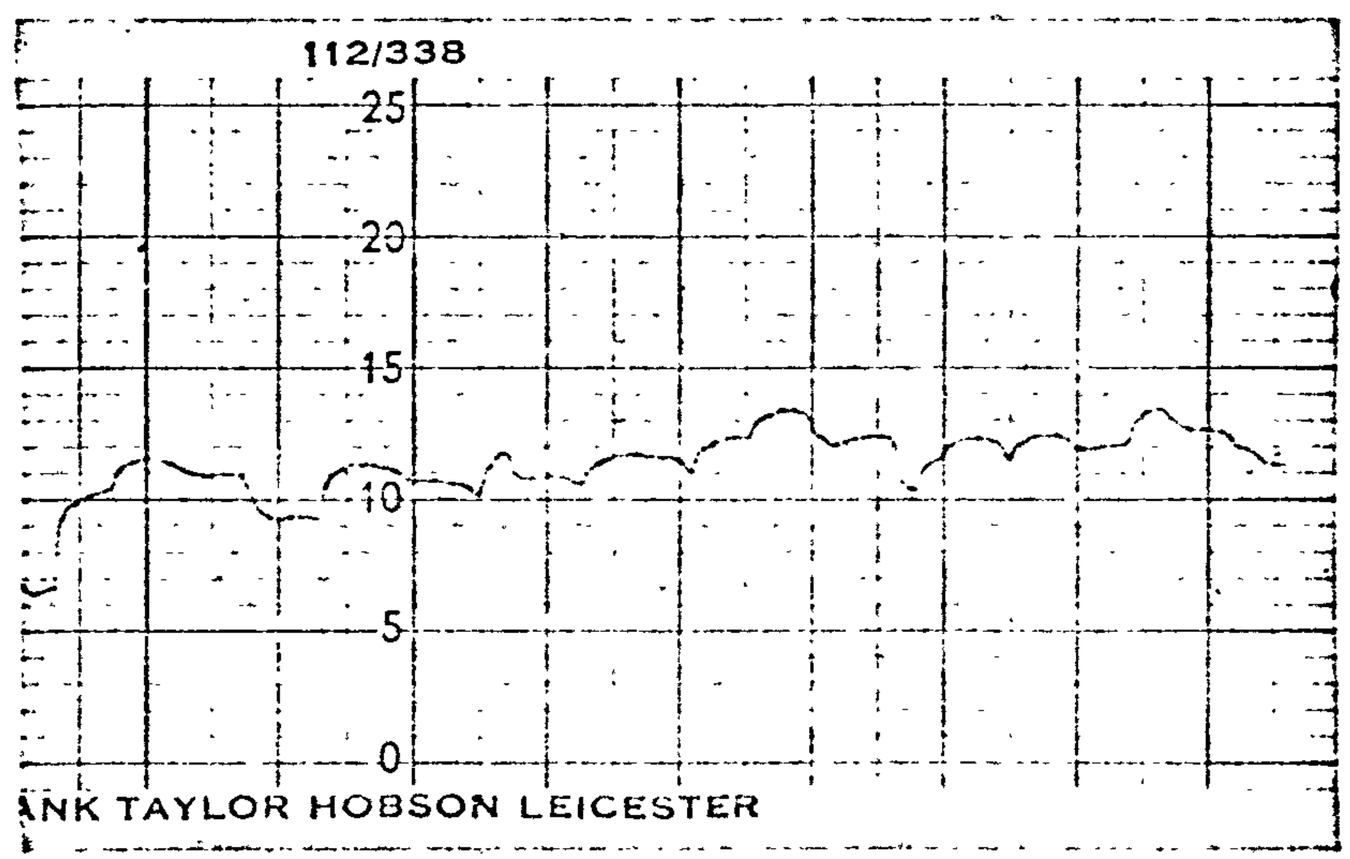

Turned Surface

Horizontal Magnification x 5

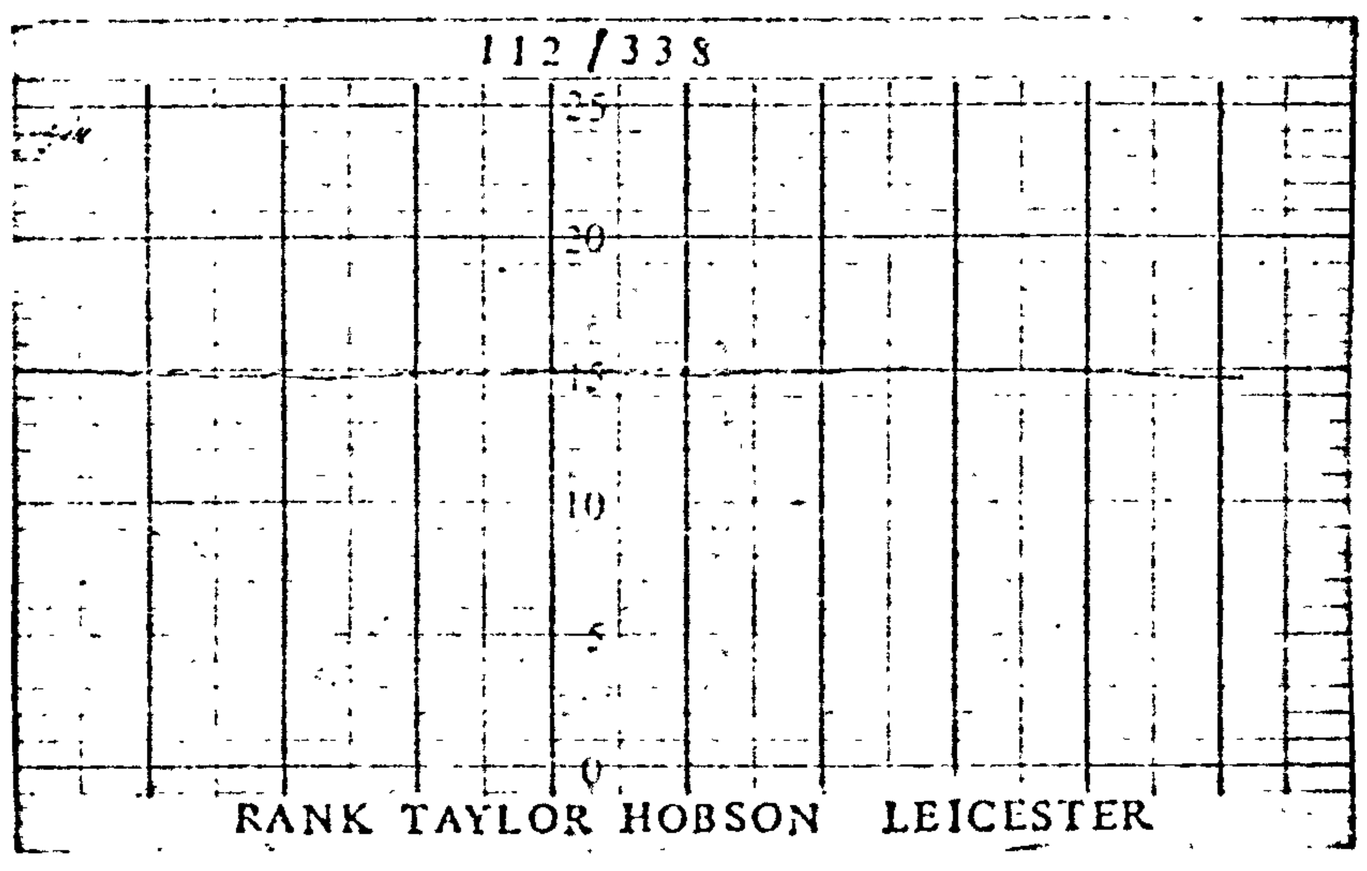

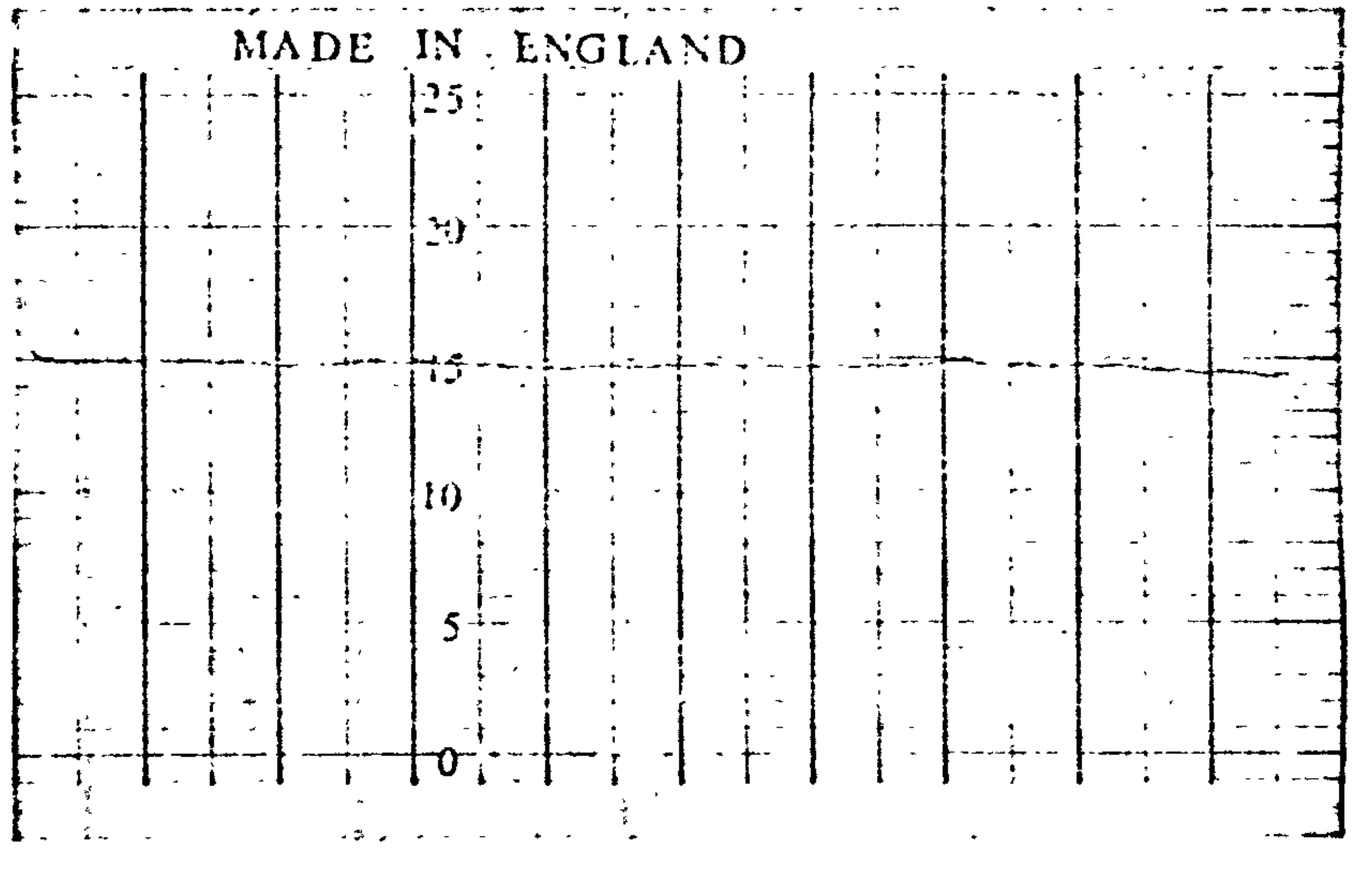

Ground Surface

Fig. 2 Sample Talylin traces taken across a diameter of the surface of turned and ground annular joints.

Surface	Direction	Mean of Deviations μm	Standard Deviation of Deviations
Turned	Radial	0·87	0·32
	Circumferential	0·90	0·30
Ground	Radial	0·116	0·046
	Circumferential	0·060	0·035

Fig. 3 Deviation of points on joint surfaces from the straight line between measuring positions

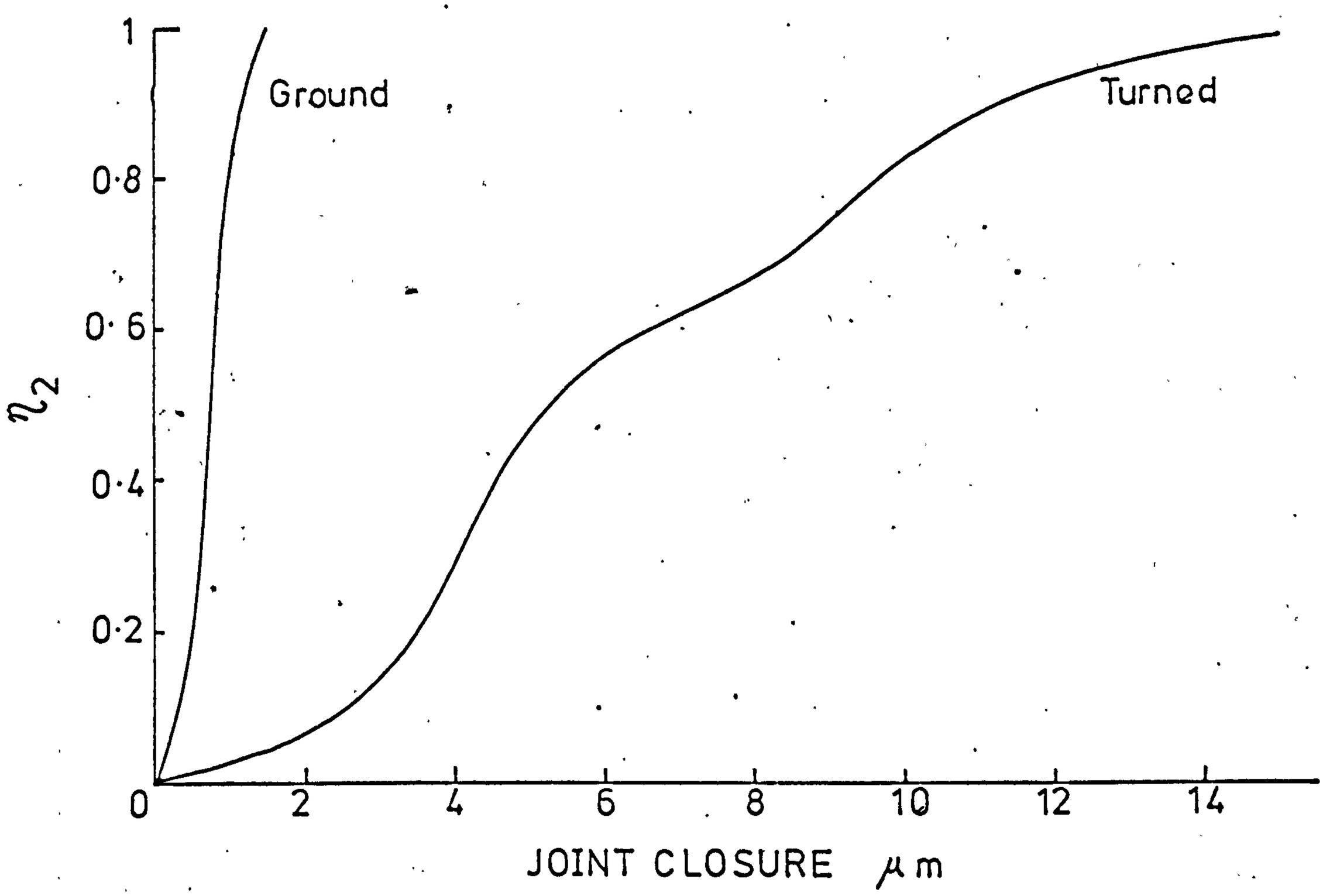

Fig. 4 Comparison of the proportionate contour area of joints with ground and turned surfaces, measured as a function of joint closure.

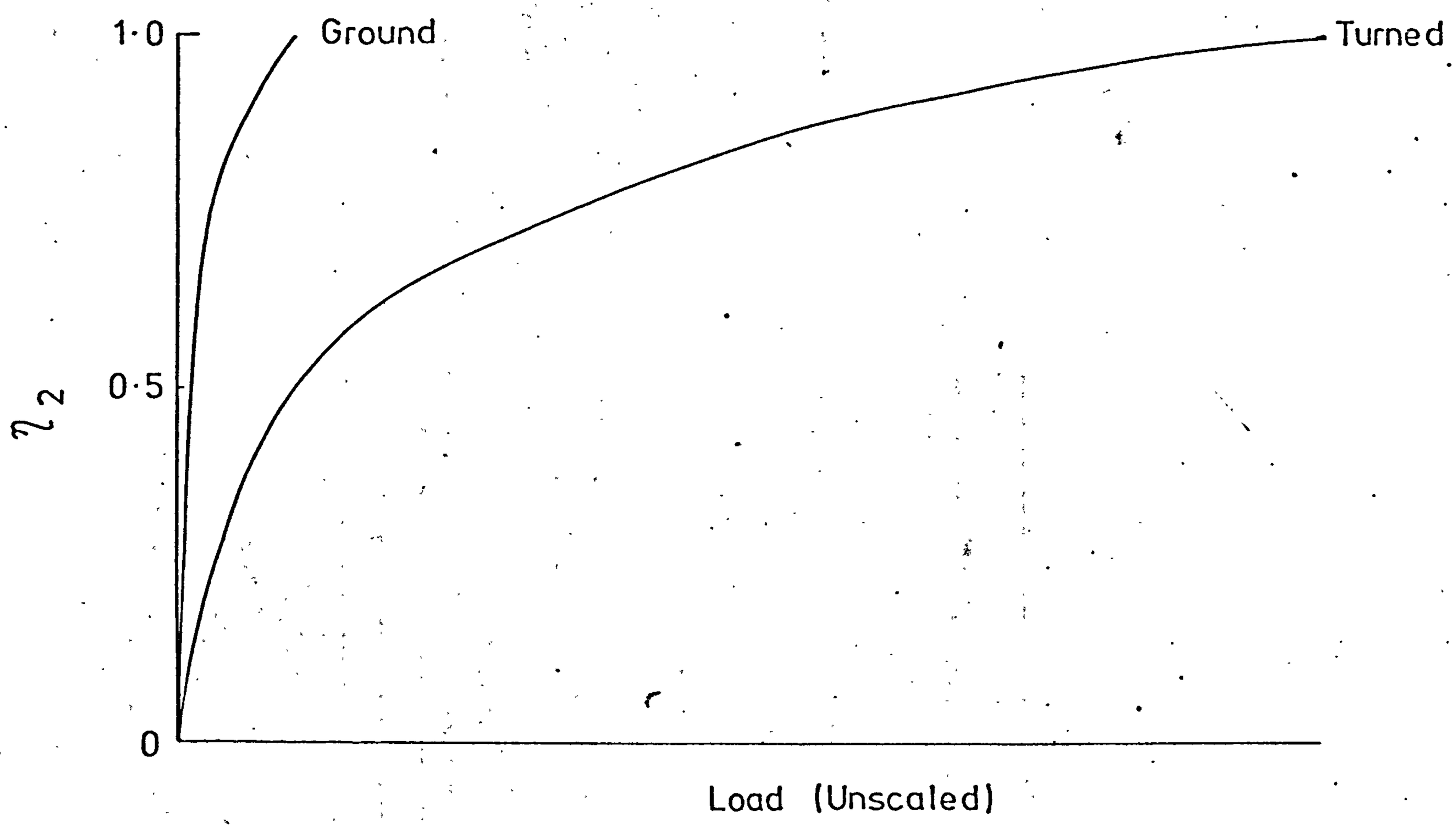

Fig. 5 Variation in η_2 with Load for Turned and Ground Joints

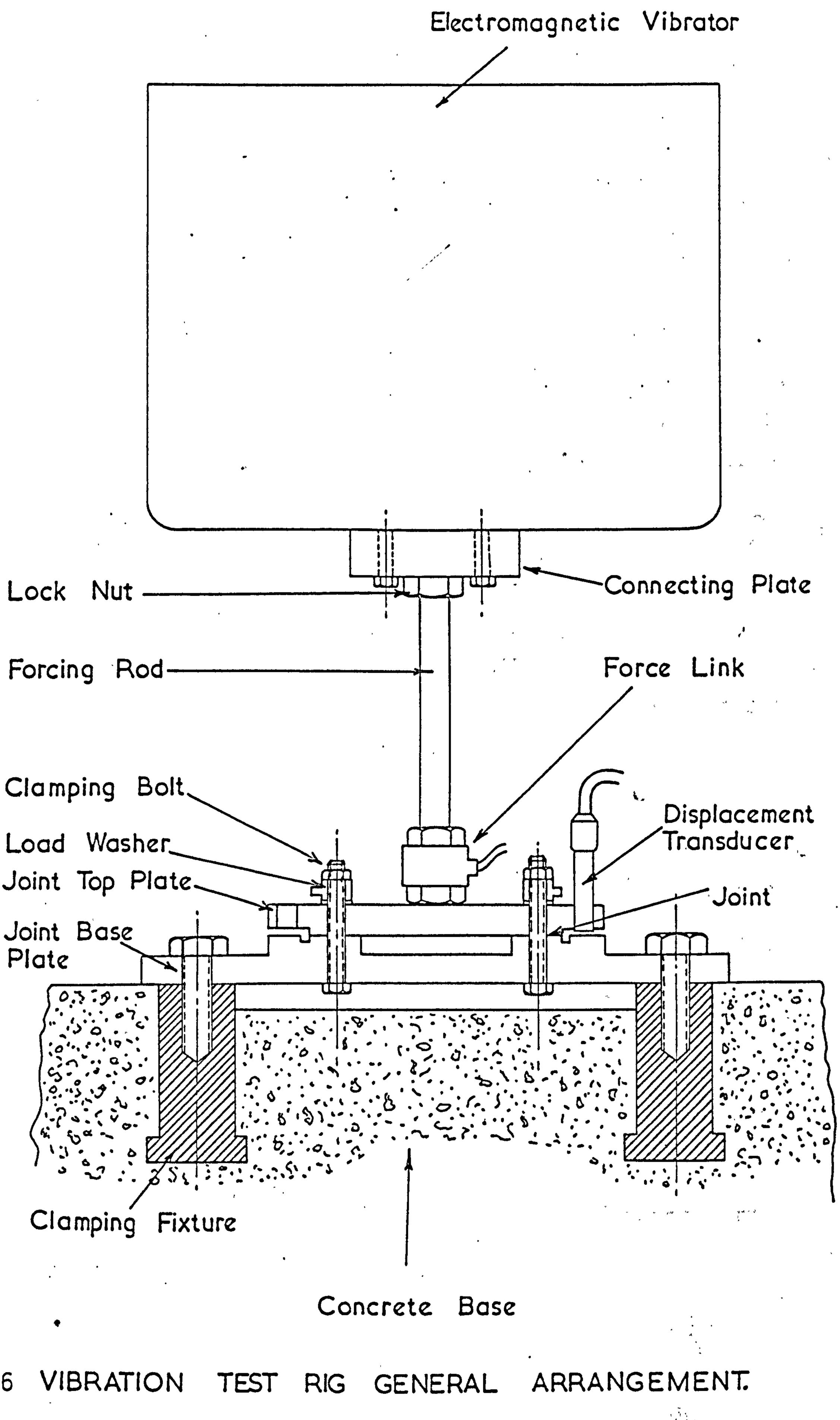

Fig 6 VIBRATION TEST RIG GENERAL ARRANGEMENT.

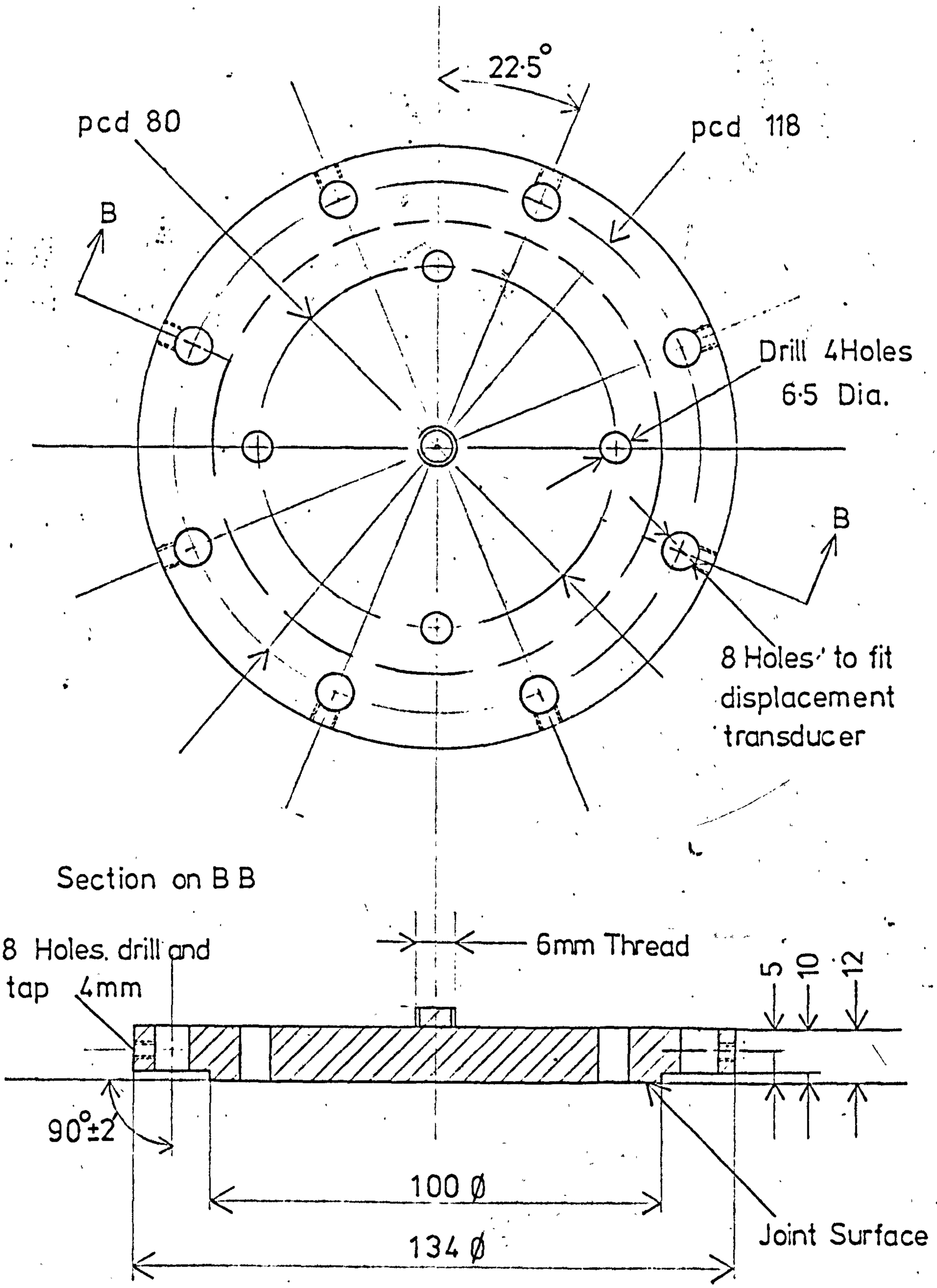

Material. EN 8 Steel

Dimensions mm.

Fig. 7 Joint Top Plate

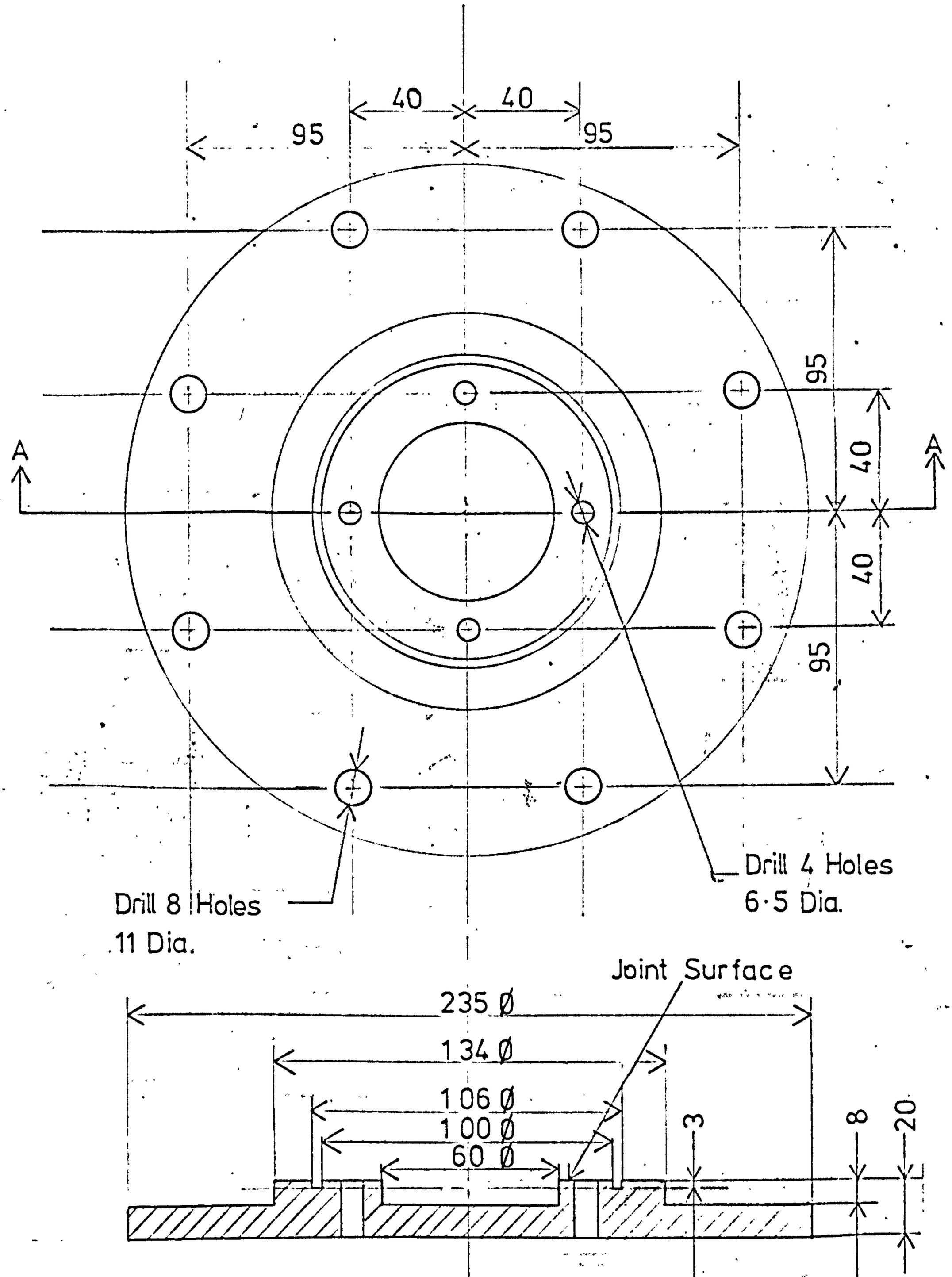

Fig. 8 Joint Base Plate

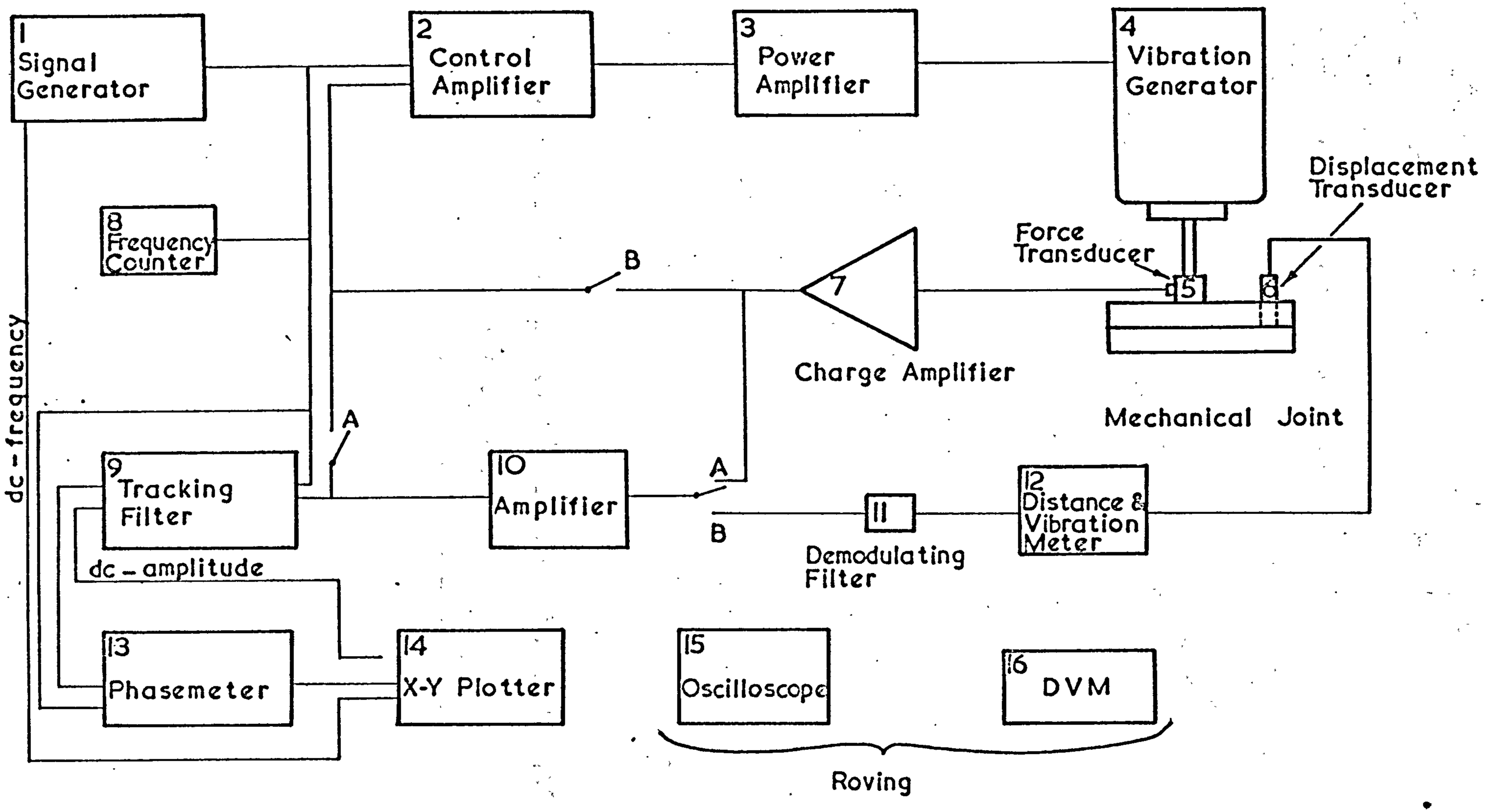

Fig. 9 Instrumentation for the measurement of dynamic joint motion.

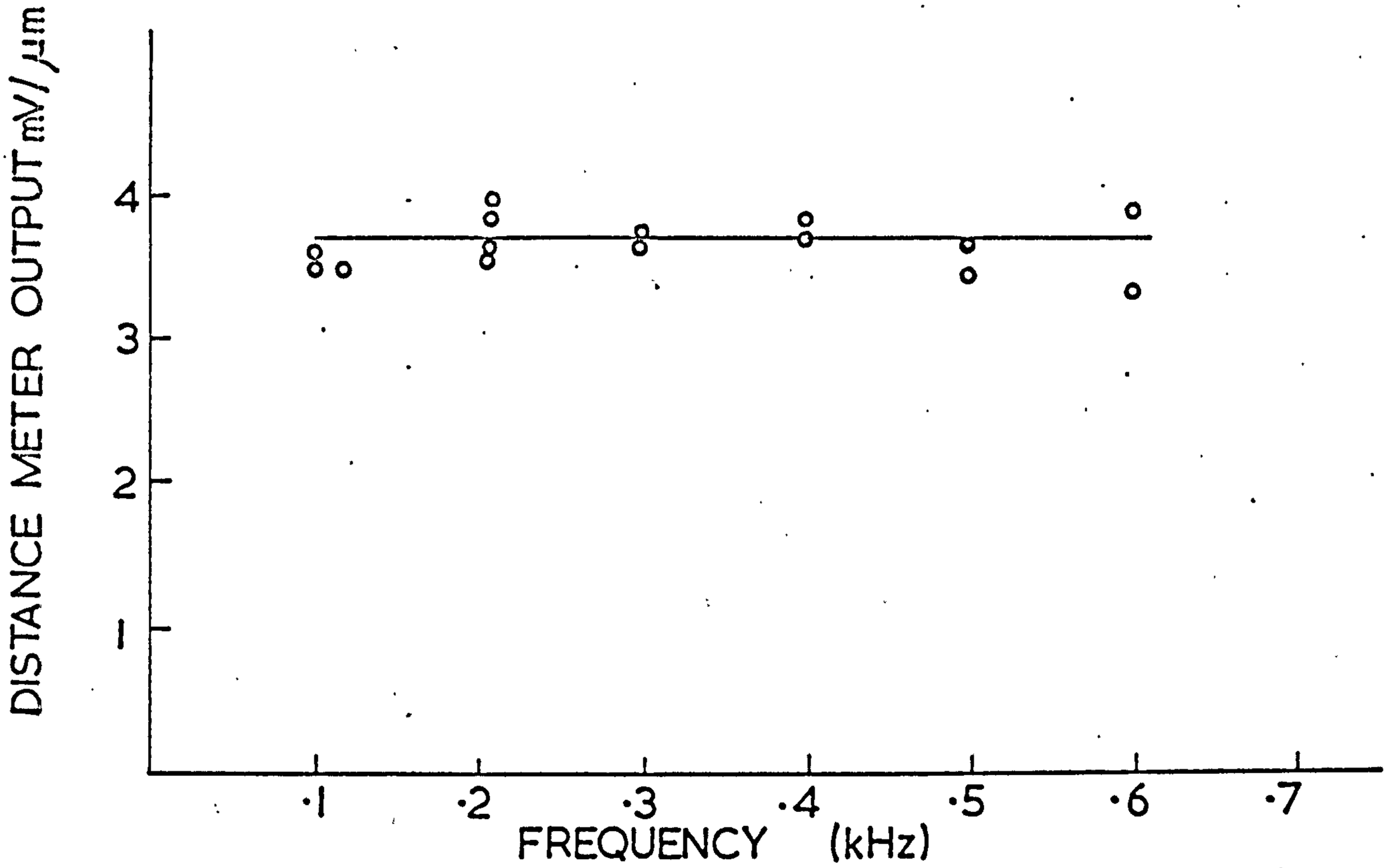

Fig 10 a) DYNAMIC AMPLITUDE CALIBRATION OF DISTANCE METER

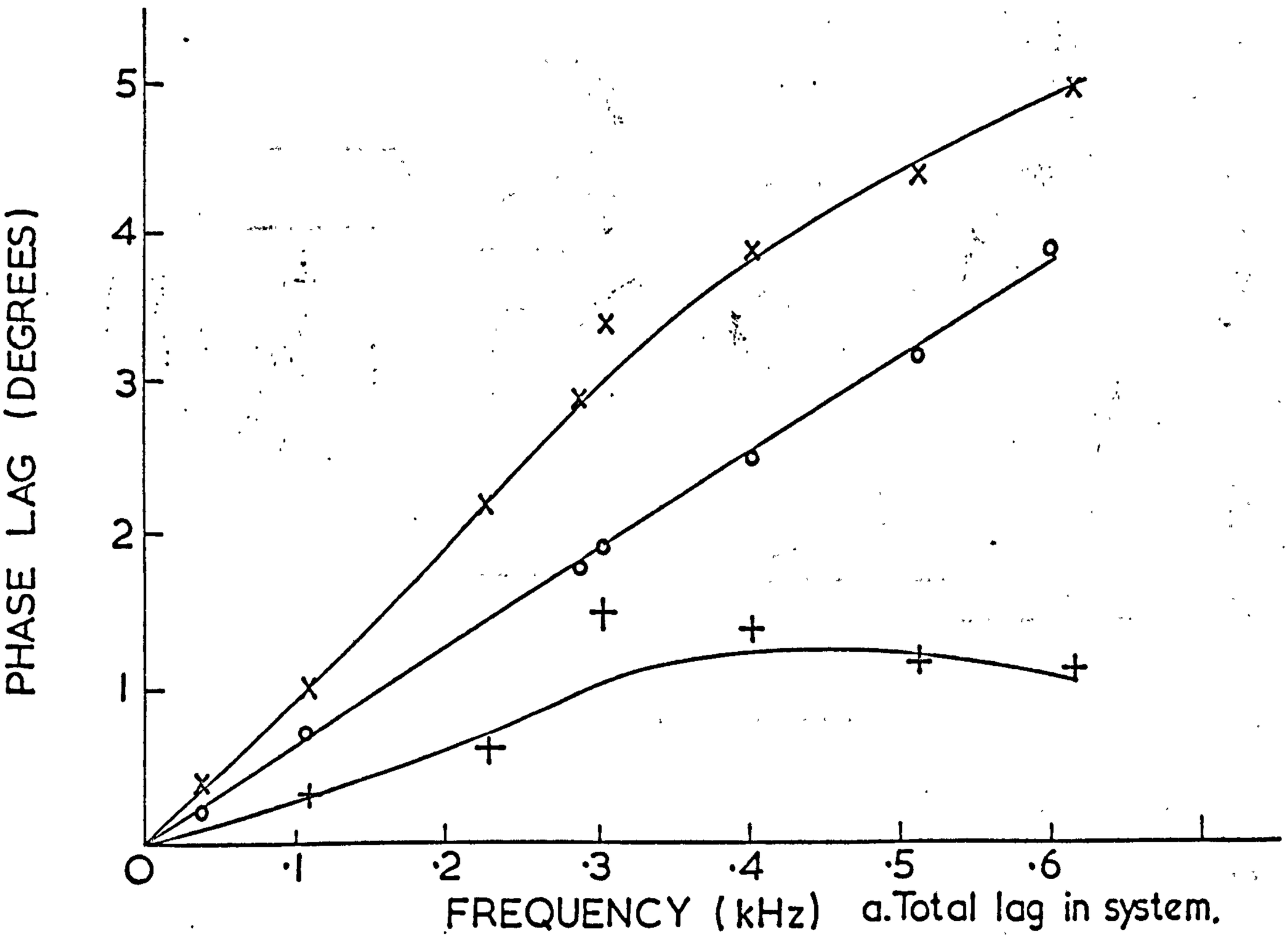

Fig 10 b) DYNAMIC PHASE CALIBRATION OF DISTANCE METER AND DEMODULATING FILTER

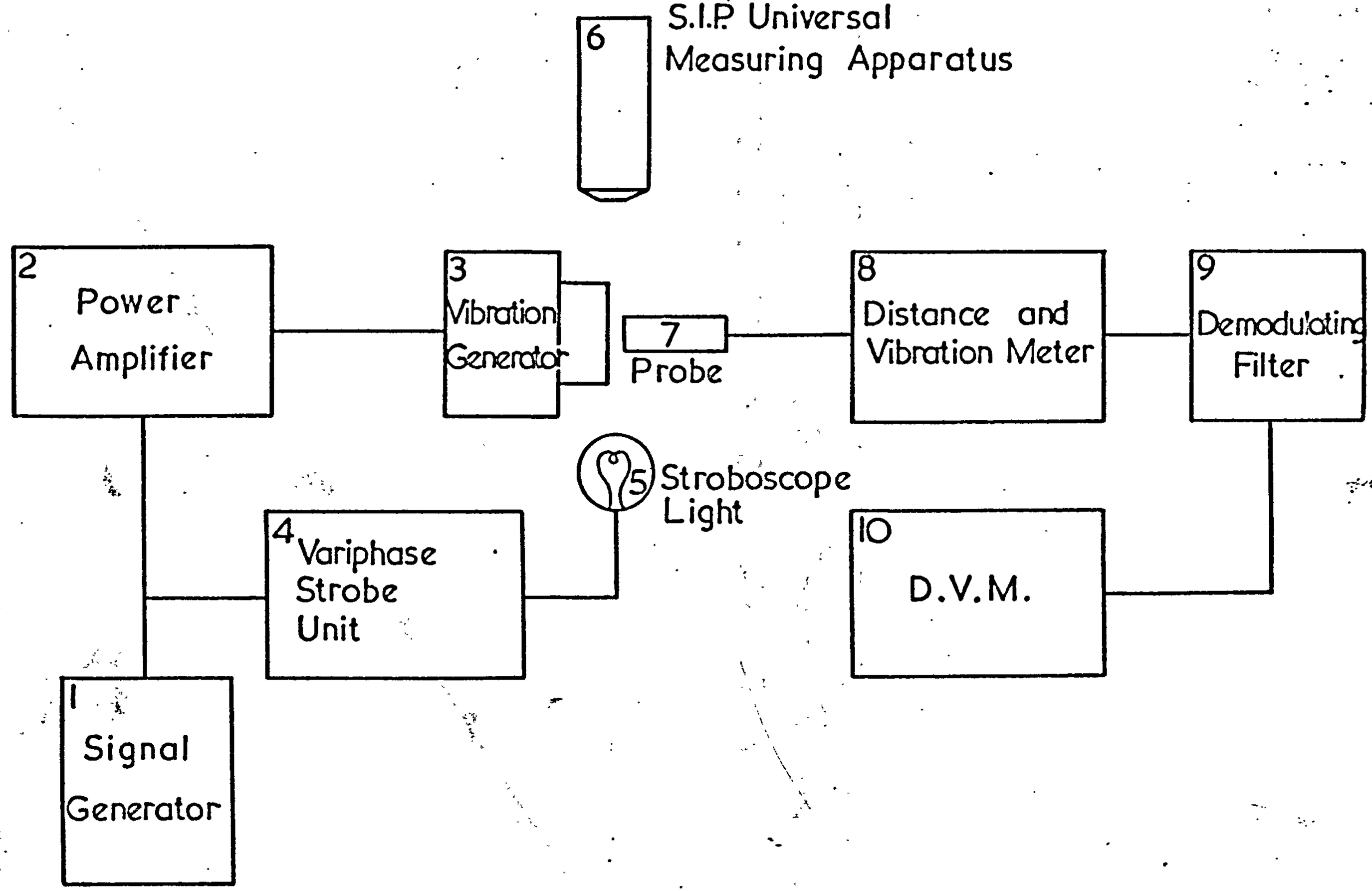

Fig 11 Apparatus for Amplitude Calibration of Wayne-Kerr Distance and Vibration Meter.

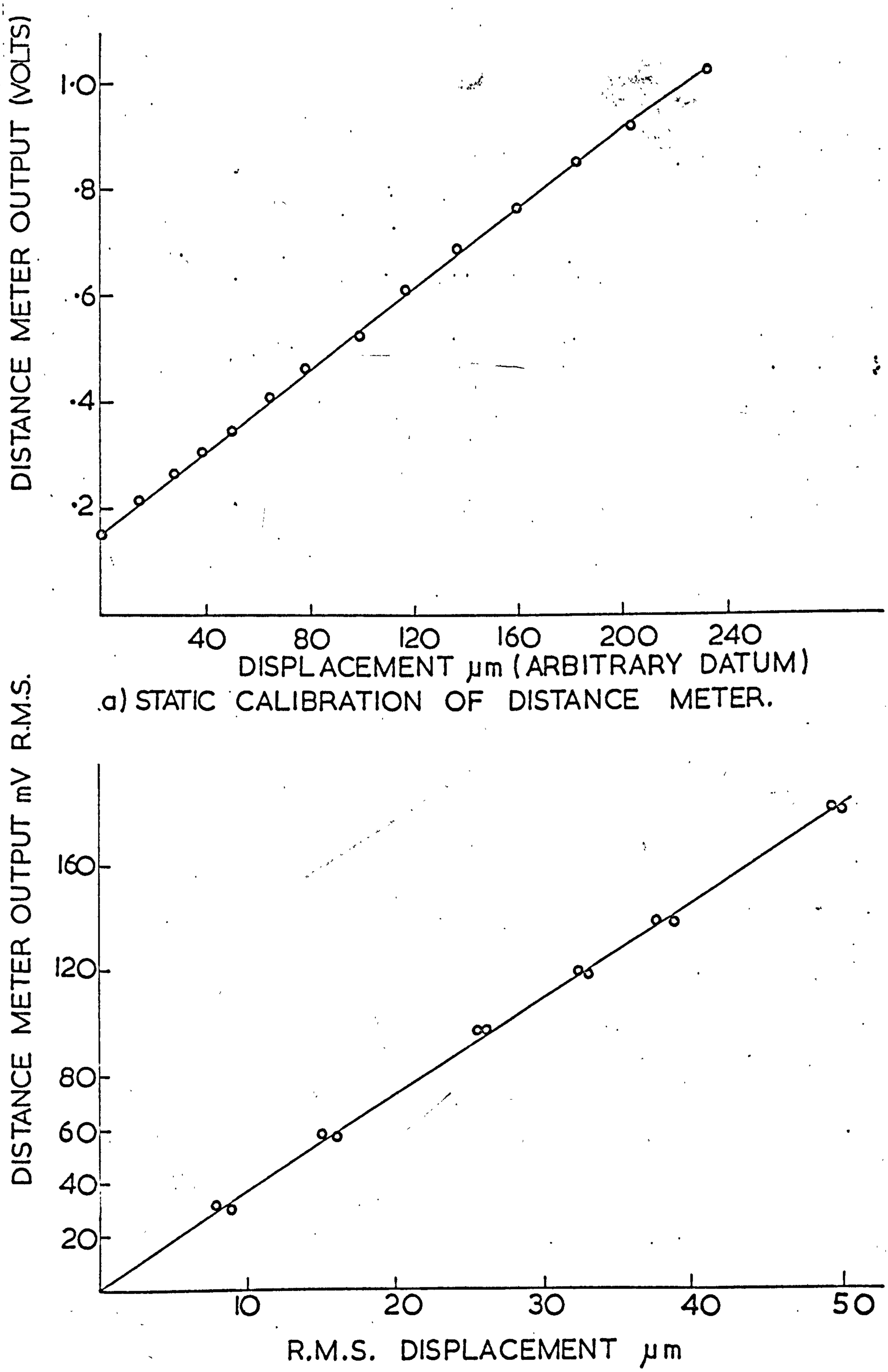
DISTANCE METER OUTPUT (VOLTS)
1·0
·8
·6
·4
·2
40
80
120
160
200
240
DISPLACEMENT μm (ARBITRARY DATUM)
a) STATIC CALIBRATION OF DISTANCE METER.
DISTANCE METER OUTPUT mV R.M.S.
160
120
80
60
40
20
10
20
30
40
50
R.M.S. DISPLACEMENT μm
b) AMPLITUDE CALIBRATION OF DISTANCE METER AT 200 Hz.

Figure 12

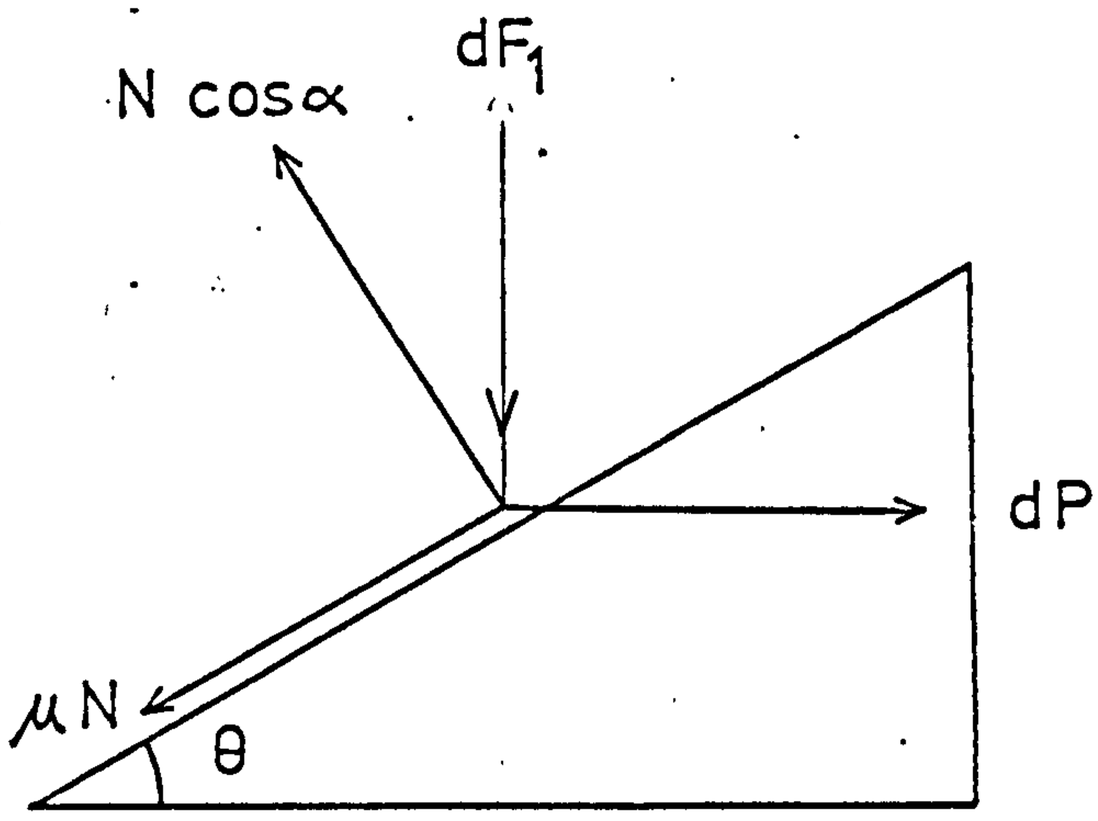

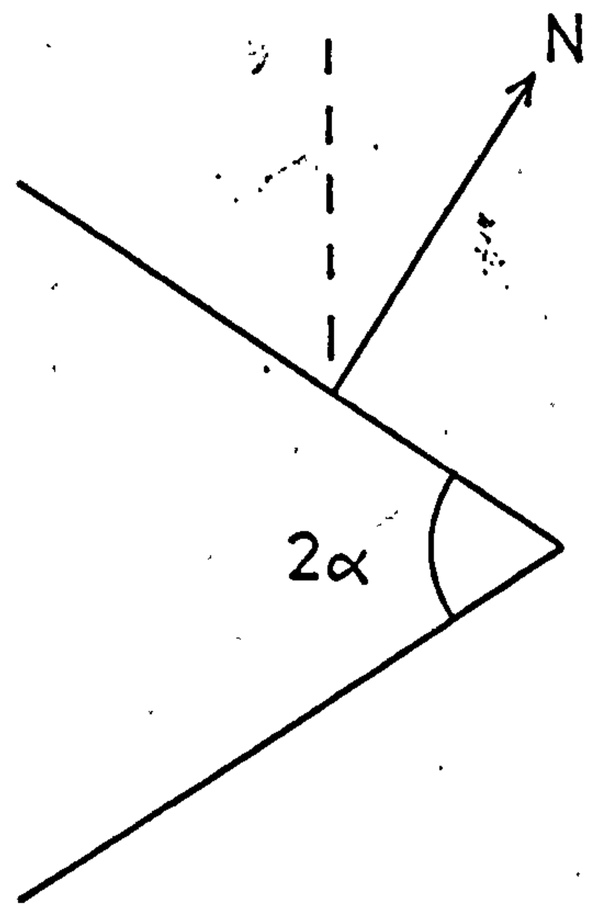

dF_1 : Element of Bolt Load carried by Section of Thread.

dP_1 : Element of Applied Load overcoming Thread Resistance.

$N \cos\alpha$: Component of Normal Reaction on Thread acting in plane of dF_1 and dP_1.

N : Frictional Resistance.

Fig 13. Thread Loading Diagram.

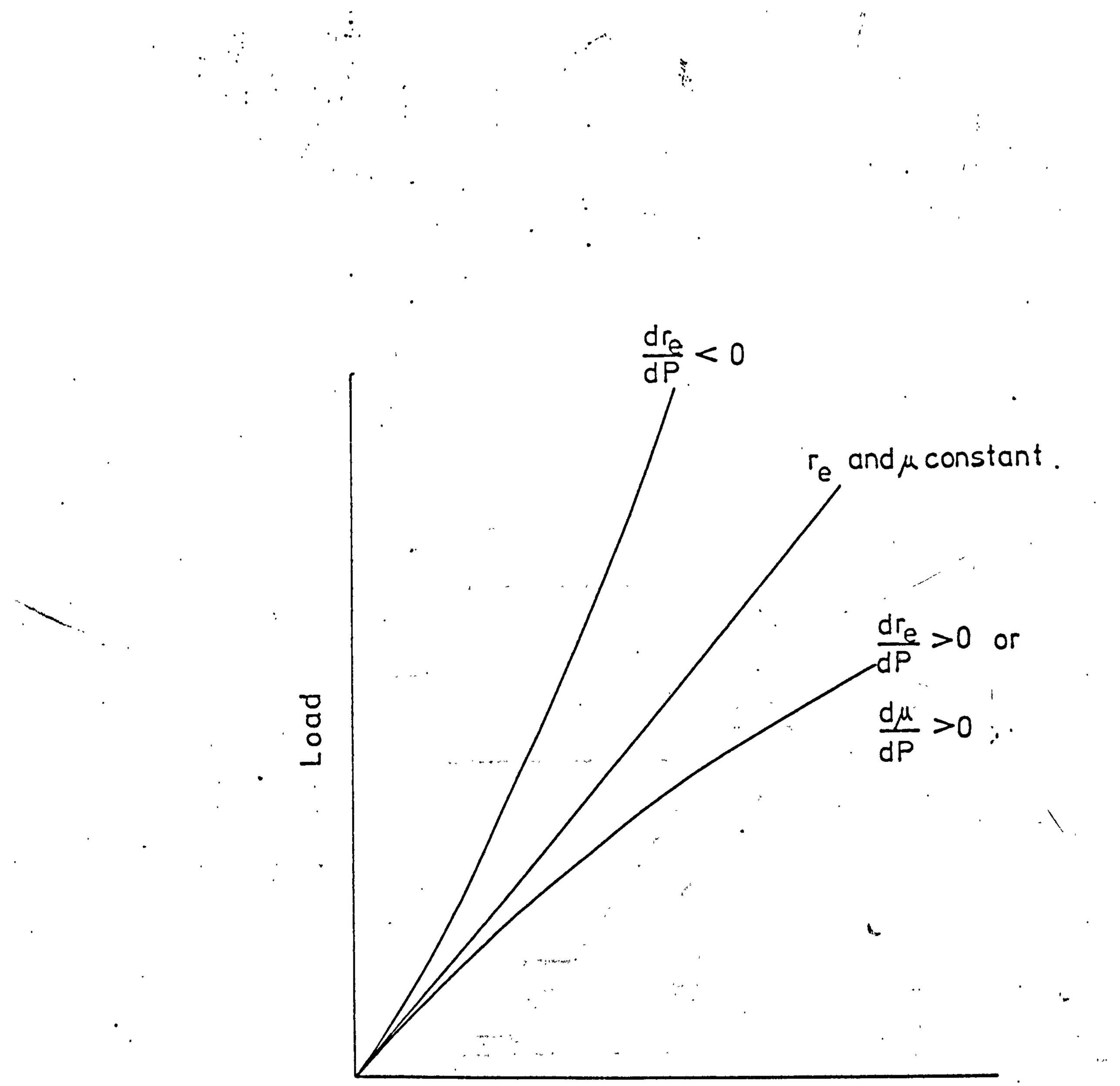

Fig. 14 Deviations from a Linear Bolt Load/ Applied Torque Relationship

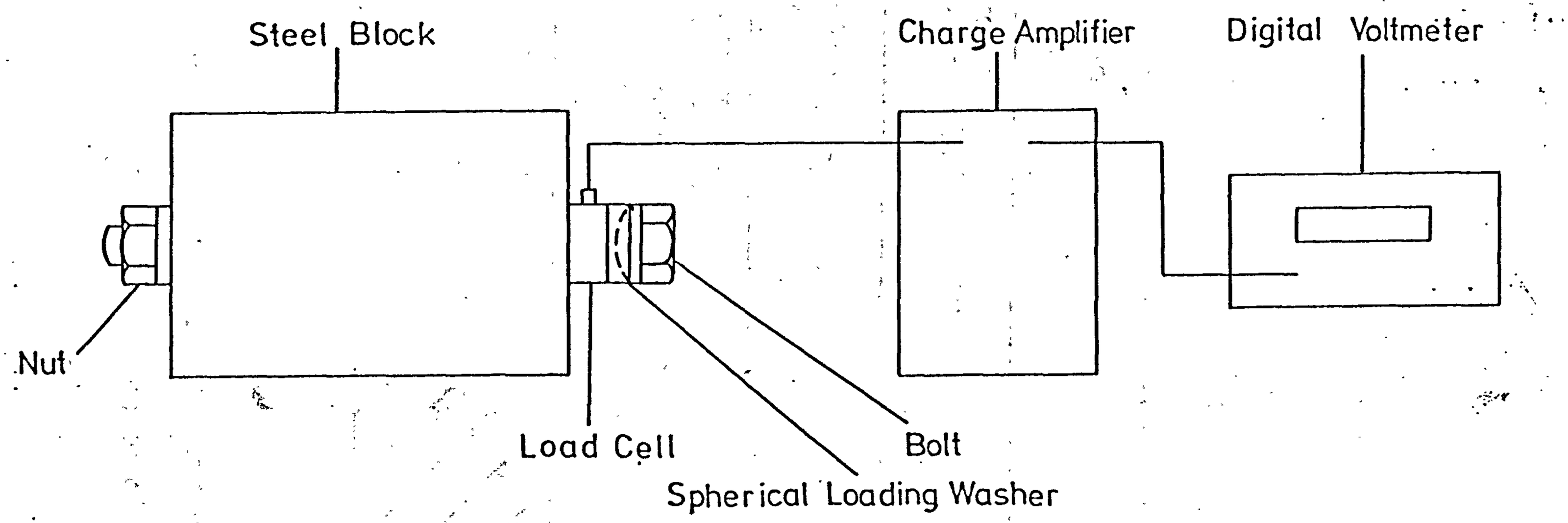

Fig. 15 Apparatus for Measurement of Bolt Load / Applied Torque Characteristic.

	Linear Solution		Quadratic Solution		
	Gradient	Standard Deviation	Linear Coeff.	Quadratic Coeff.	Standard Deviation
12mm. as from stores	498	321	450	13·8	309
12mm. machine oil lubricated	526	476	458	19·3	452
12mm. ground nut face and washer	523	407	531	-18·7	383
6mm. as from stores	872	92	1120	-230	75
Mean of standard devs. from curves fitted to results taken from individual 6mm. bolts.		85·5			63·6
Mean of standard devs. from curves fitted to results from single loading cycles of 6mm. bolts.		60·5			24·1

Fig. 16 Linear and quadratic curve fits on the experimental measurements of the variation of bolt load with applied torque. (Units : m^{-1})

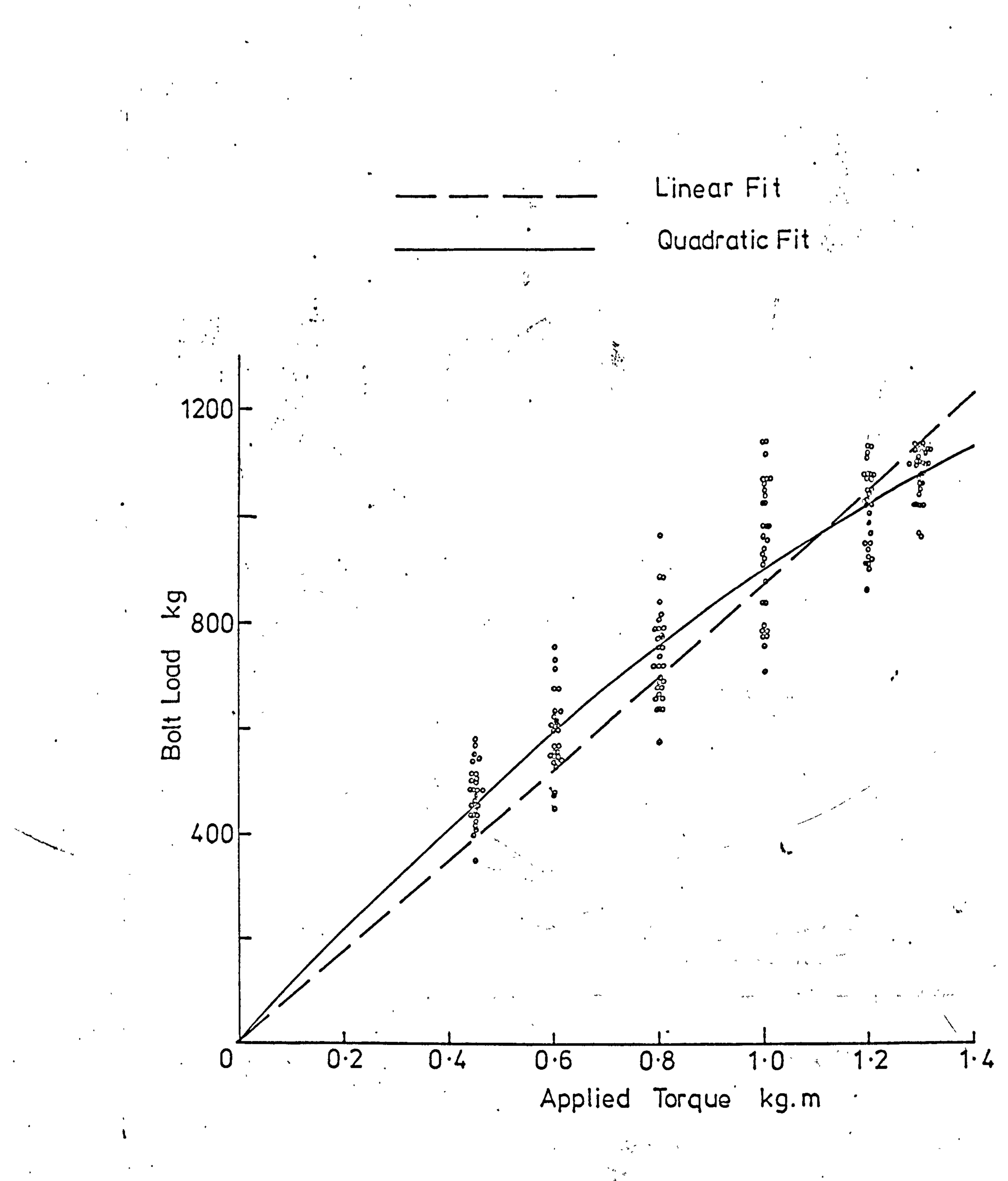

Fig. 17 Variation in Bolt Load with Applied Torque : Aggregate Results from 6mm Bolts.

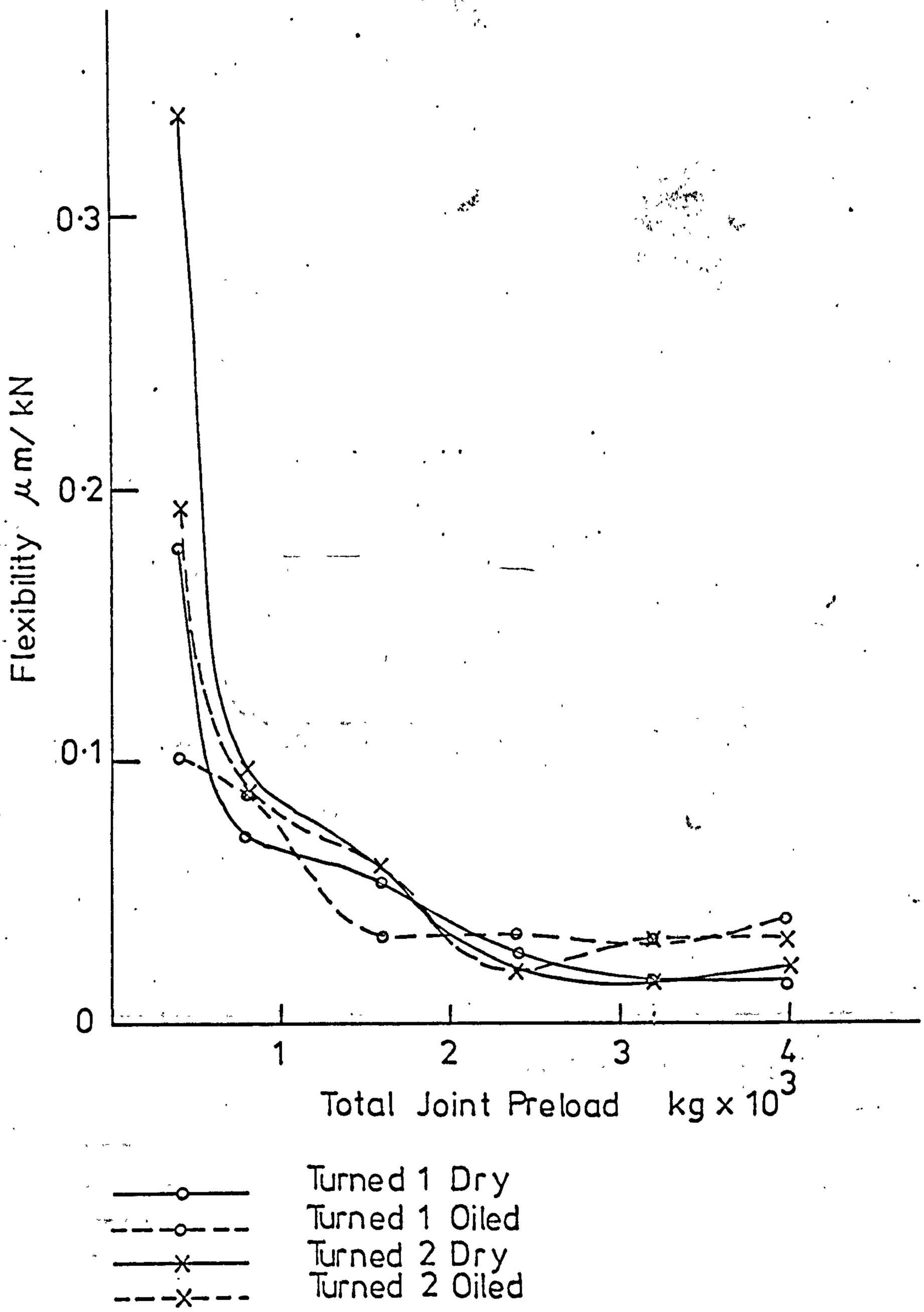

Fig. 18 Variation of Rms. Flexibility of Turned Joints with Preload.

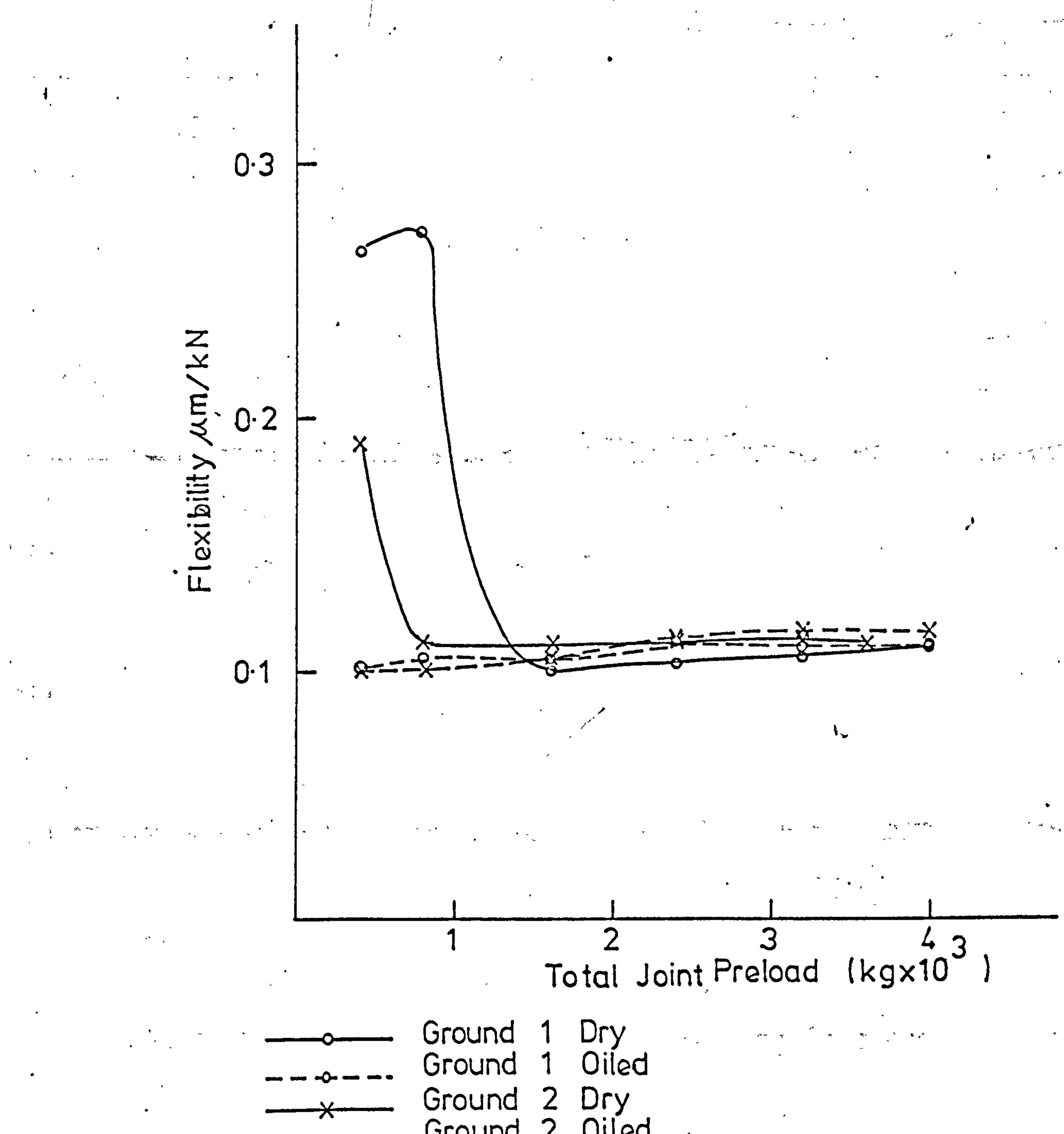

Fig. 19 Variation of Rms. Joint Flexibility of Ground Joints with Preload.

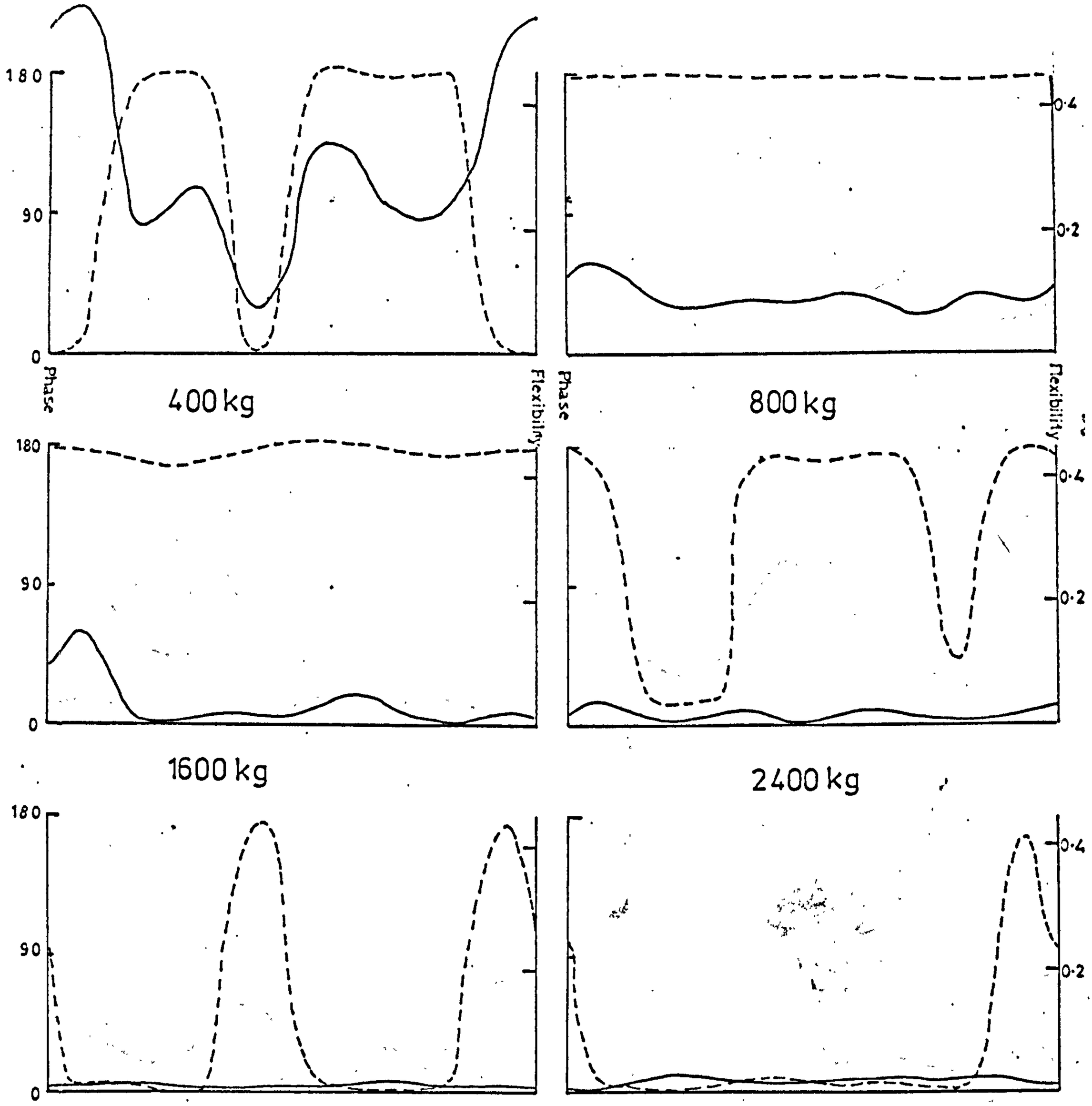

Fig 20 Variation in the Dynamic Flexibility of a Turned Dry Joint and of the Phase Lag between the joint motion and the applied force, plotted as a function of position around the joint annulus, for different joint preloads.

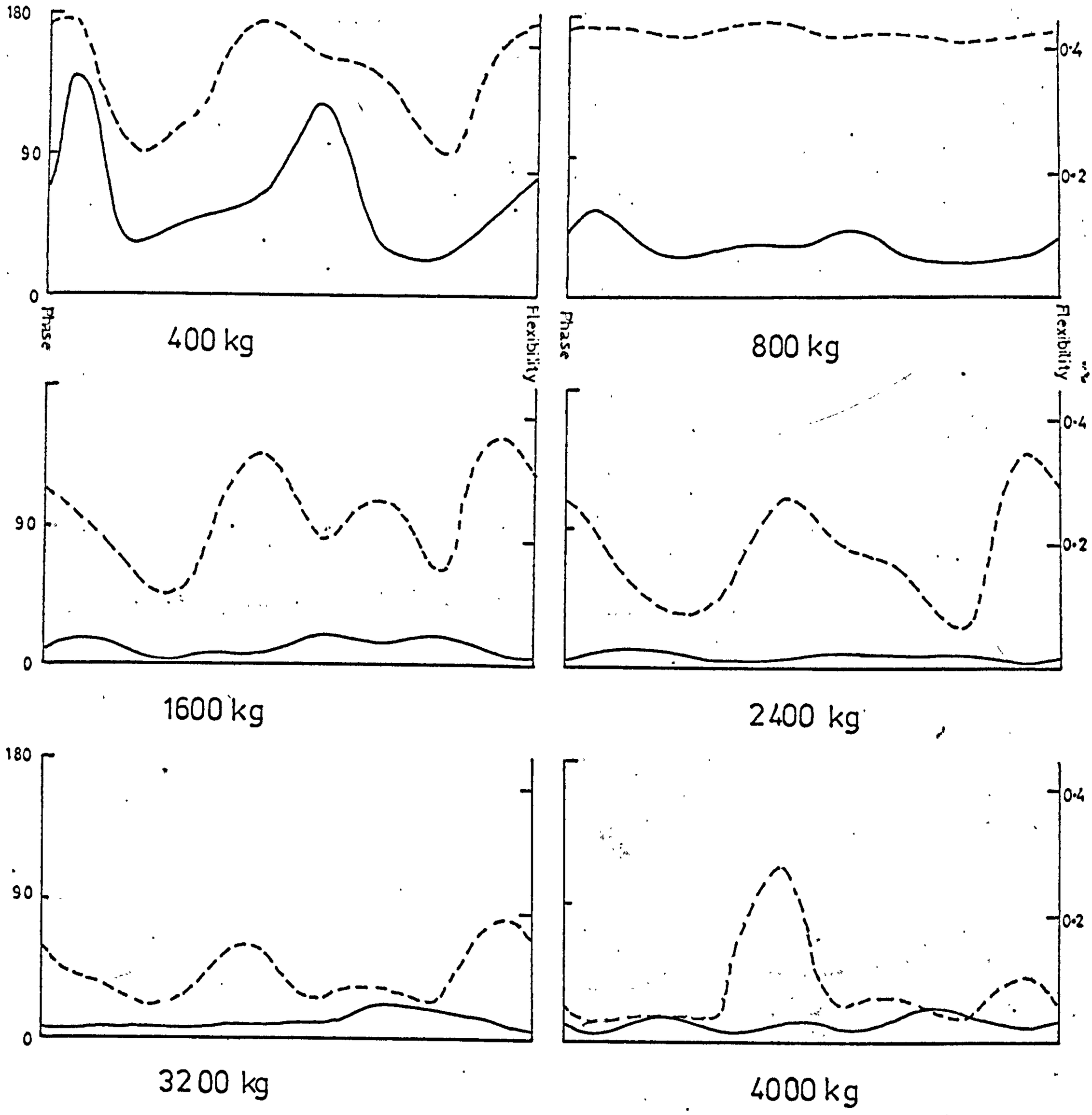

Fig. 21 Variation in the Dynamic Flexibility of a Turned Oiled Joint and of the Phase Lag between the Joint motion and the applied force, plotted as a function of position around the joint annulus, for different joint preloads.

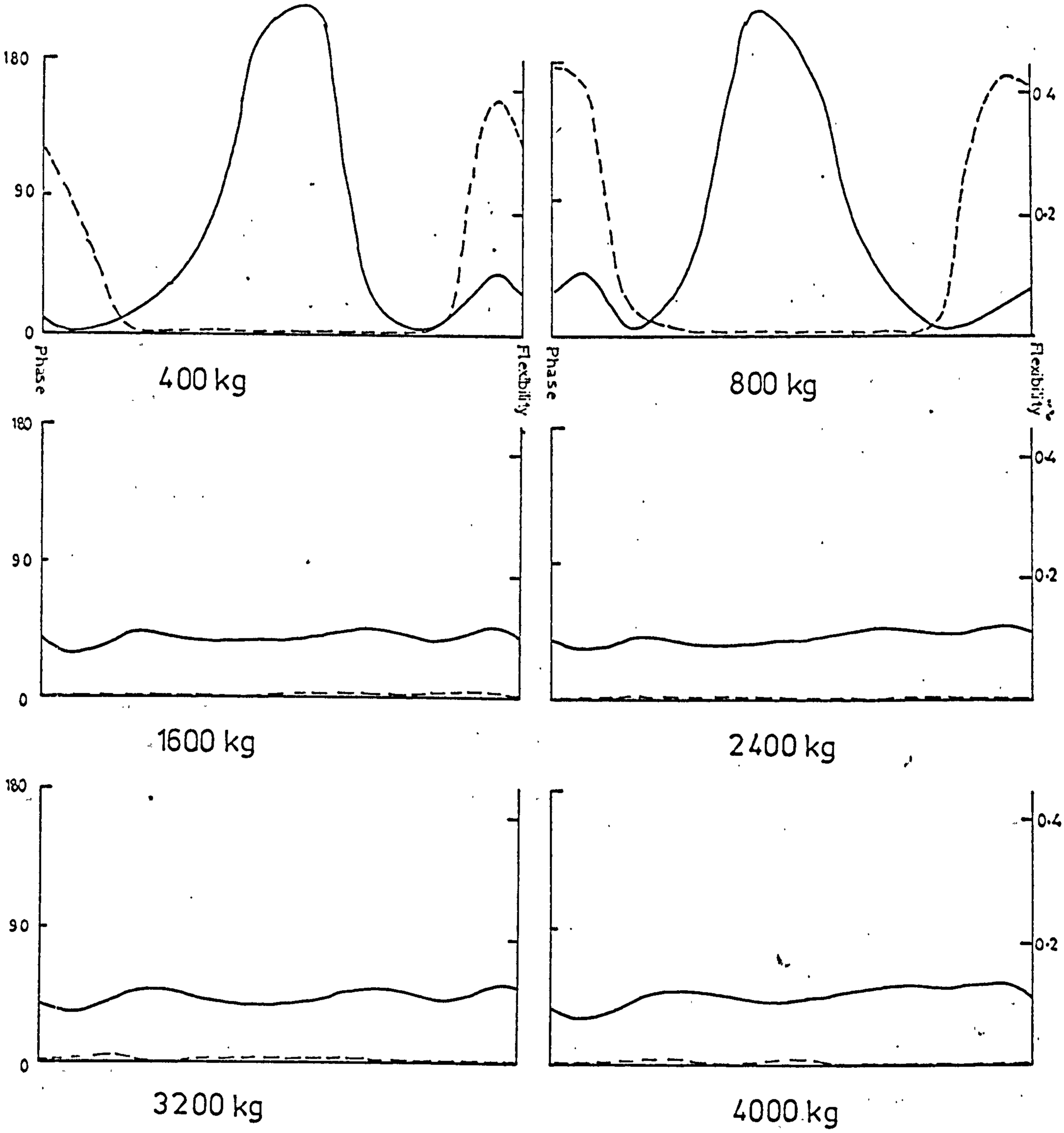

Fig. 22 Variation in the Dynamic Flexibility of a Ground Dry Joint and of the Phase Lag between the joint motion and the applied force, plotted as a function of position around the joint annulus, for different joint preloads.

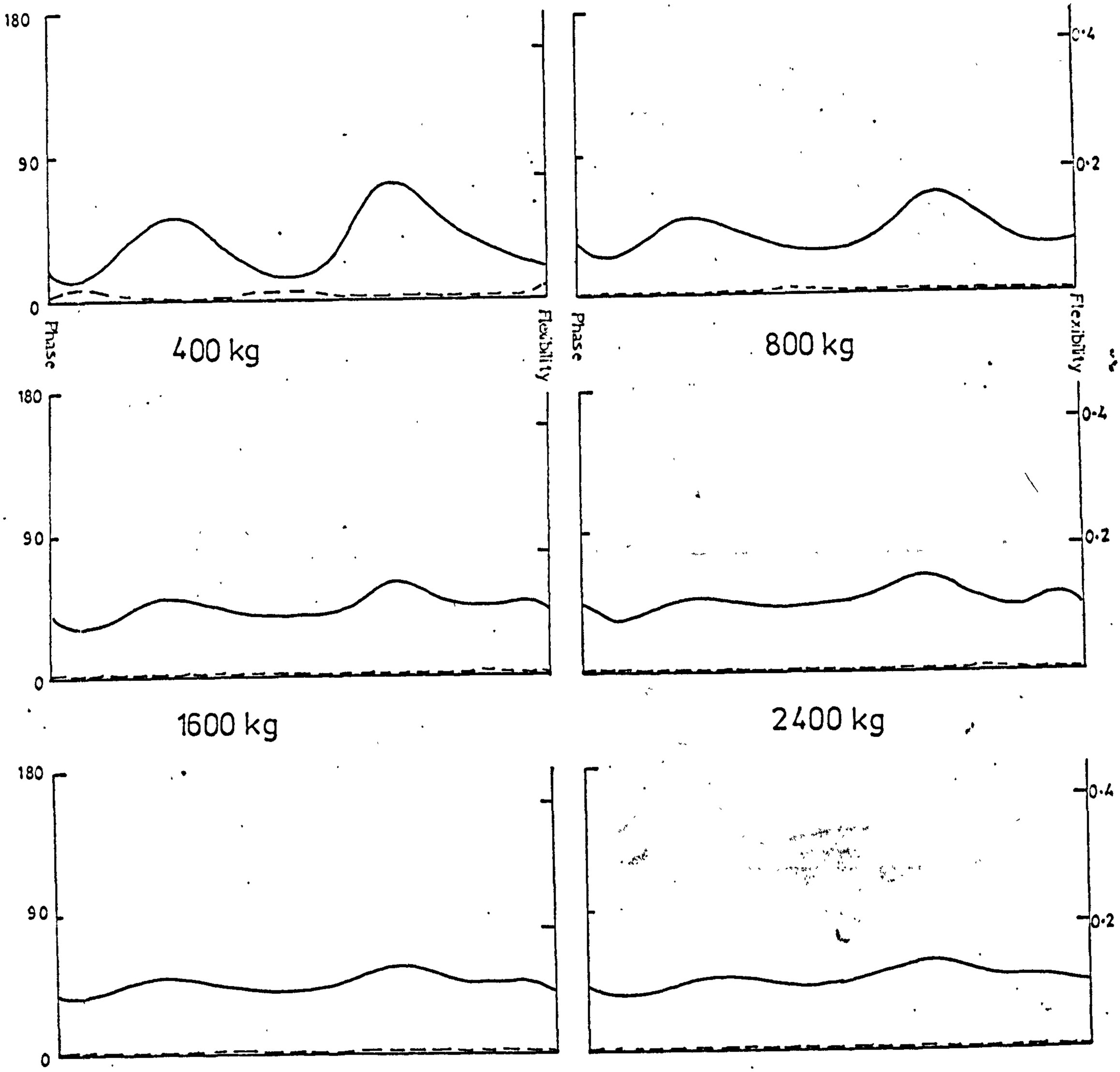

Fig 23. Variation in the Dynamic Flexibility of a Ground Oiled Joint and of the Phase Lag between the joint motion and the applied force, plotted as a function of position around the joint annulus, for different joint preloads.

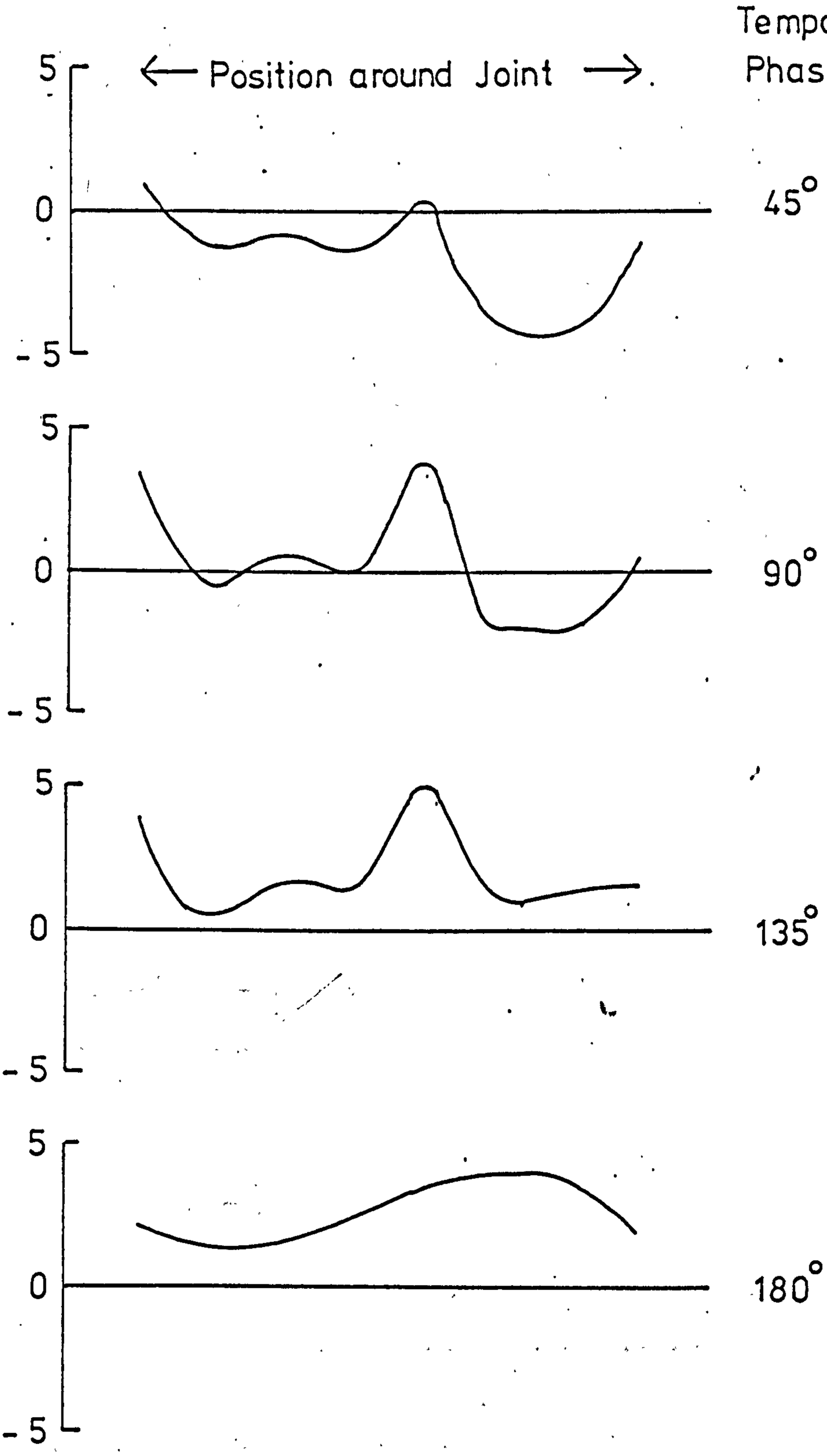

Exciting Force: 20N rms at 200 Hz

Fig. 24 Variation in the deflected profile of a turned oiled joint over a half cycle of forced excitation. Joint preload 1600kg.

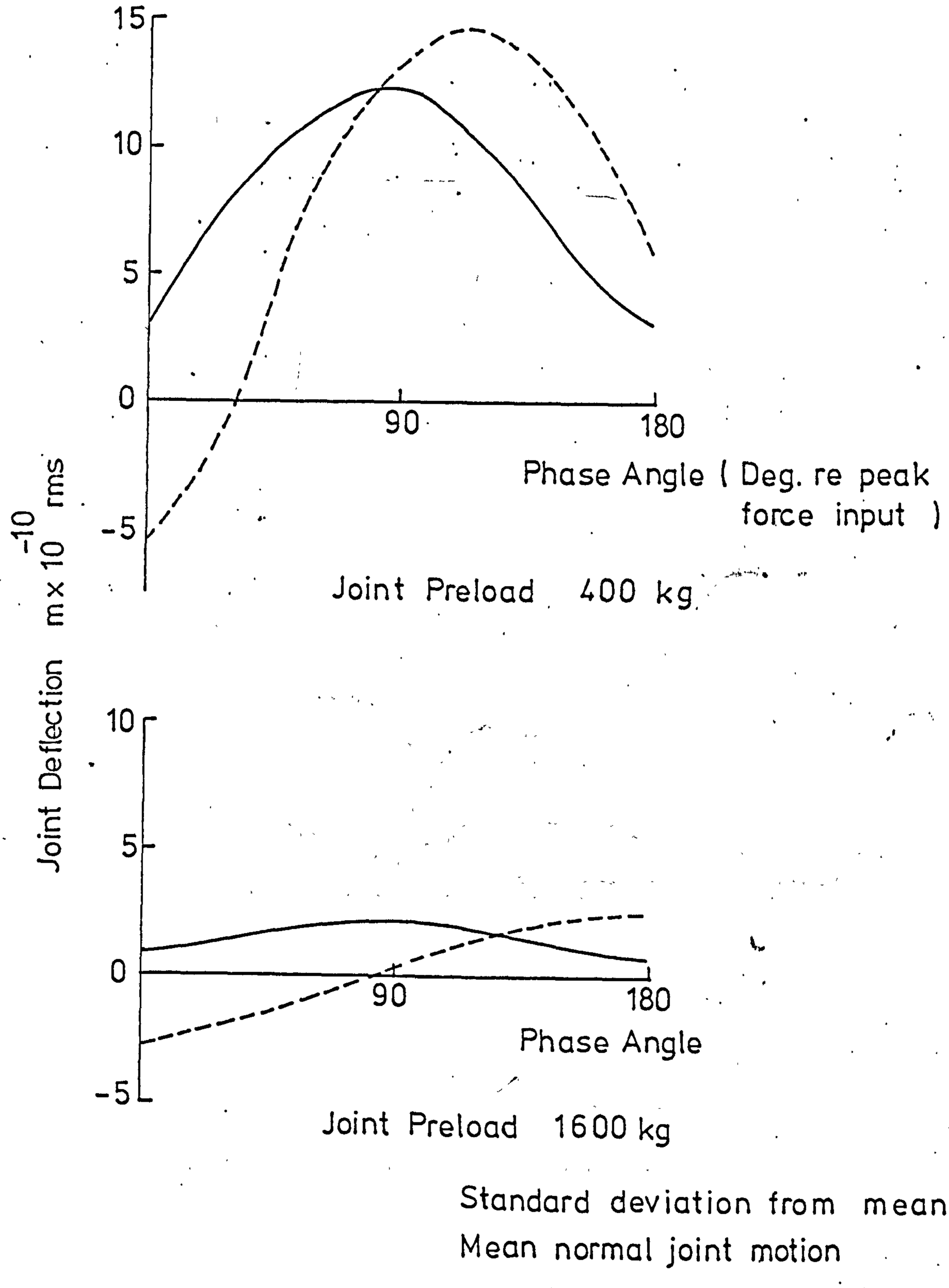

Fig 25. Comparison of the variation of the mean normal motion of a turned oiled joint, and the standard deviation of points on the joint annulus from this mean, as a function of time, for two joint preloads.

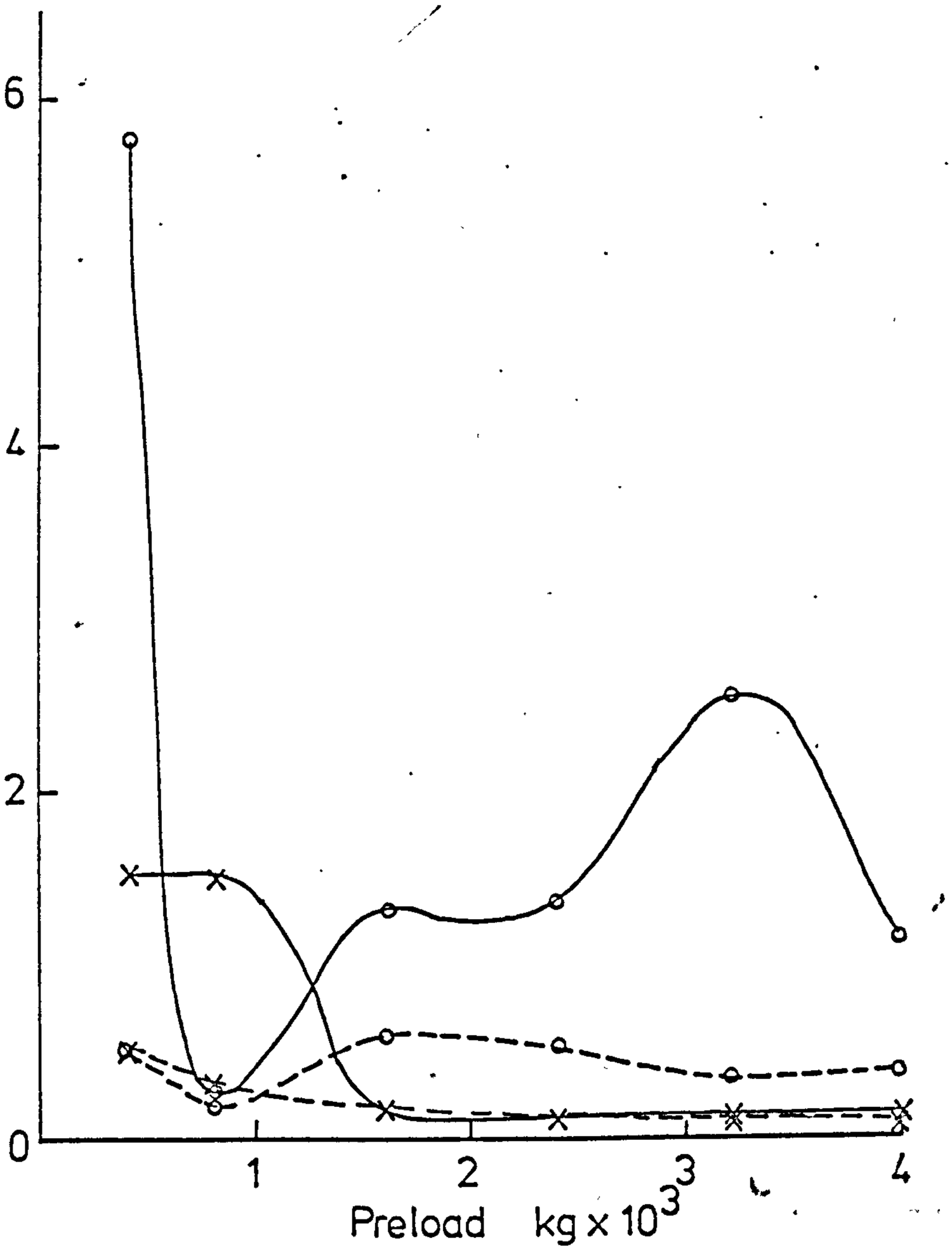

Fig.26 Variation, as a function of joint preload, of the ratio of the standard deviation of the joint motion from the mean level, to the mean level of normal motion averaged around the joint annulus.

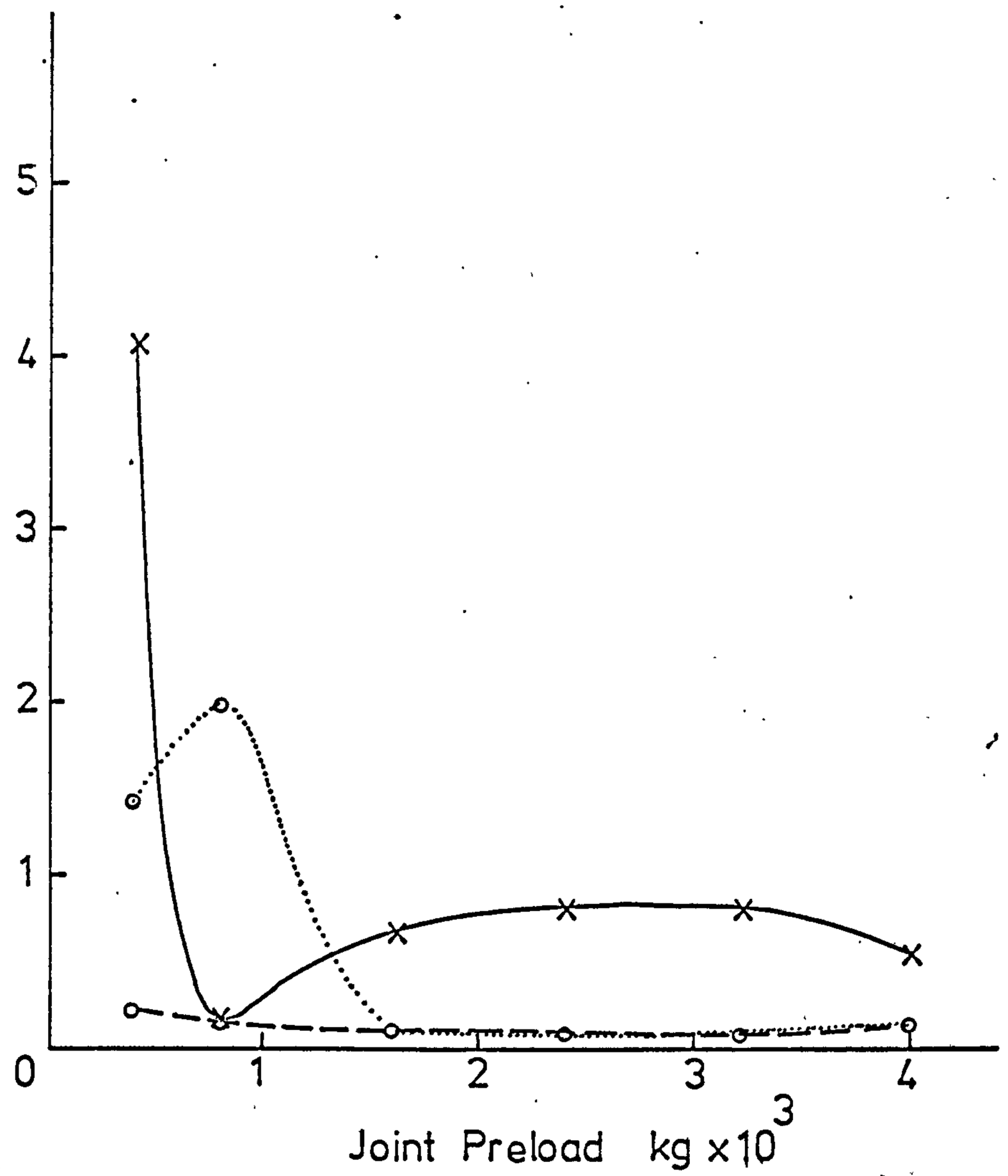

Fig.27 Variation in the ratio of Rocking to Normal motion with joint preload.

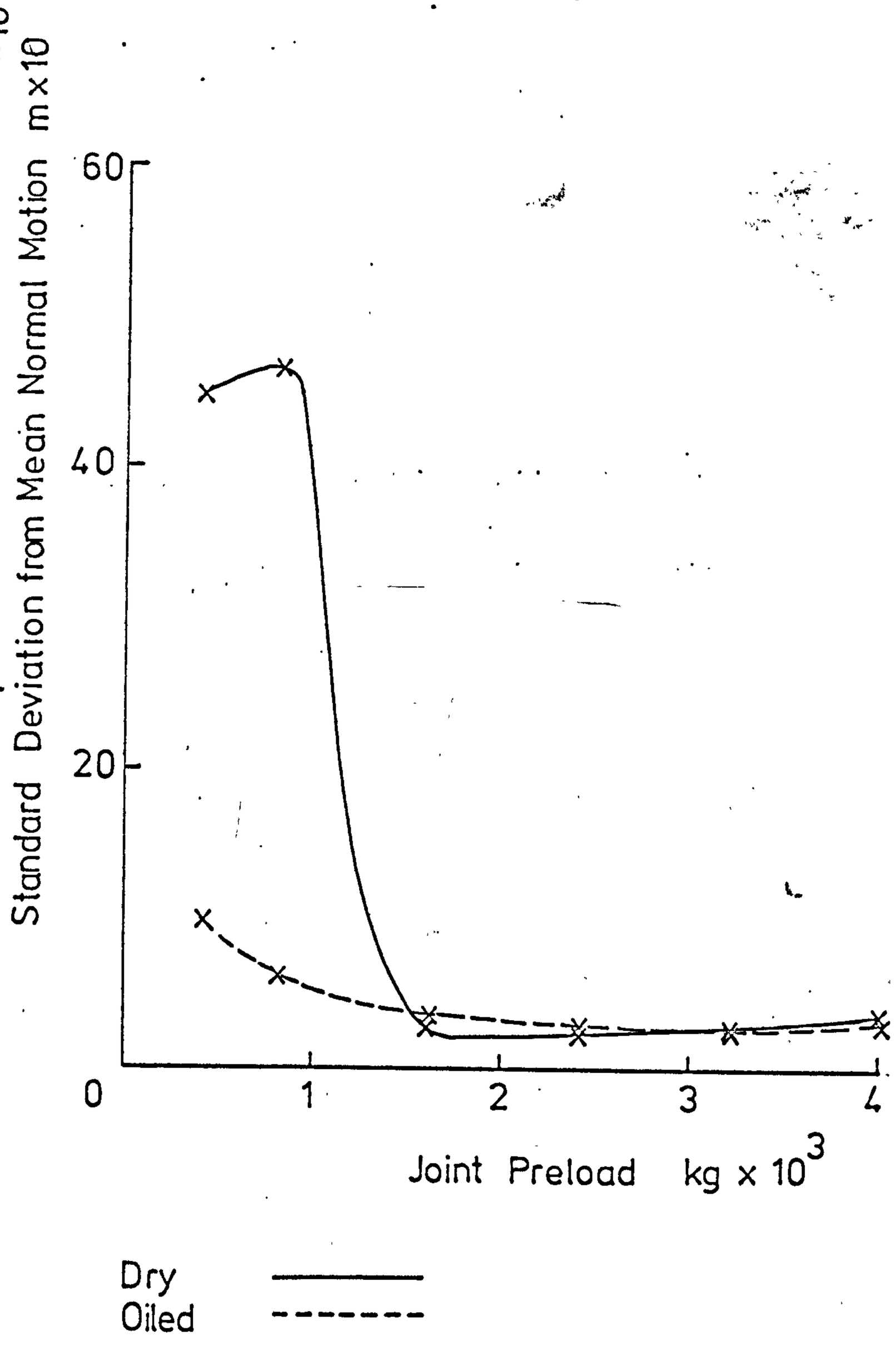

Fig. 28. Variation in the Standard Deviation of the motion of a ground joint from the mean normal motion averaged around the joint annulus.

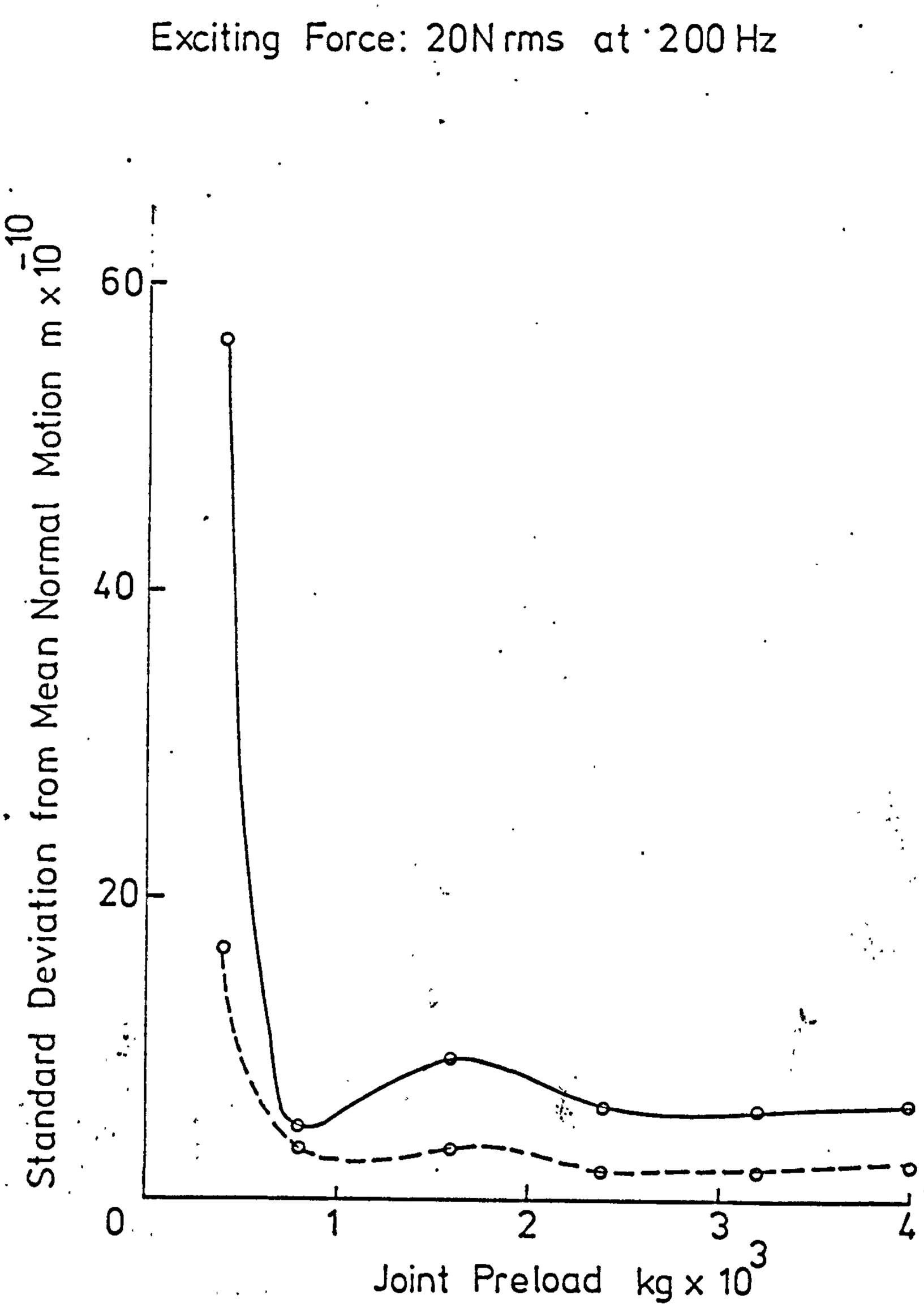

Fig. 29. Variation in the Standard Deviation of the motion of a turned joint from the mean normal motion averaged around the joint annulus.

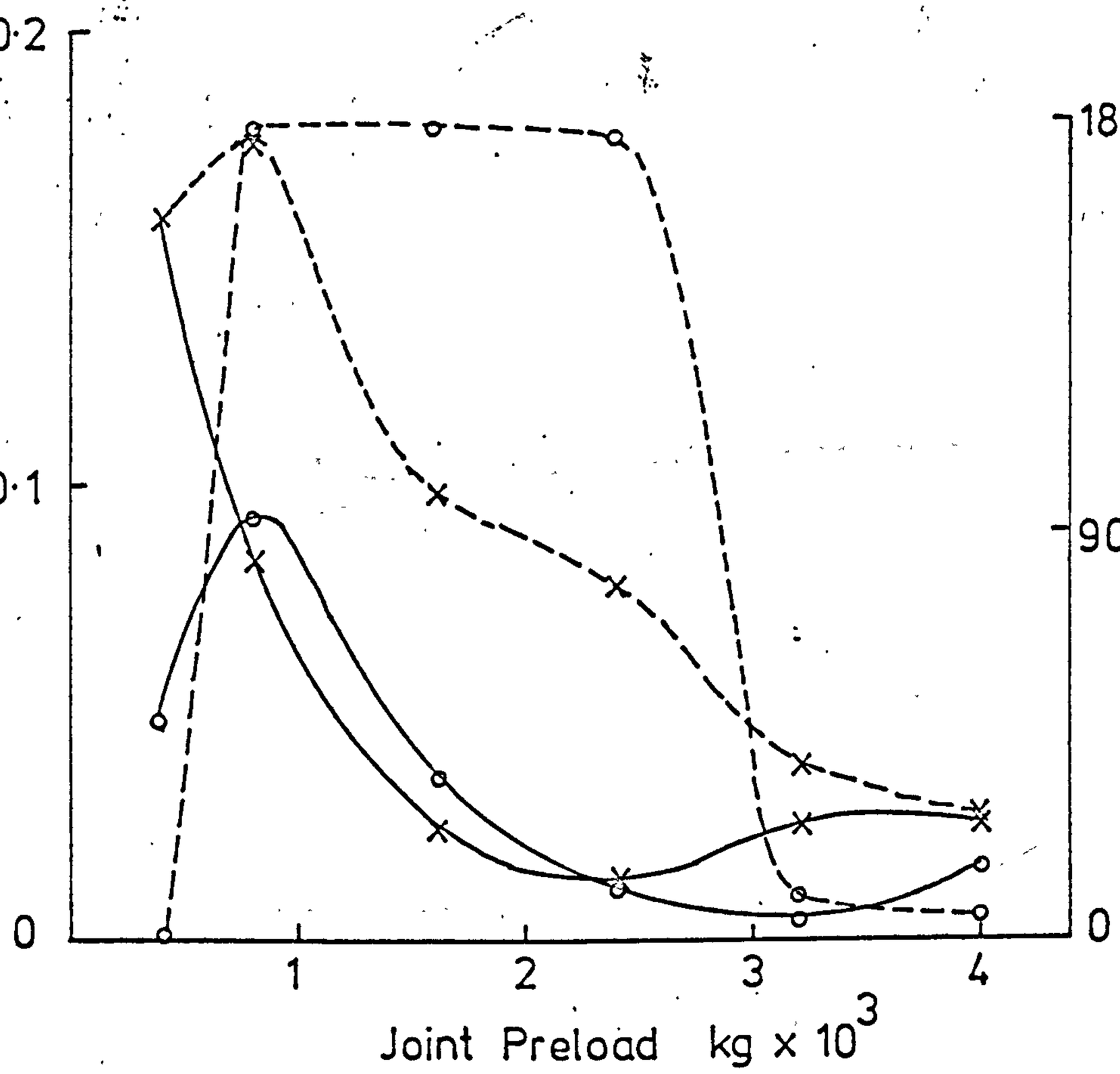

Fig. 30 Variation in the Normal Flexibility of a turned joint, and of the Phase Lag between the joint motion and the applied force, with joint preload.

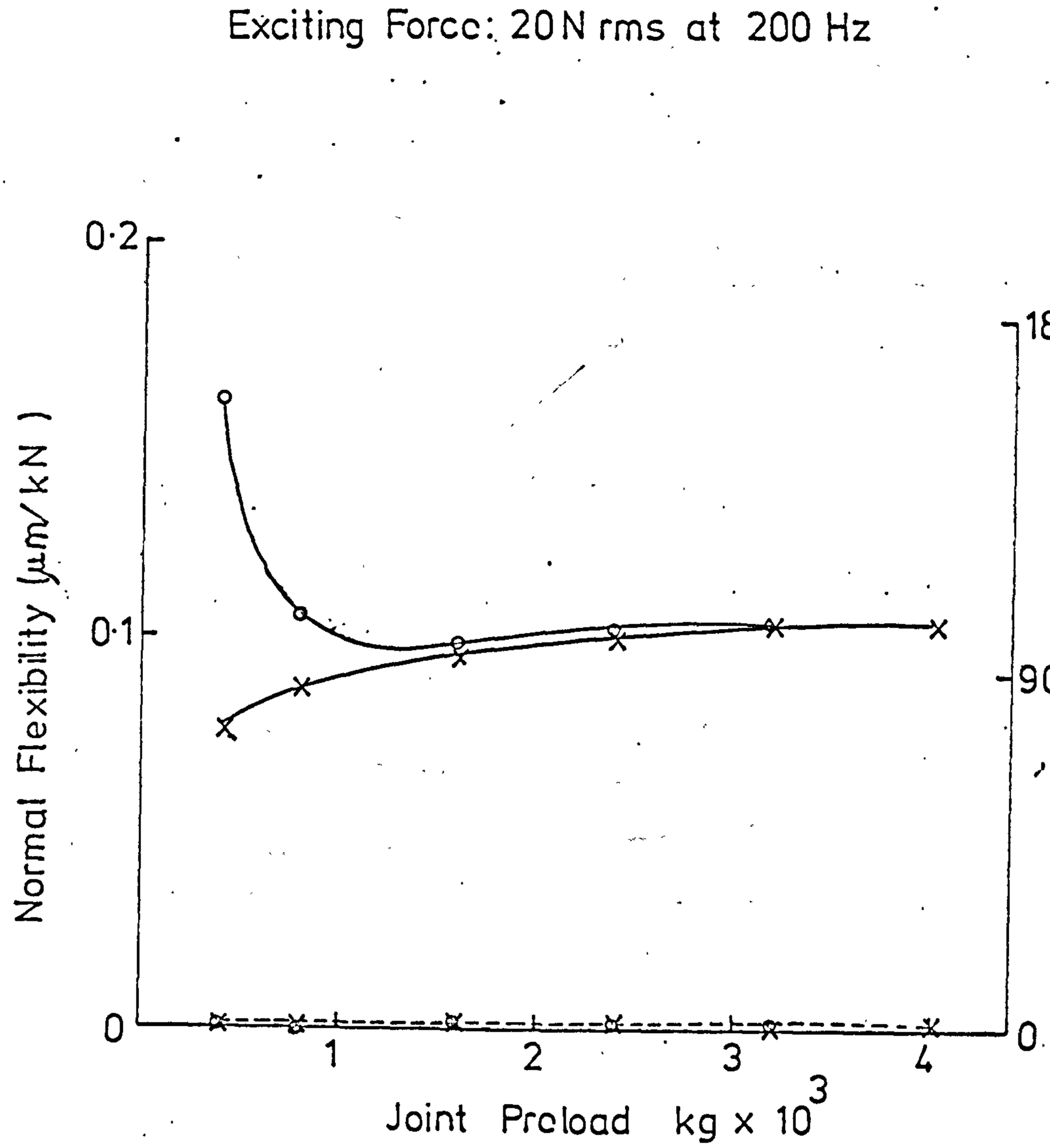

Fig. 31 Variation in the Normal Flexibility of a Ground joint, and of the Phase Lag between the joint motion and the applied force „ with joint preload.

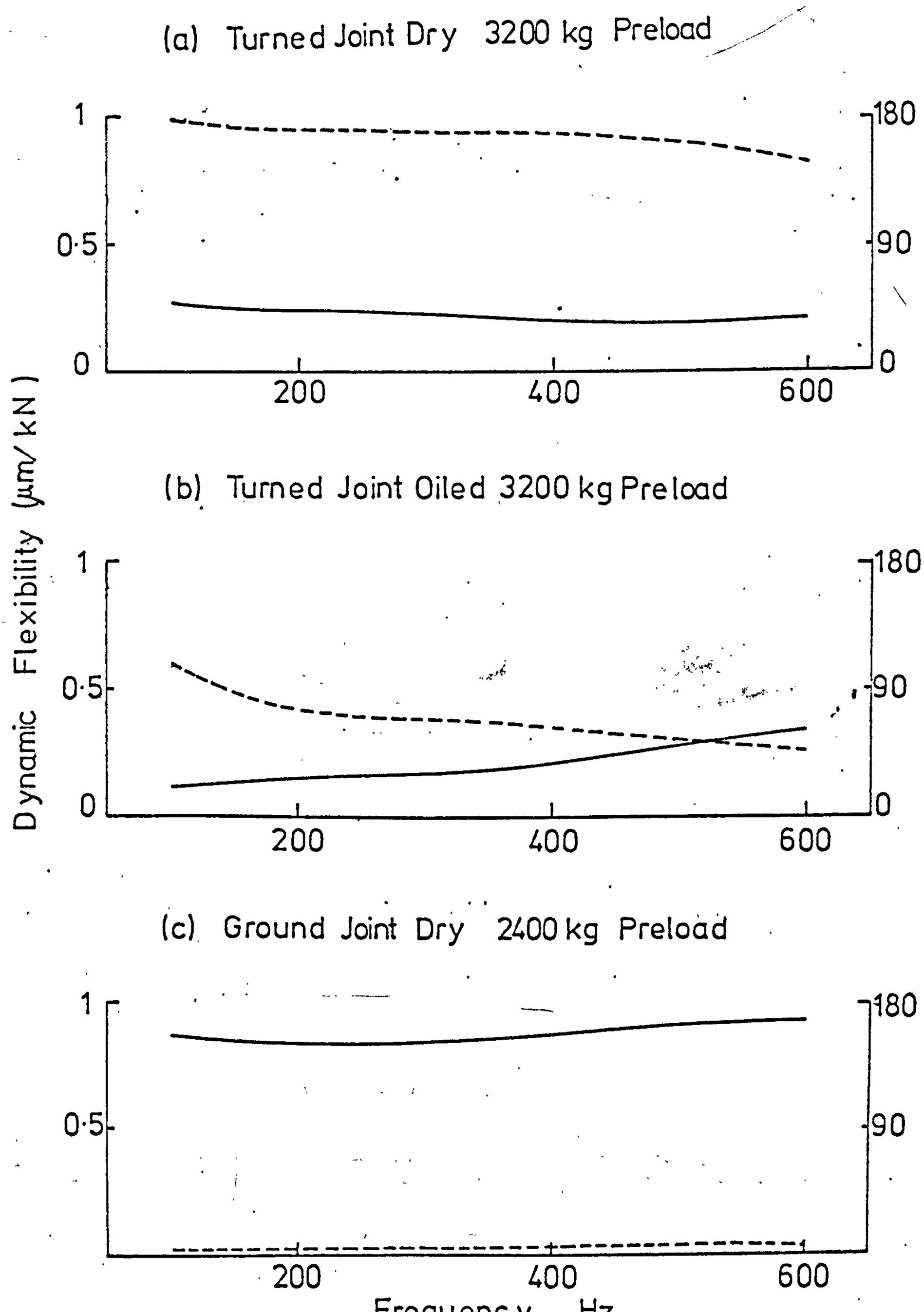

Fig. 32 Typical frequency responses of test joints

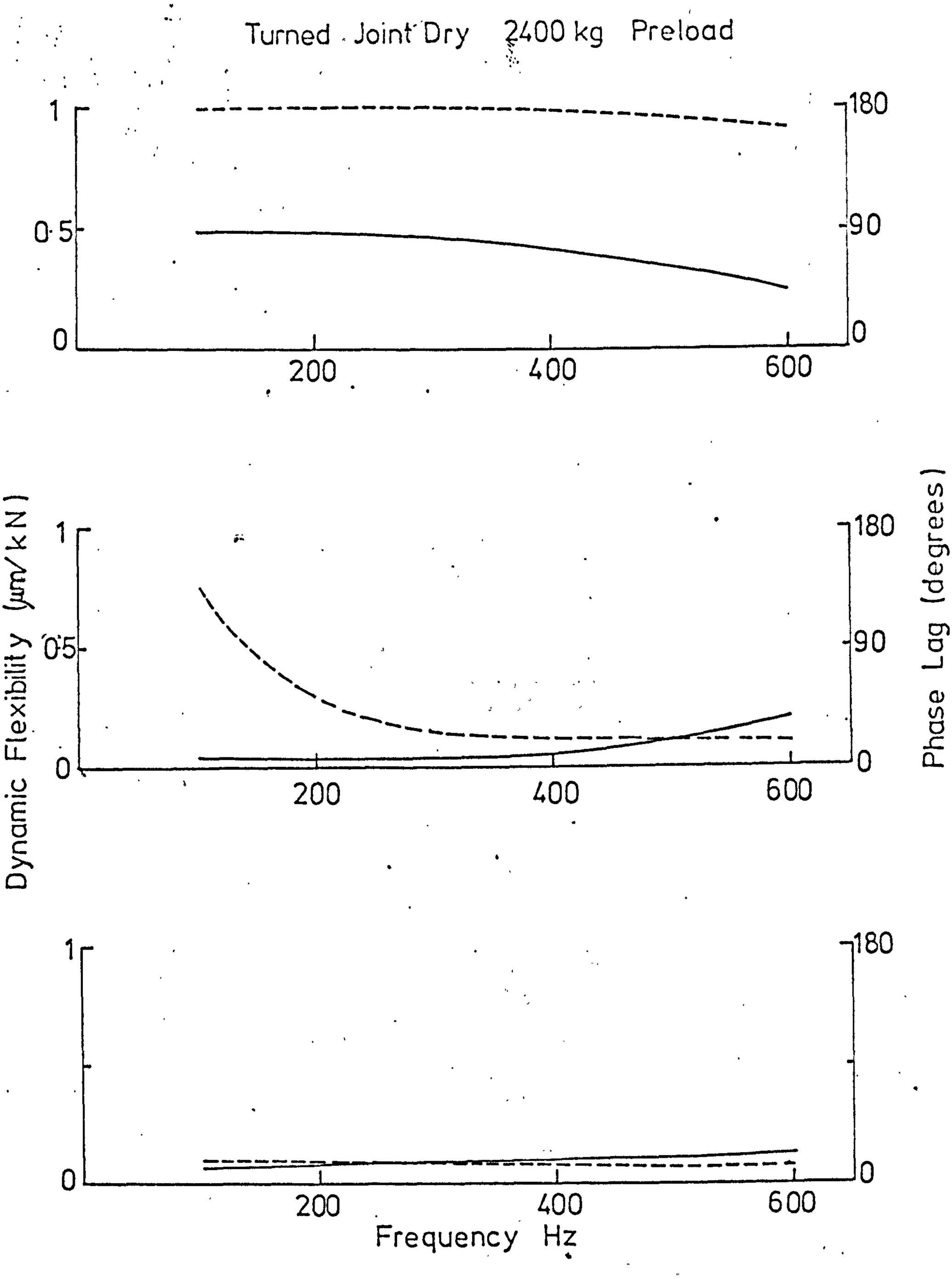

Fig. 33 Variation in frequency response at different positions within a single joint

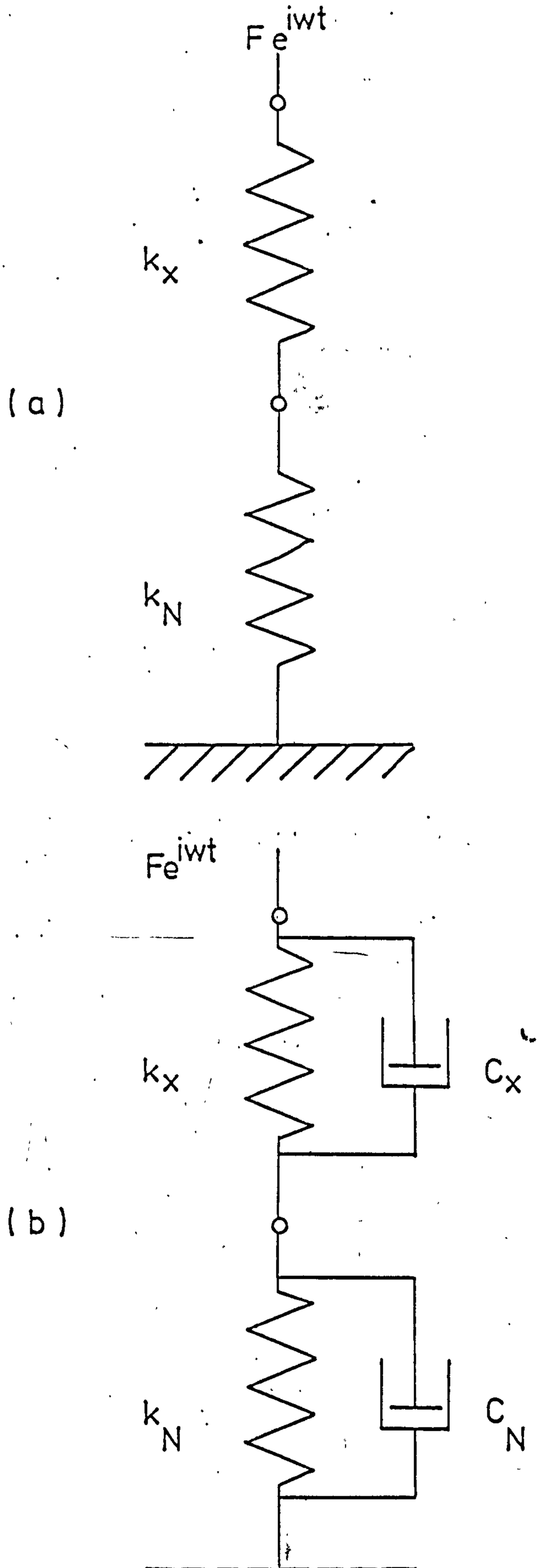

Fig. 34 Joint Models

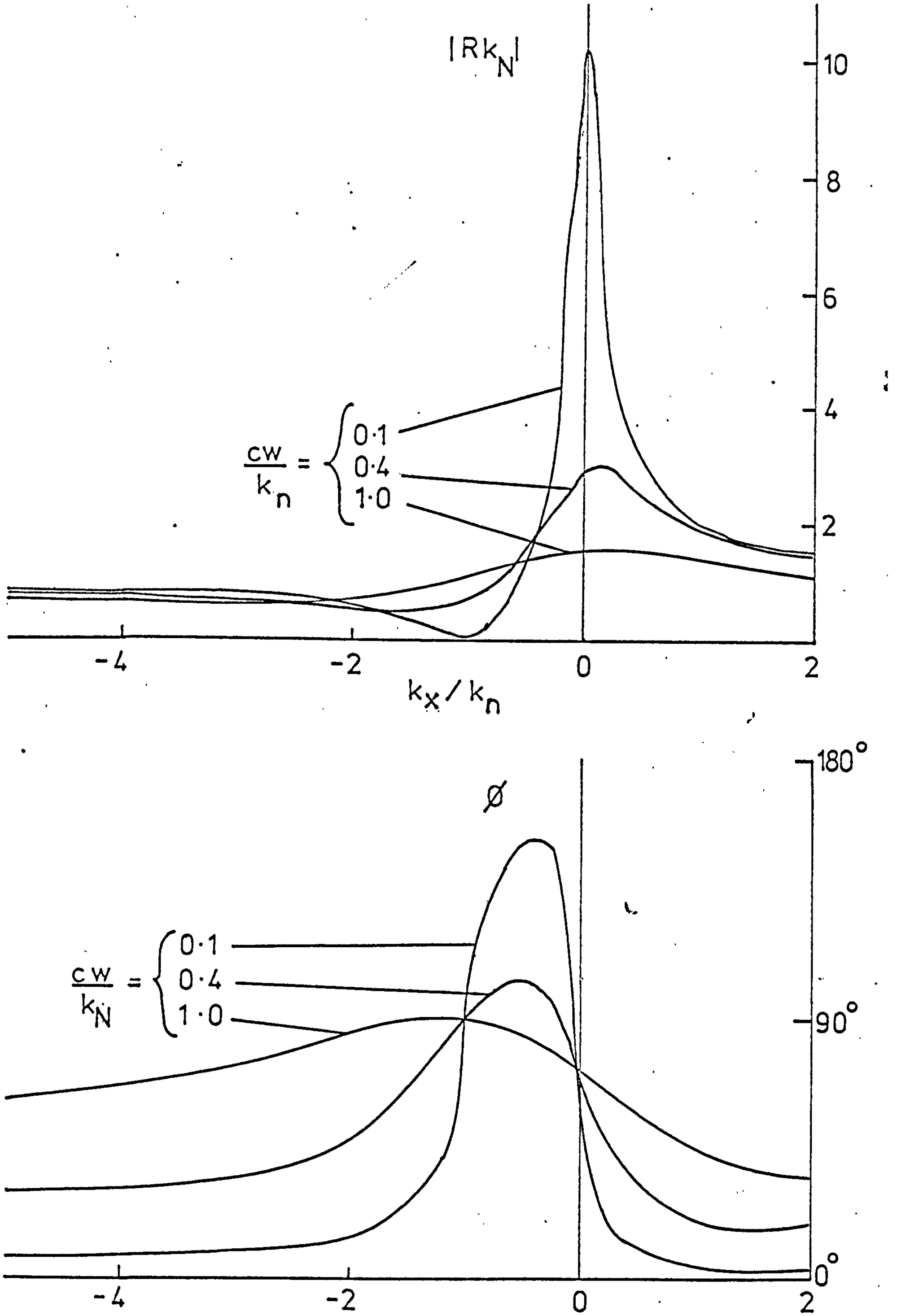

Fig. 35 Variation of $|Rk_n|$ and ϕ with k_x/k_n for different values of $\frac{cw}{k_n}$

$c_n = c_x = c$

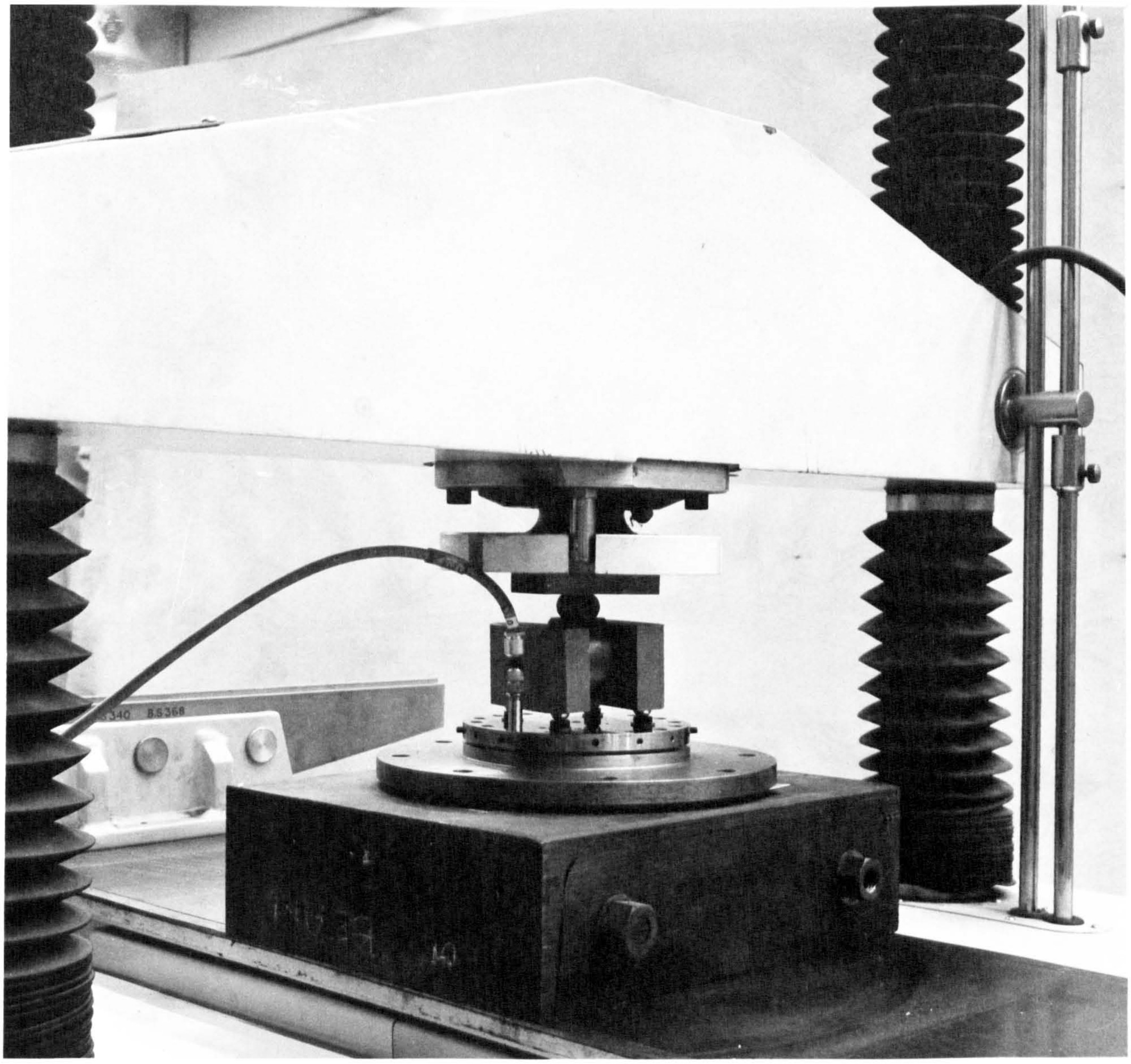

Fig. 36 Static loading rig : annular joints

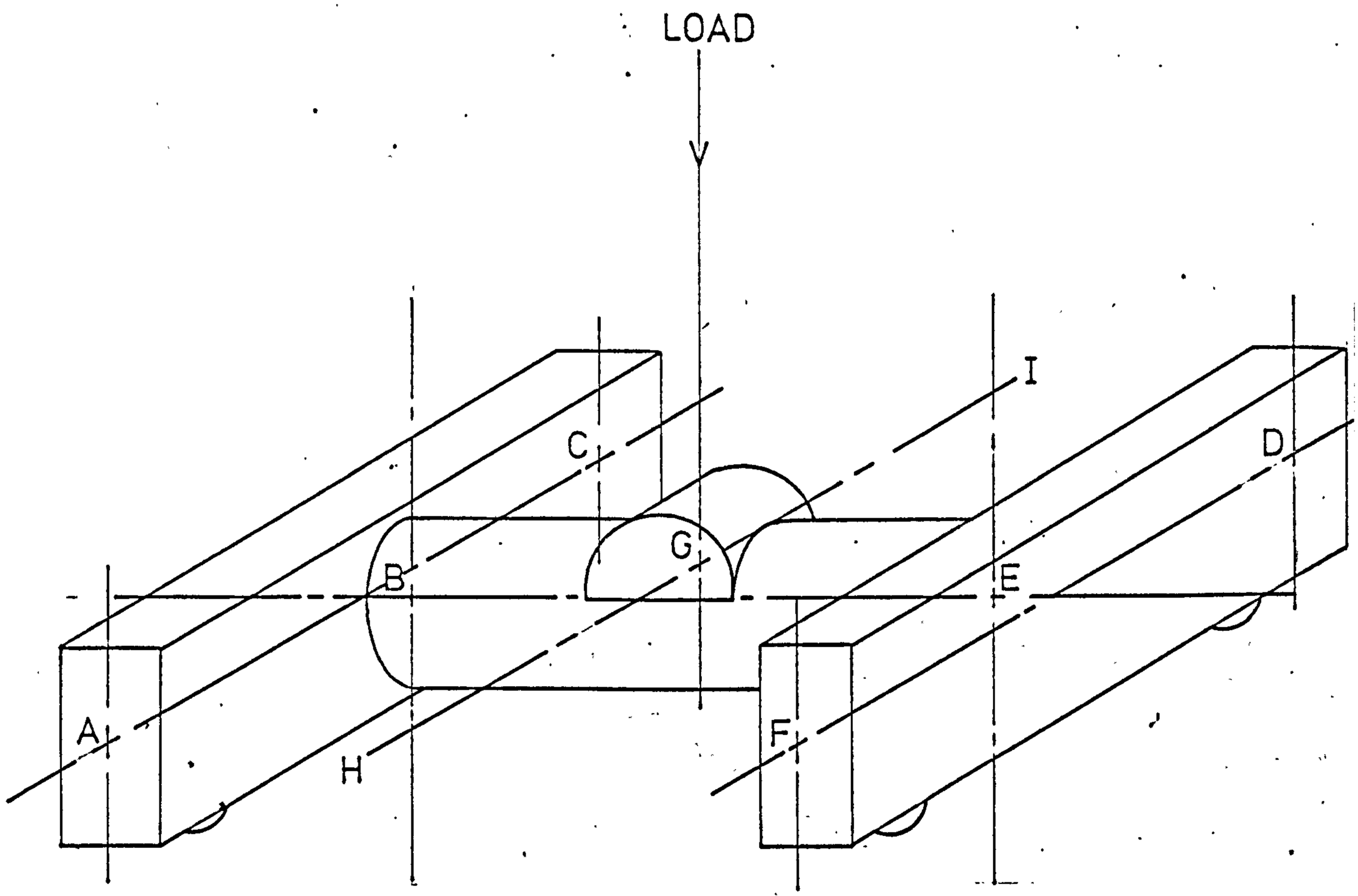

Fig. 37 Diagrammatic representation of rig used to apply four equal static loads to an annular joint.

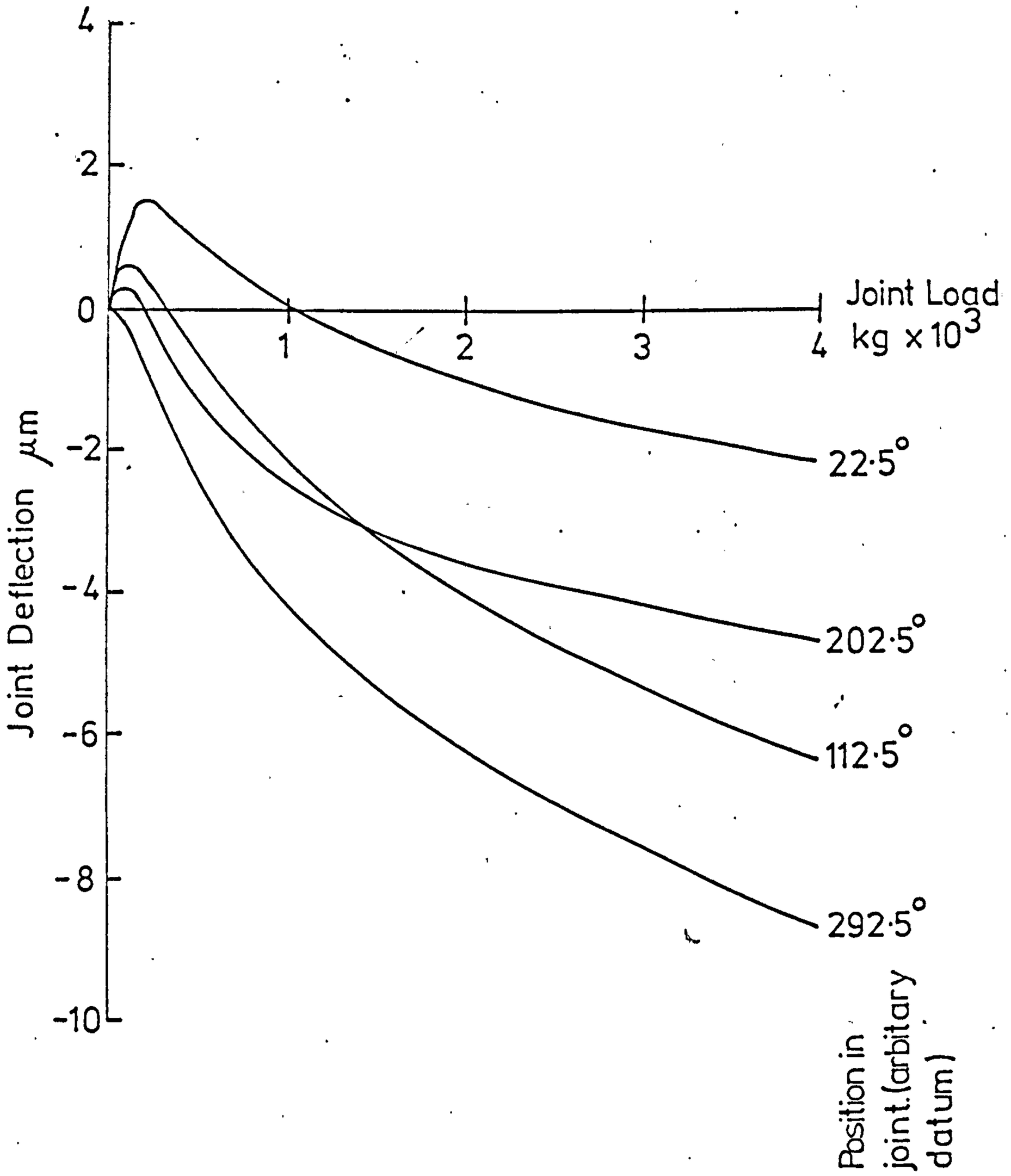

Fig. 38 Static load/deflection curves at various positions around an annular turned joint

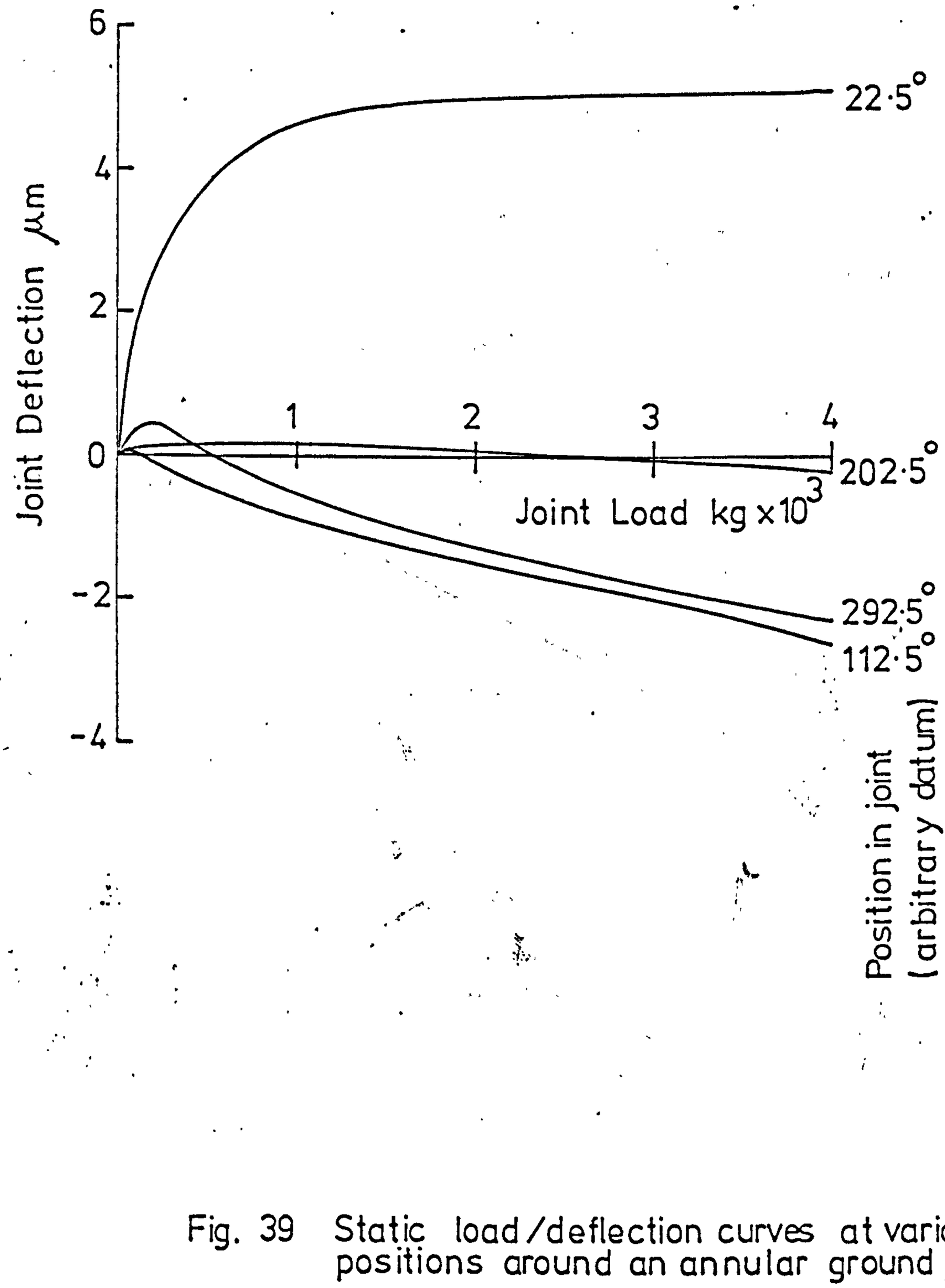

Fig. 39 Static load/deflection curves at various positions around an annular ground joint

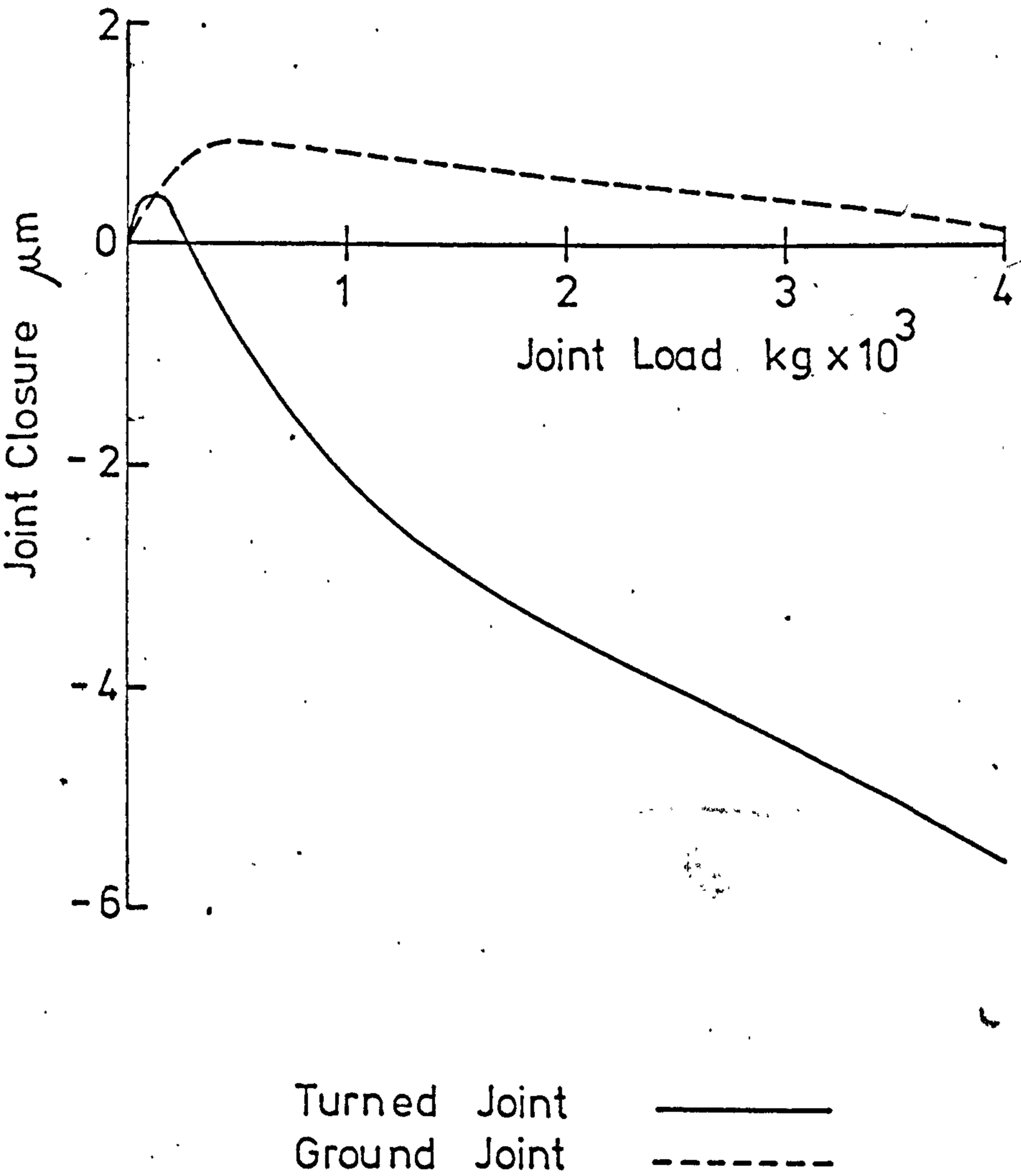

Turned Joint ————
Ground Joint - - - - - - -

Fig. 40 Variation with static preload, of the mean closure of points on an annular test joint at an angular displacement of 22.5° from the bolt holes.

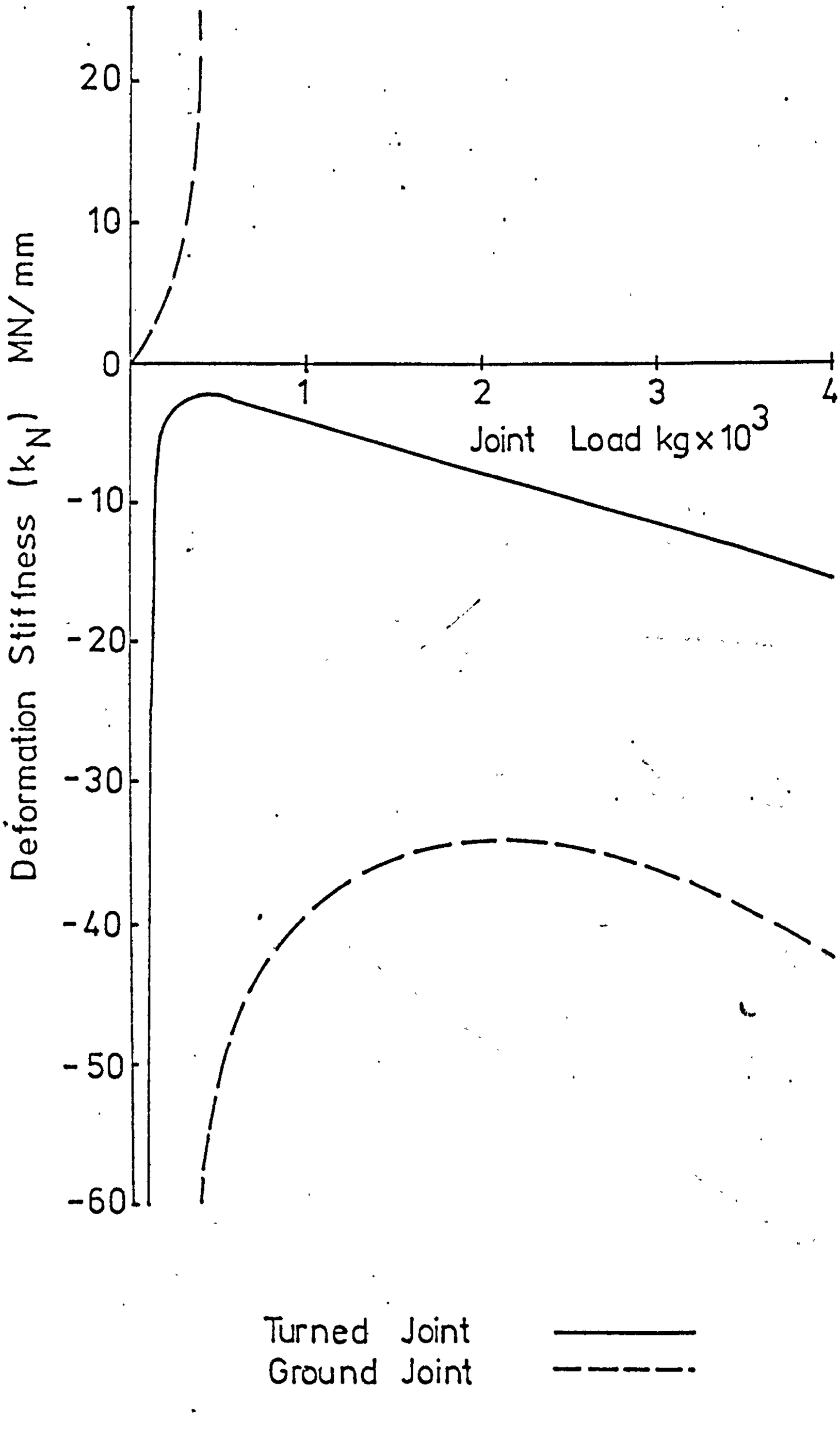

Fig. 41 Variation with applied preload, of the deflection stiffness (k_x) of turned and ground annular joints.

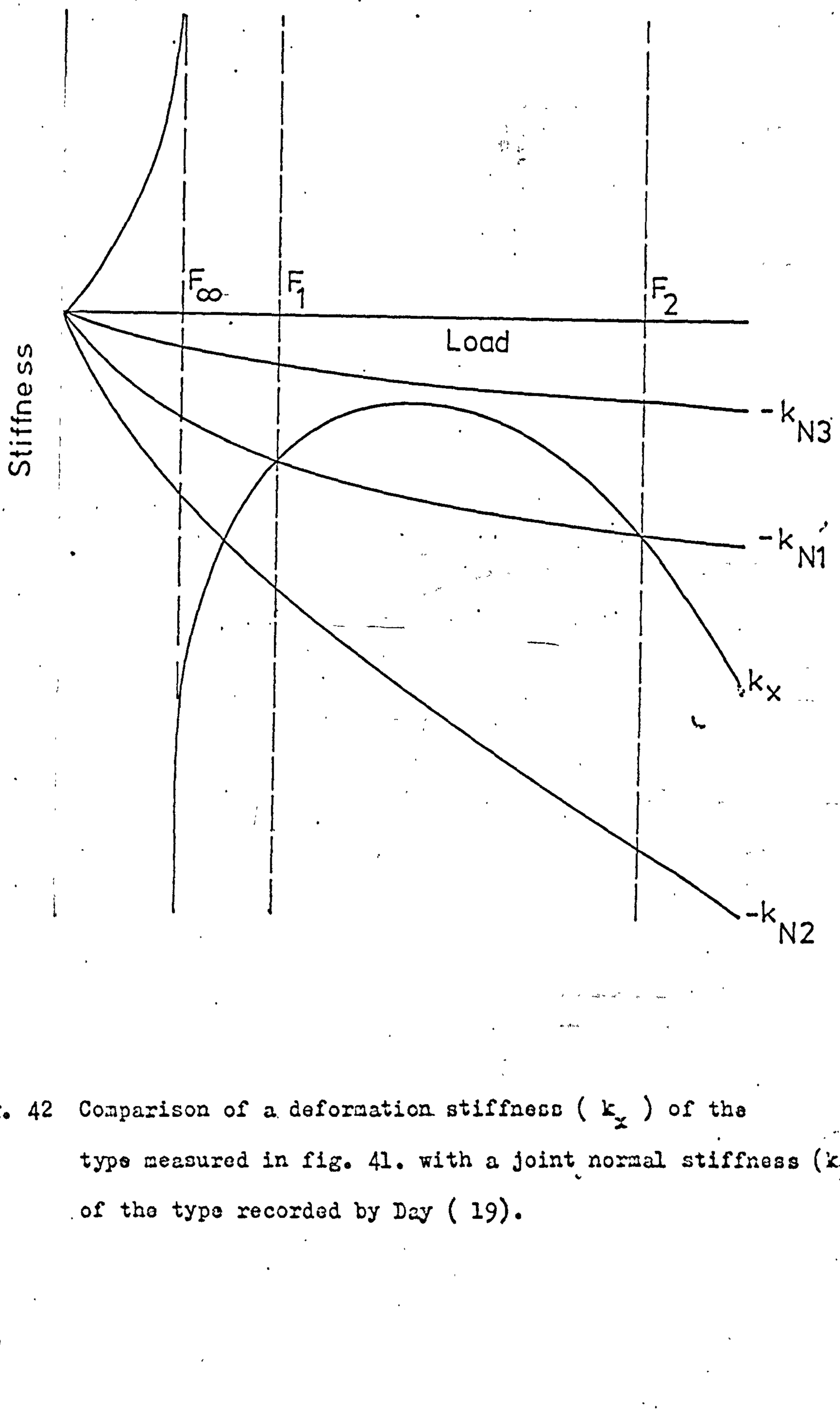

Fig. 42 Comparison of a deformation stiffness (k_x) of the type measured in fig. 41. with a joint normal stiffness (k_N) of the type recorded by Day (19).

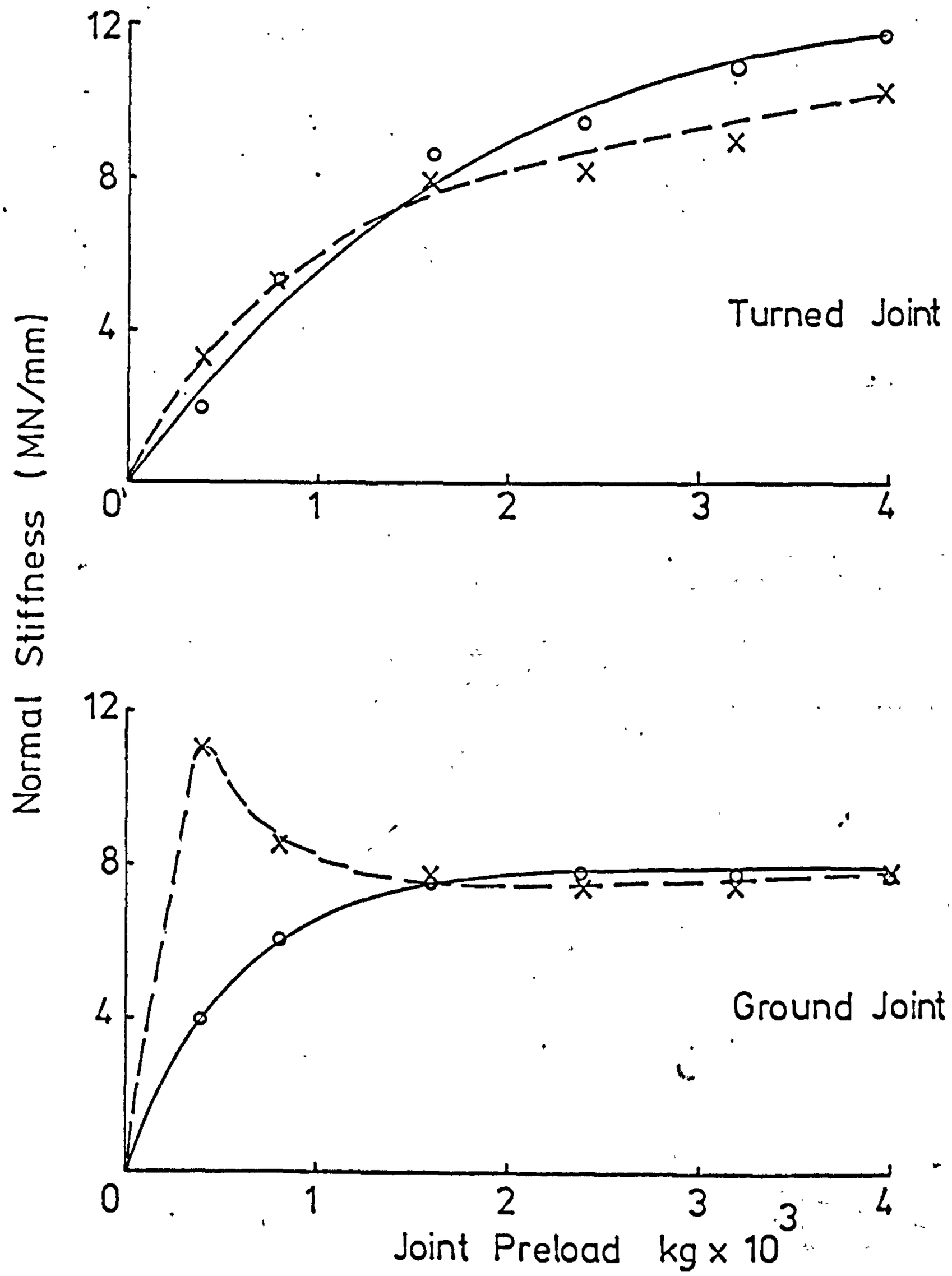

Fig. 43 Variation with preload of the normal stiffness of turned and ground annular joints.

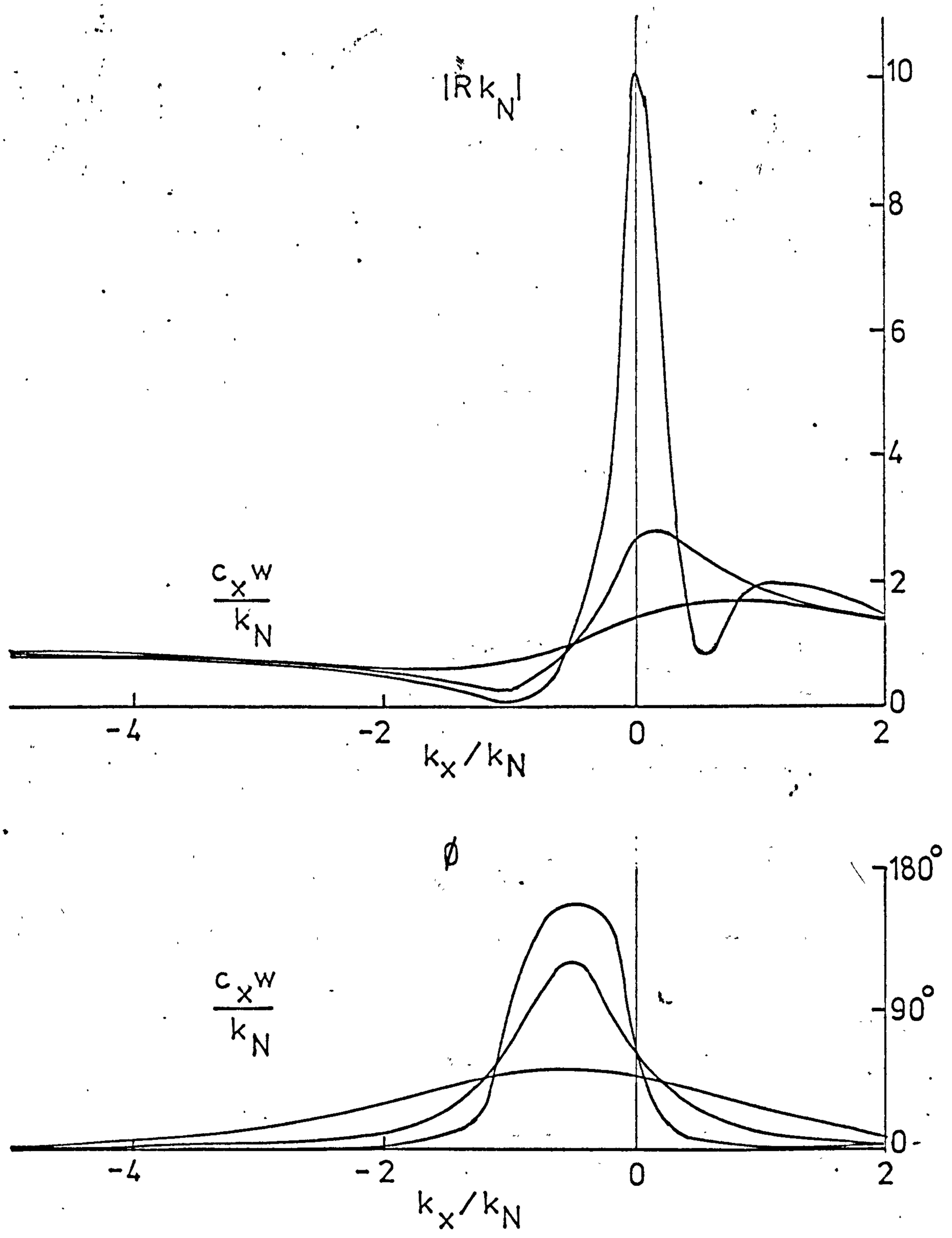

Fig. 44 Variation of $|Rk_N|$ and ϕ with k_x/k_N for different values of $\frac{c_x w}{k_N}$

$c_N = 0.$

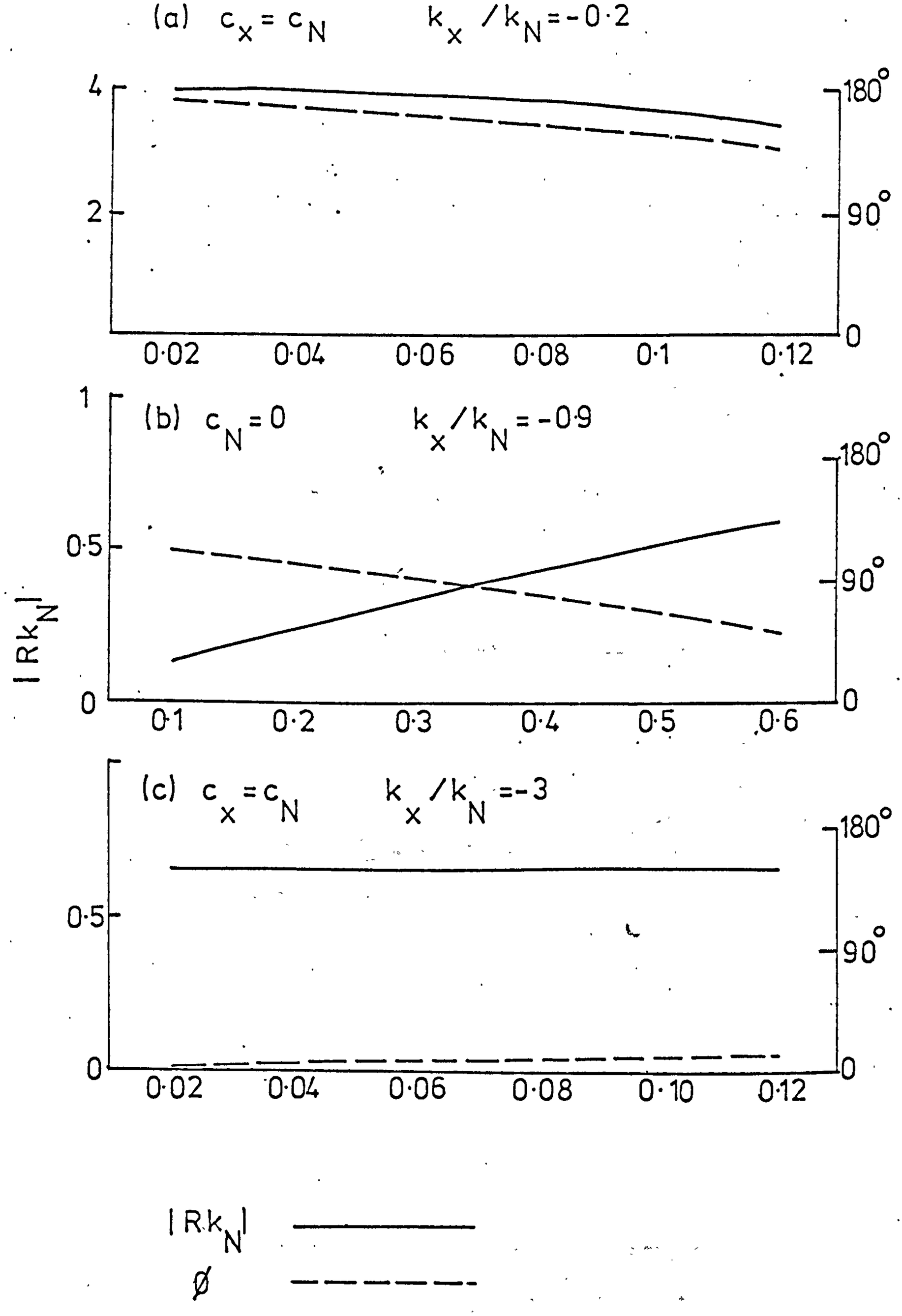

Fig. 45 Frequency response of joint model under various conditions.

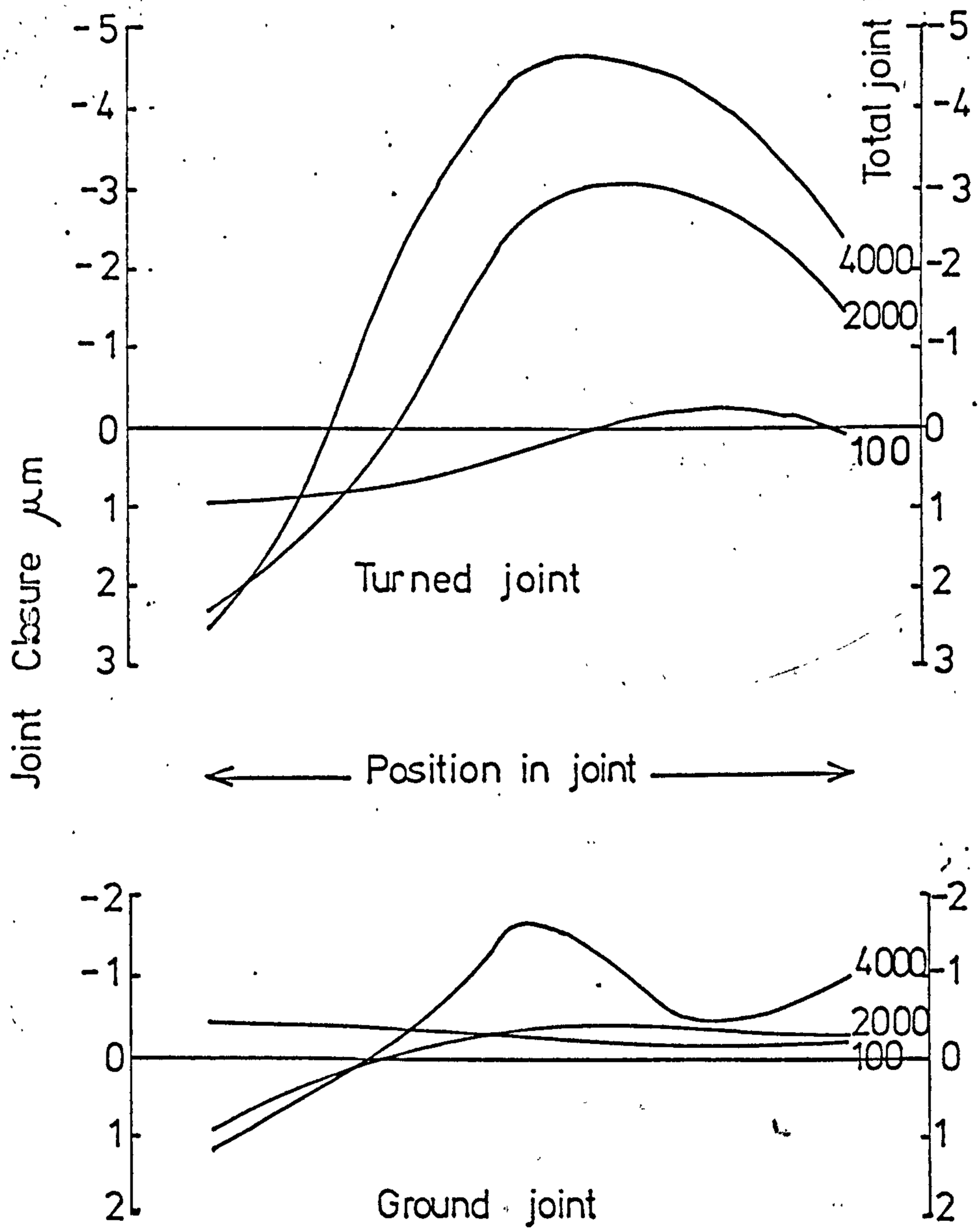

Fig. 46 Joint closure, under static simulated bolt load, over a quadrant of an annular joint.

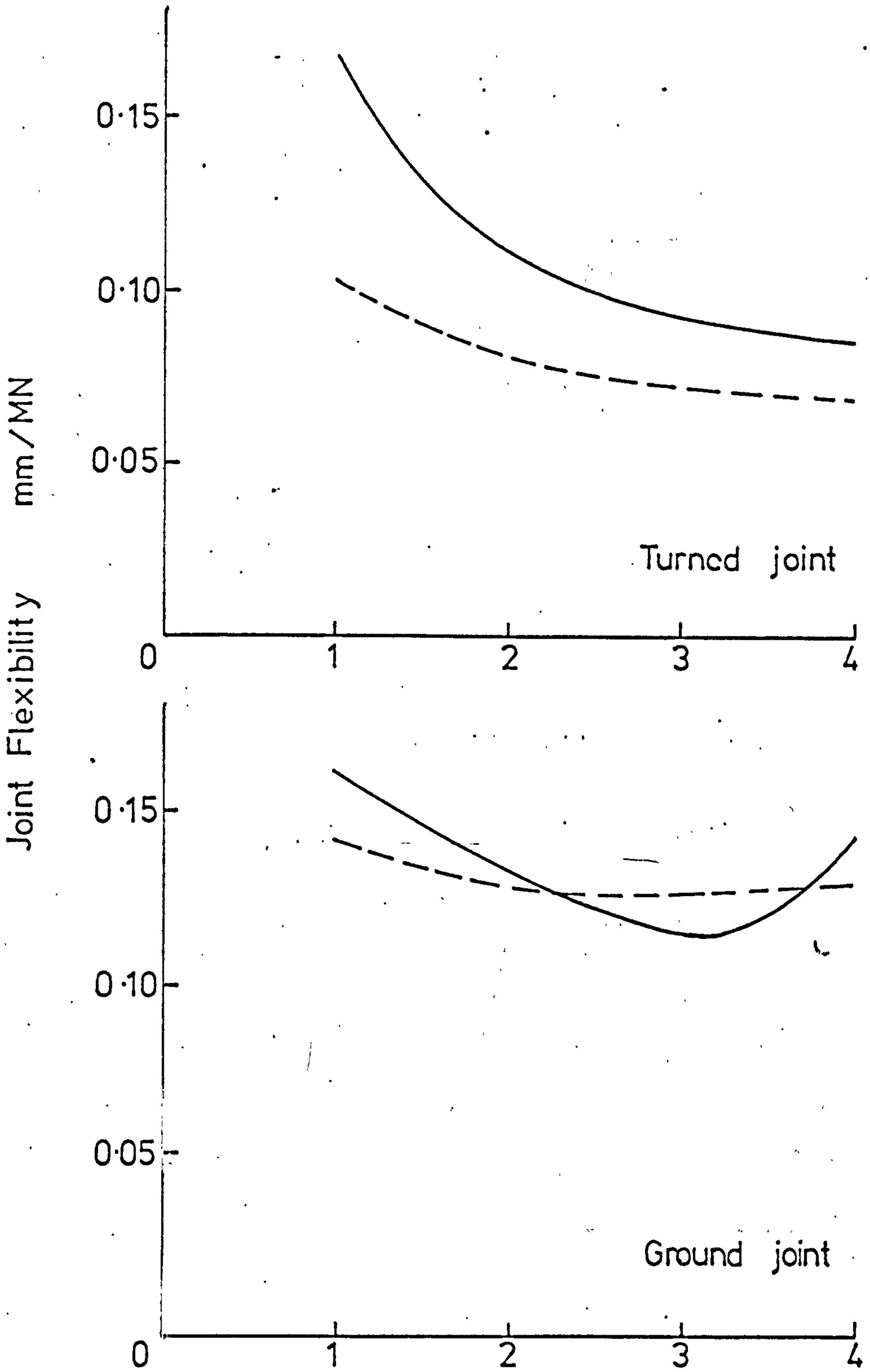

Fig. 47 Comparison of the variation with preload of the Rms and normal flexibilities of an annular joint.

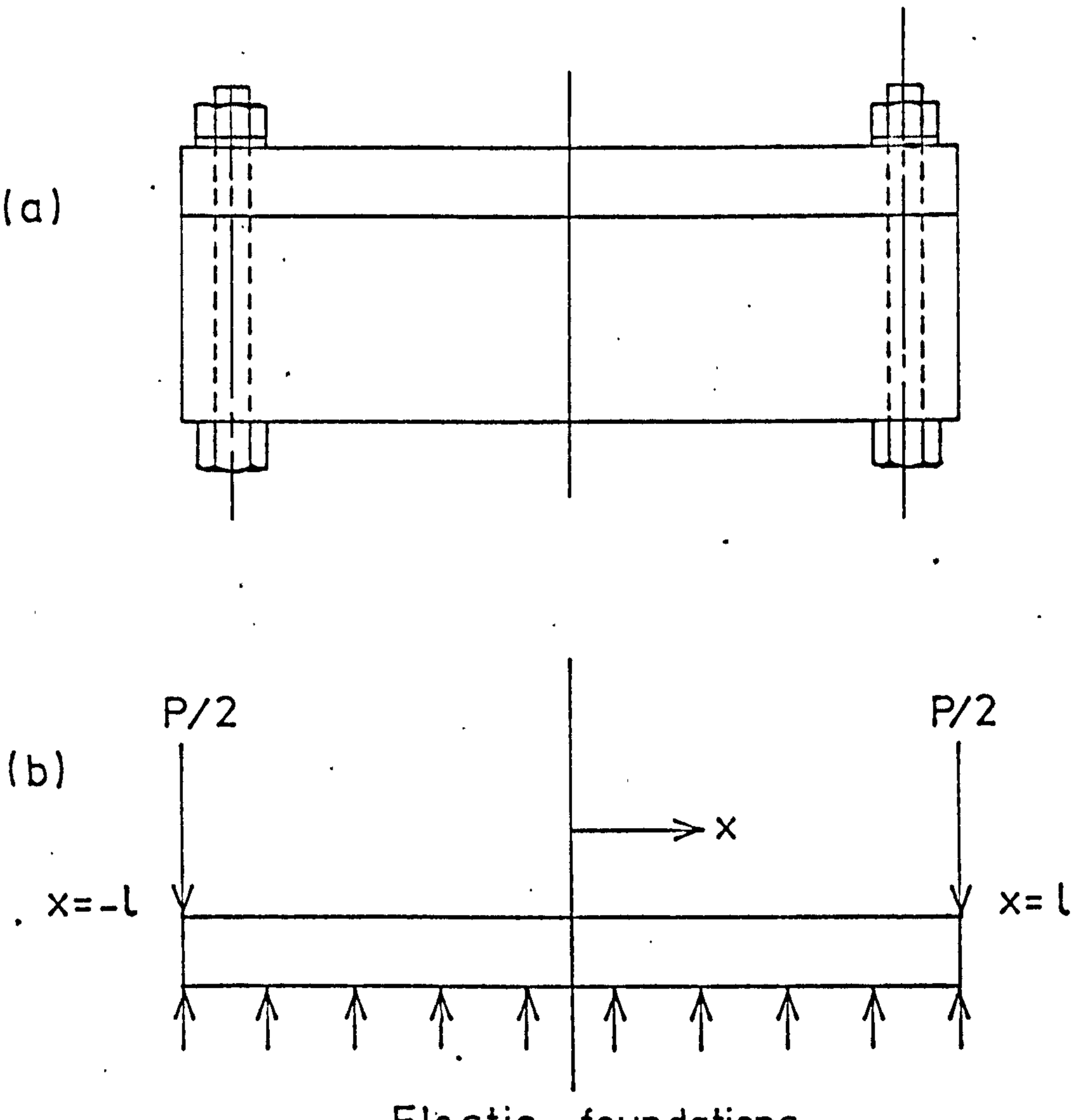

Fig. 48 Rectangular joint models.

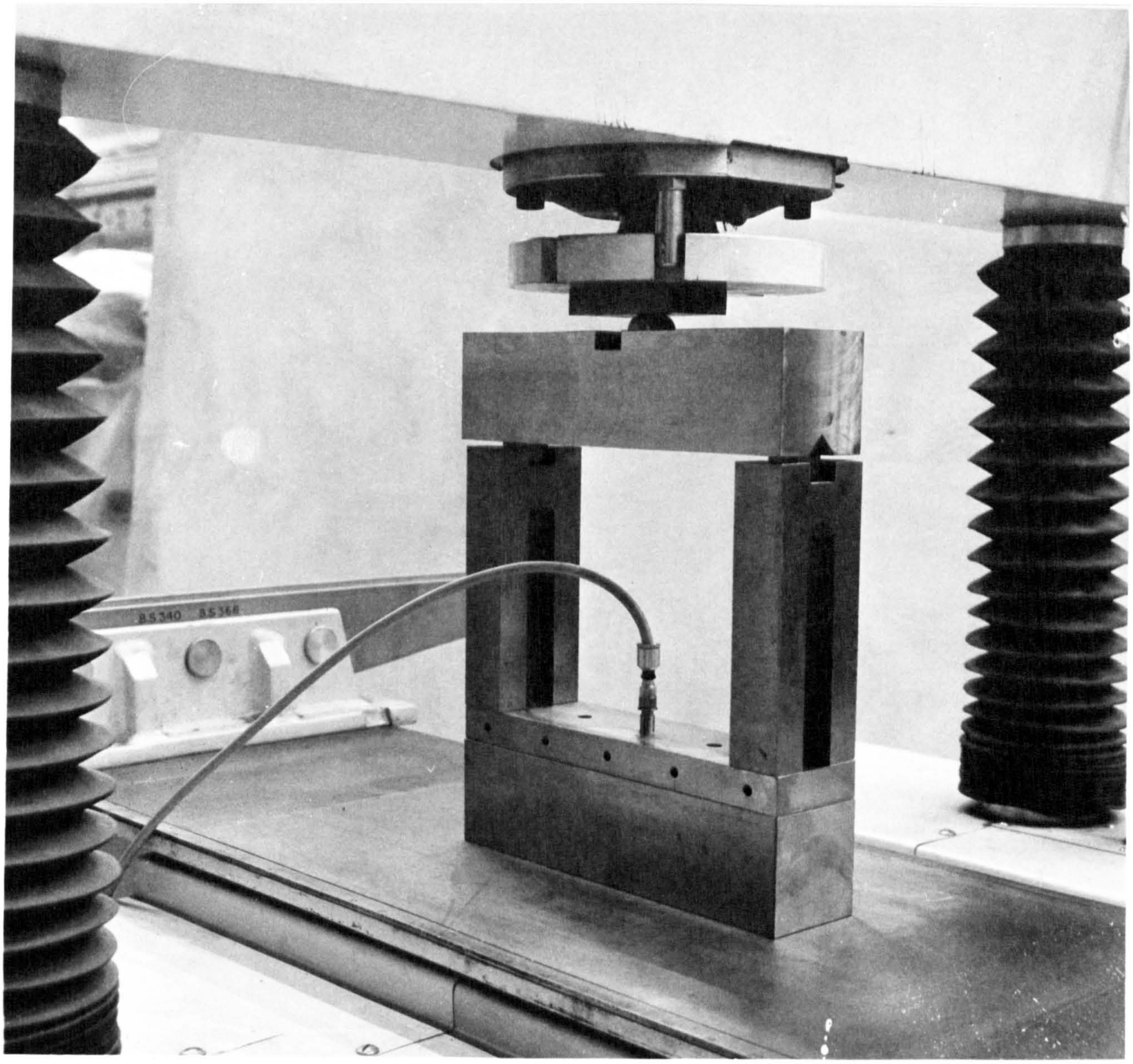

Fig. 49 Static loading rig: rectangular joints

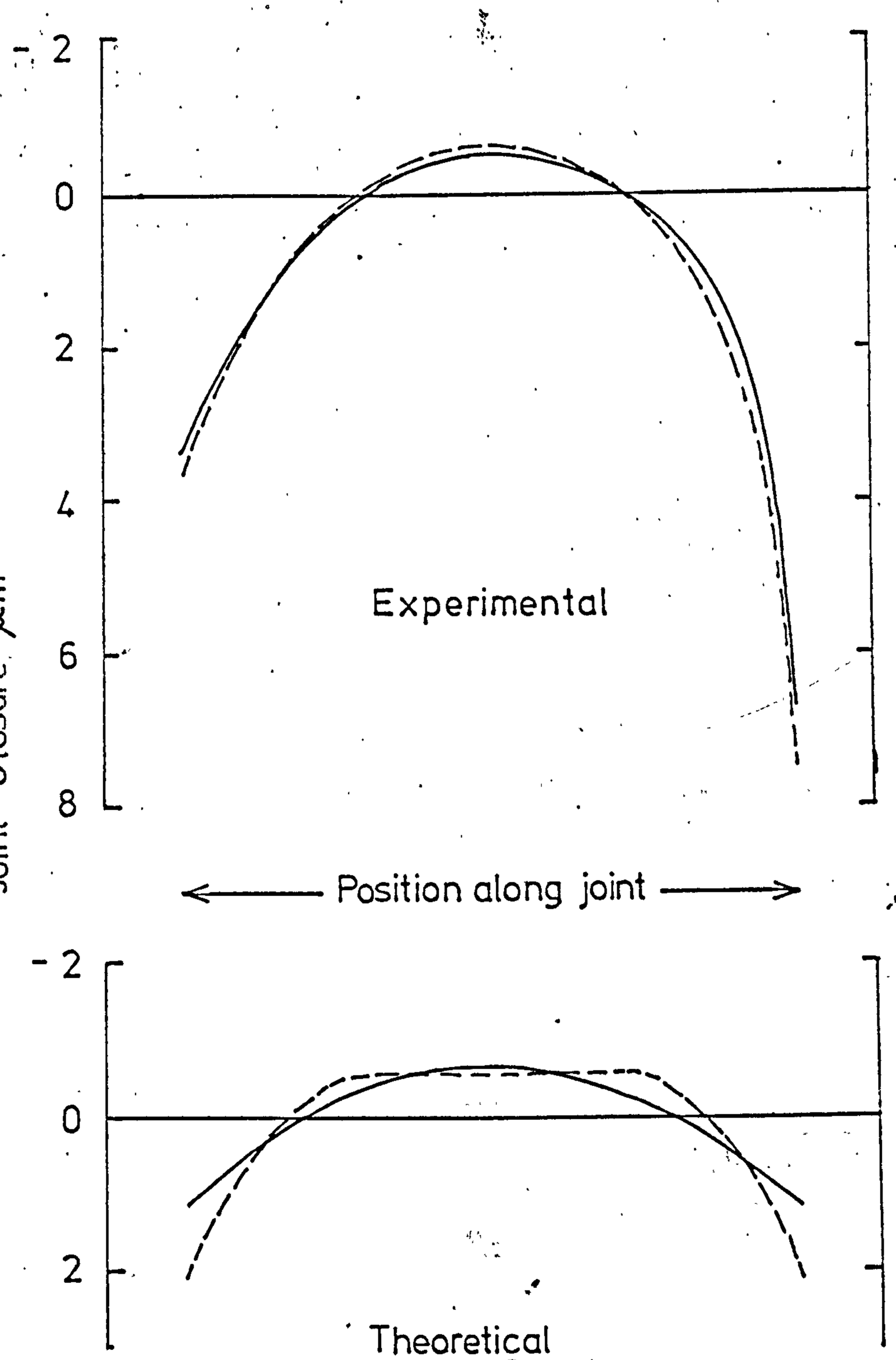

Fig. 50 Experimental and theoretical values of the closure in a ground joint formed between a rectangular plate, 1x6x20 cm. and a nominal solid.

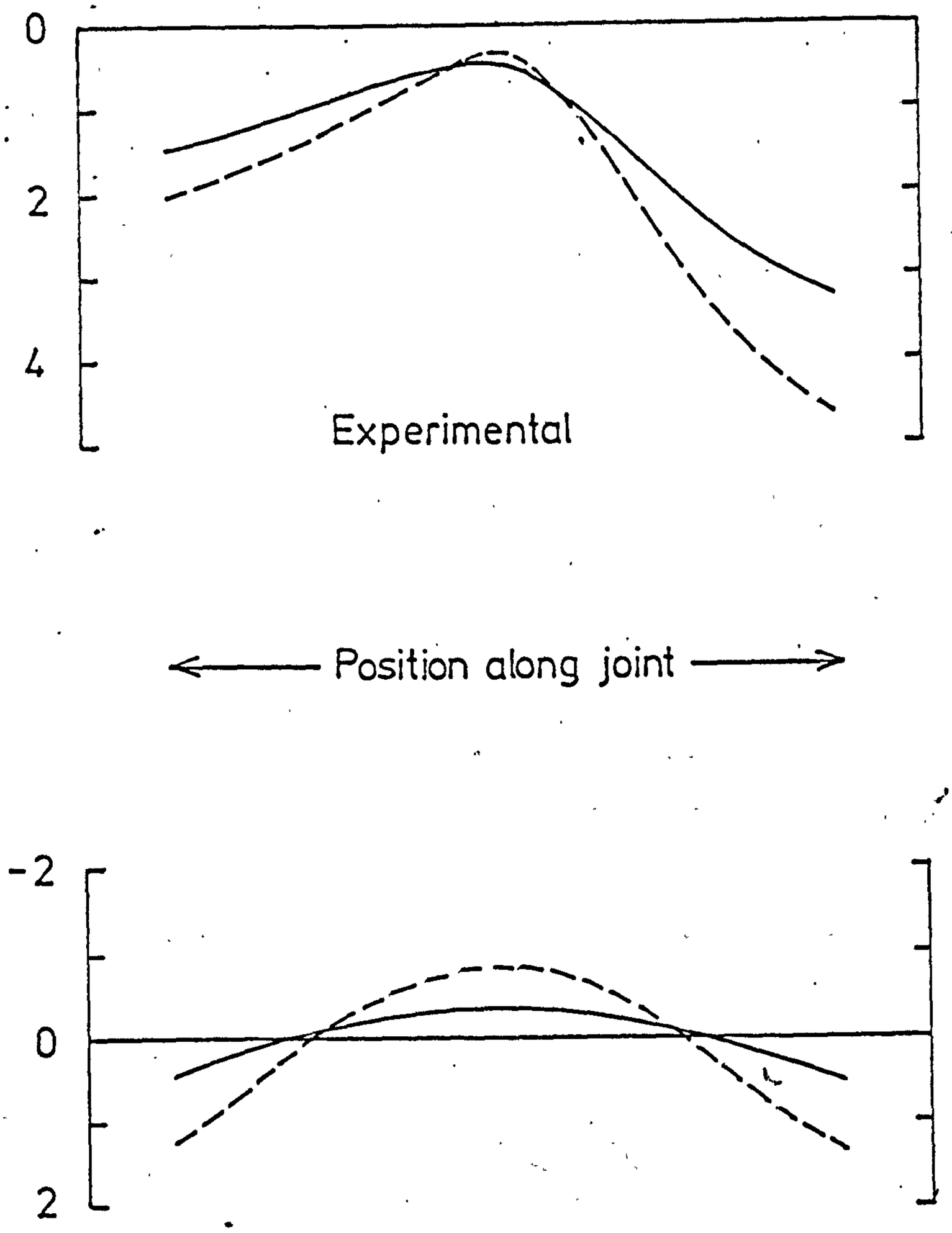

Fig. 51 Experimental and theoretical values of closure in a ground joint formed between a rectangular plate 2x6x20 cm. and a nominal solid.

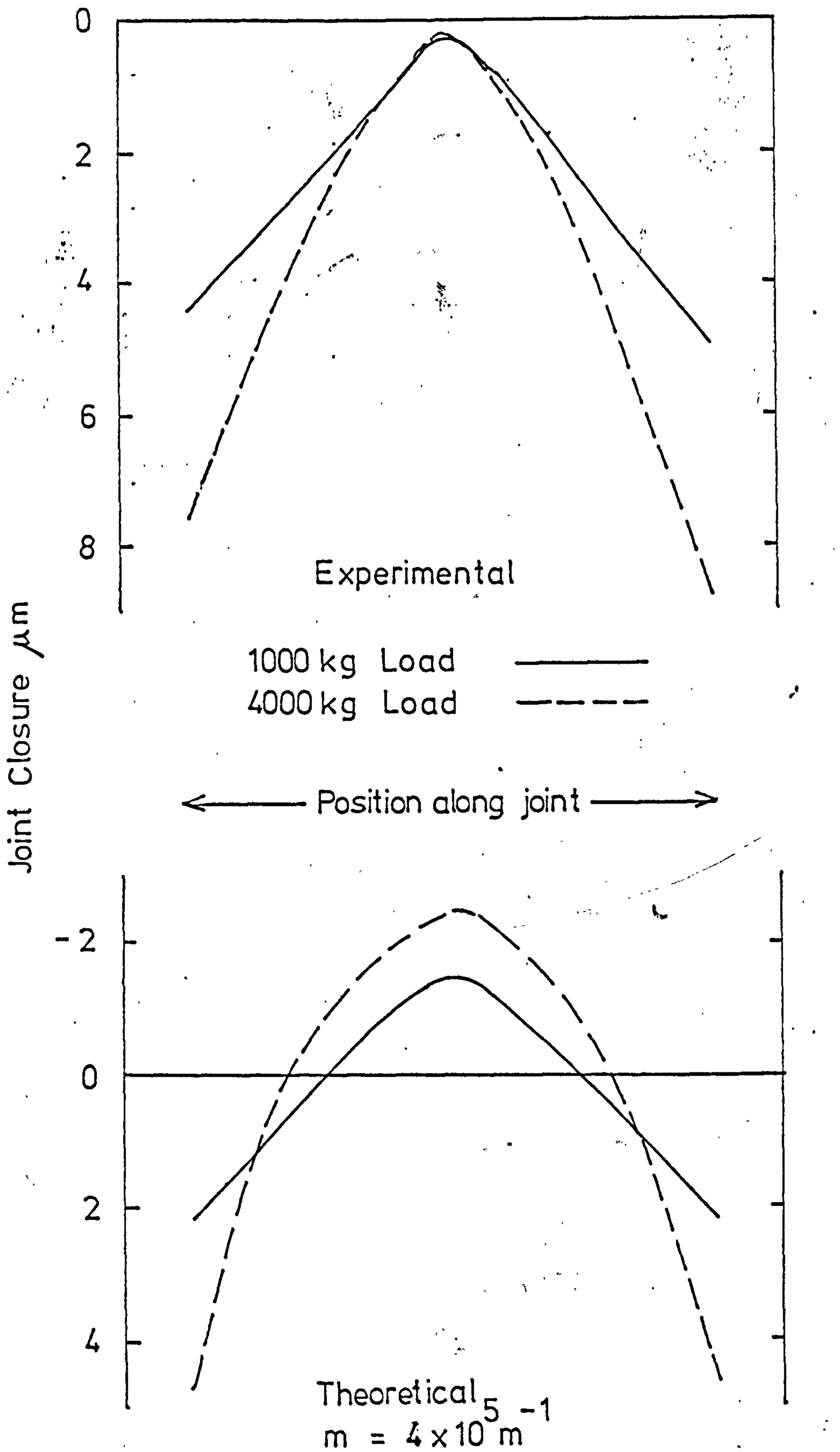

Fig. 52 Experimental and theoretical values of closure in a milled joint formed between a rectangular plate 1x6x20 cm. and a nominal solid.

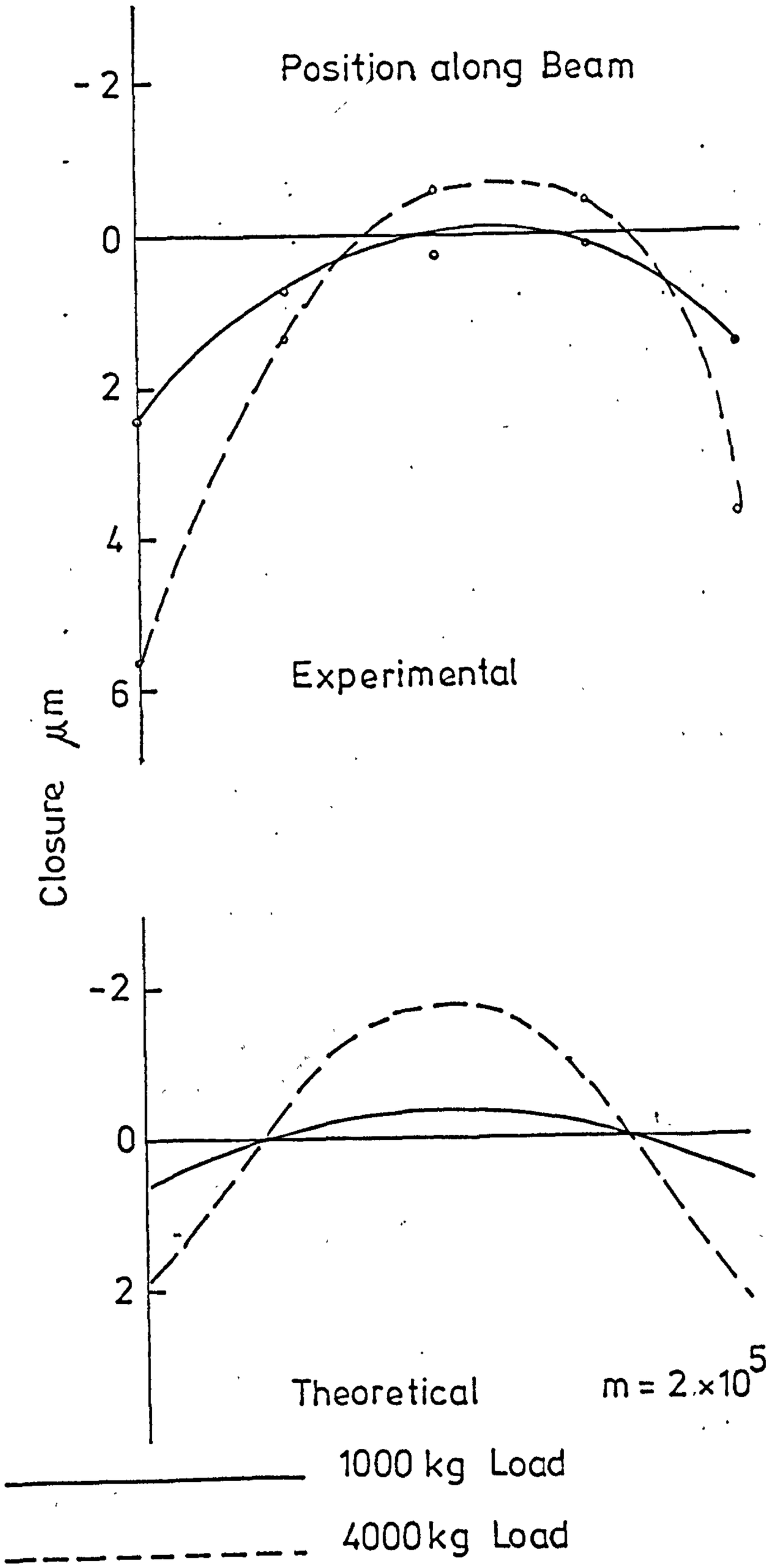

Fig. 53. Experimental and theoretical values of closure in a milled joint formed between a rectangular plate 2x6x20 cm. and a nominal solid.

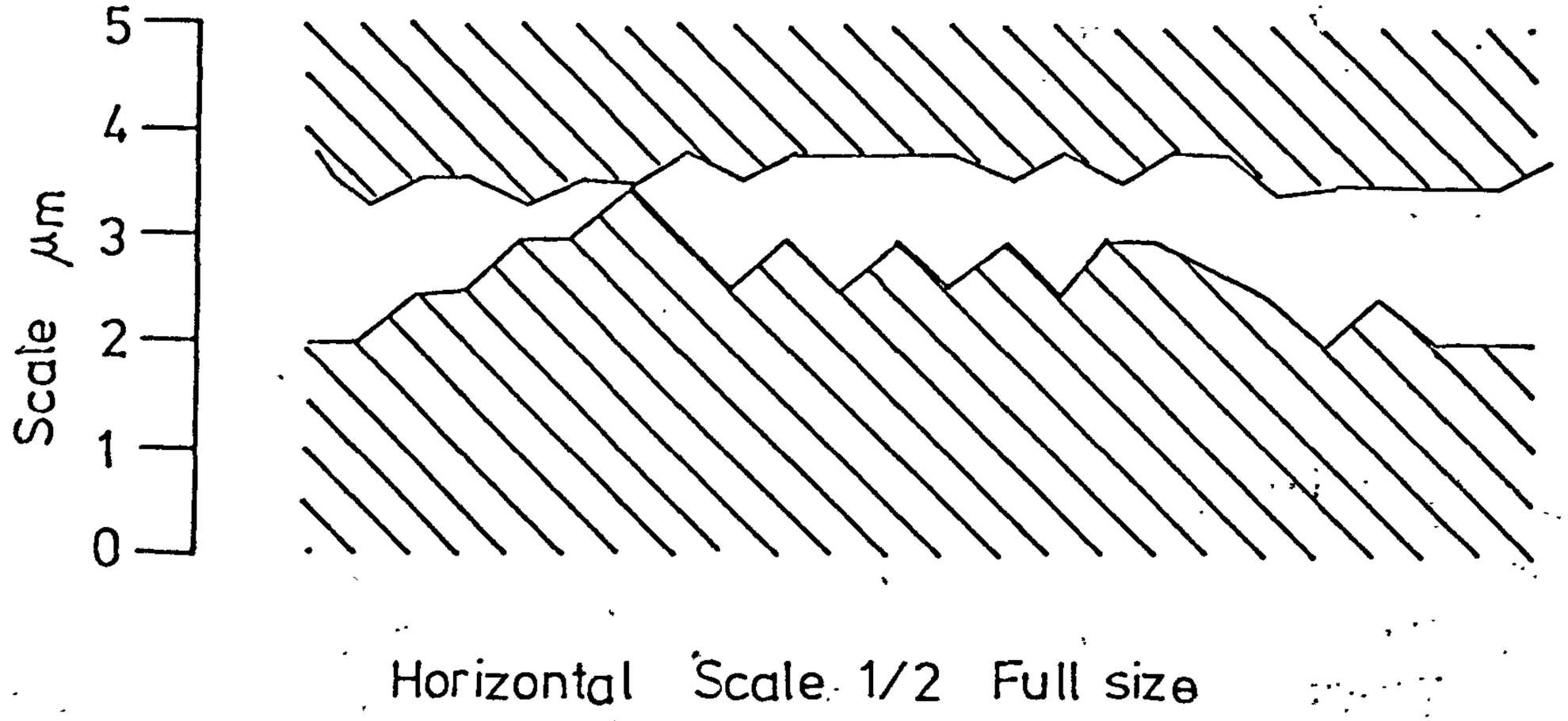

Fig. 54 Surface profile along the mid-axis of a ground joint formed between a rectangular plate 2x6x20 cm. and a nominal solid.

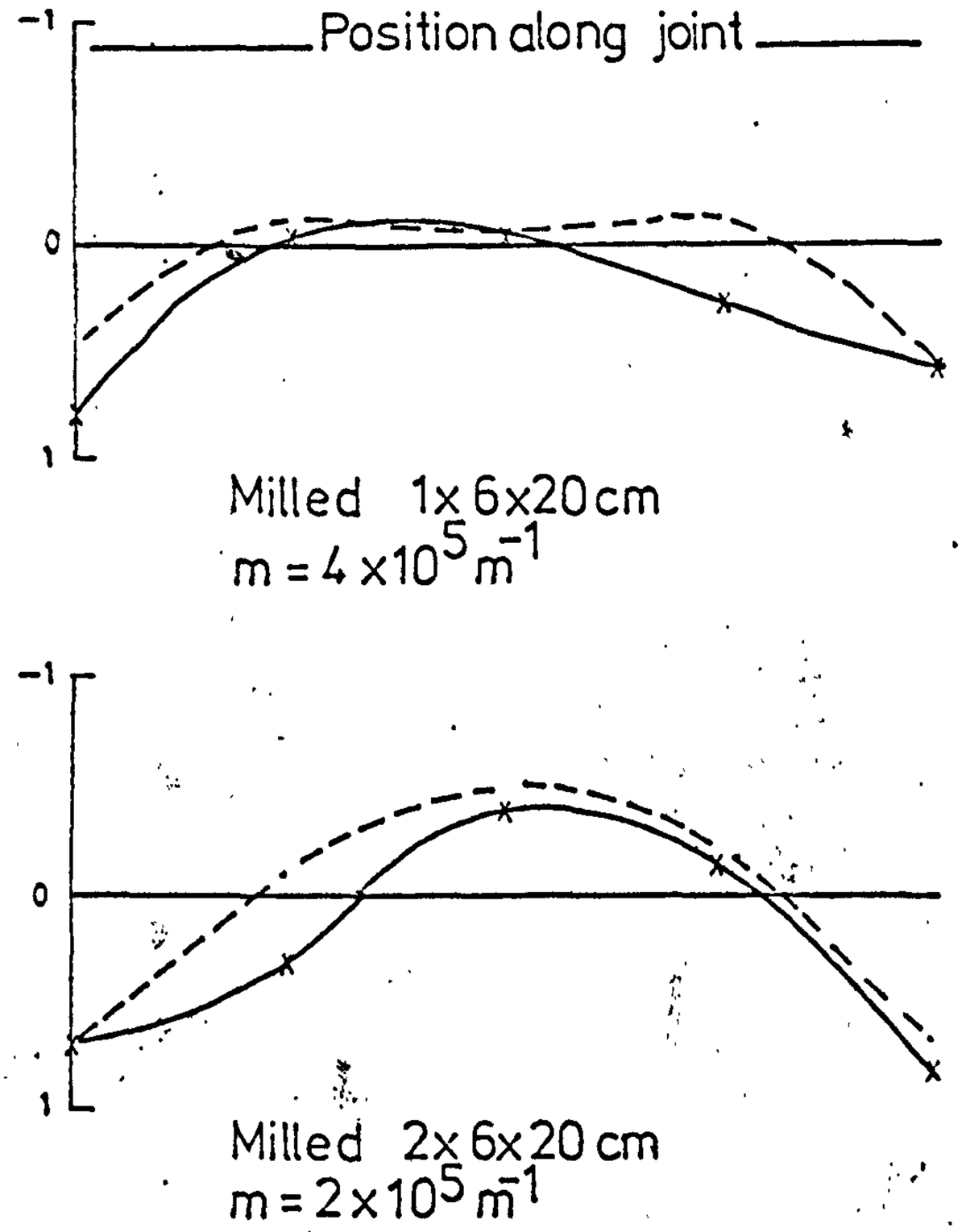

Fig. 55. Experimental and theoretical values of the closure of ground and milled rectangular joints between applied loads of 3000 kg. and 4000kg.